https://www.mdc-berlin.de/de/veroeffentlichungstypen/clinical-journal-club

Als gemeinsame Einrichtung von MDC und Charité fördert das Experimental and Clinical Research Center die Zusammenarbeit zwischen Grundlagenwissenschaftlern und klinischen Forschern. Hier werden neue Ansätze für Diagnose, Prävention und Therapie von Herz-Kreislauf- und Stoffwechselerkrankungen, Krebs sowie neurologischen Erkrankungen entwickelt und zeitnah am Patienten eingesetzt. Sie sind eingeladen, uns beizutreten. Bewerben Sie sich!

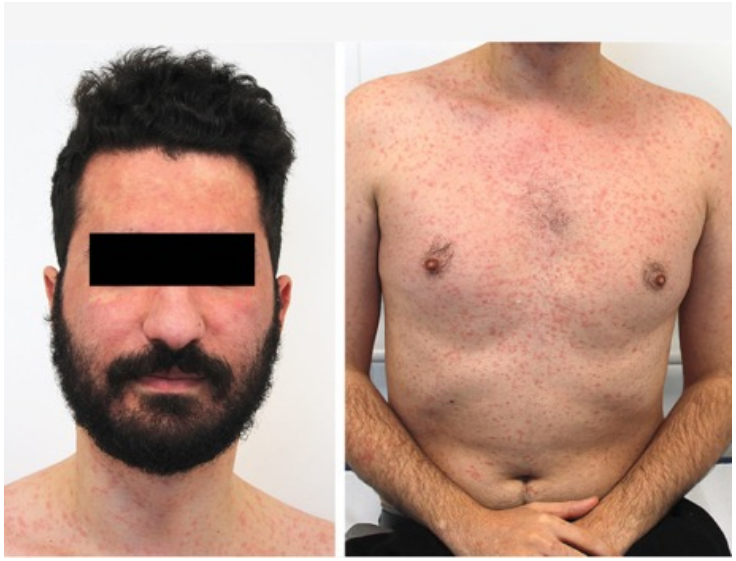

A previously healthy 26-year-old man presented with a 5-day history of fever, nausea, and vomiting and a 2-day history of an itchy rash. The rash had started behind his ears and then spread to his face and entire body. The patient was a refugee from a Middle Eastern country and had had limited vaccinations. Well-demarcated erosions were also present on the buccal mucosa on both sies of the mouth.
What is the most likely etiology of these erosions?

Aphthous ulcers

Forchheimer spots

Fordyce spots

Herpes stomatitis

Koplik spots

The appearance of the erosions on the buccal mucosa was consistent with Koplik spots. Measles was suspected on the basis of this patient's typical exanthem and enanthem. The diagnosis of primary measles infection was confirmed after serologic testing for antimeasles IgM and IgG was positive. A quantitative real-time polymerase-chain-reaction assay for measles virus performed on a blood sample was also positive. Treatment with antipyretic medications was initiated. Two weeks after presentation, the patient had recovered without complications.

Fordyce-Flecken (oder Fordyce-Drüsen) sind harmlose, 1-5 mm große, weißlich-gelbe oder hautefarbene Talgdrüsen, die oft an Lippen, im Mundraum oder im Genitalbereich auftreten.

Koplik-Flecken
sind ein frühes, wegweisendes Anzeichen für Masern. Sie erscheinen 2–3 Tage vor dem Hautausschlag als winzige, weiße, sandkornartige Flecken auf rotem Grund, typischerweise an der Innenseite der Wangen (Wangenschleimhaut) gegenüber den Backenzähnen. Diese hochinfektiösen Läsionen verschwinden oft, wenn der Hautausschlag beginnt.

Forchheimer-Flecken
sind kleine, rote Petechien (Punktblutungen) auf dem weichen Gaumen, die als flüchtiges Enanthem bei Röteln, Scharlach oder Masern auftreten. Sie erscheinen oft kurz vor oder während des typischen Hautausschlags, insbesondere bei Röteln, wo sie in etwa 20% der Fälle beobachtet werden. Benannt sind sie nach dem Pädiater Frederick Forchheimer.

Multiple myeloma is a cancer of the bone marrow plasma cells that produce antibodies, leading to the buildup of abnormal cells, bone destruction, kidney dysfunction, and immune system suppression. Common symptoms include severe bone pain (often back or ribs), fractures, fatigue, infections, and anemia. It typically affects older adults and is managed with chemotherapy, targeted therapies, and stem cell transplants.

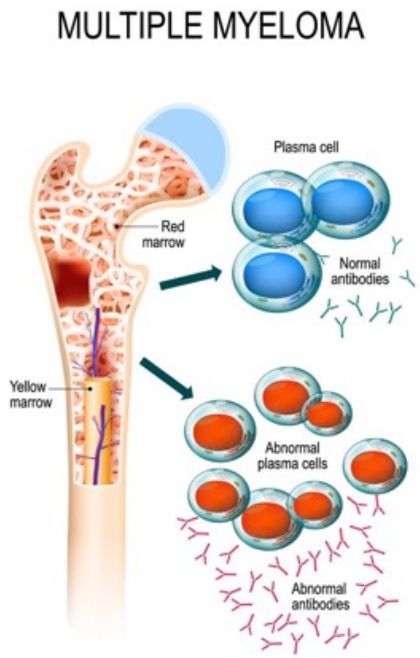

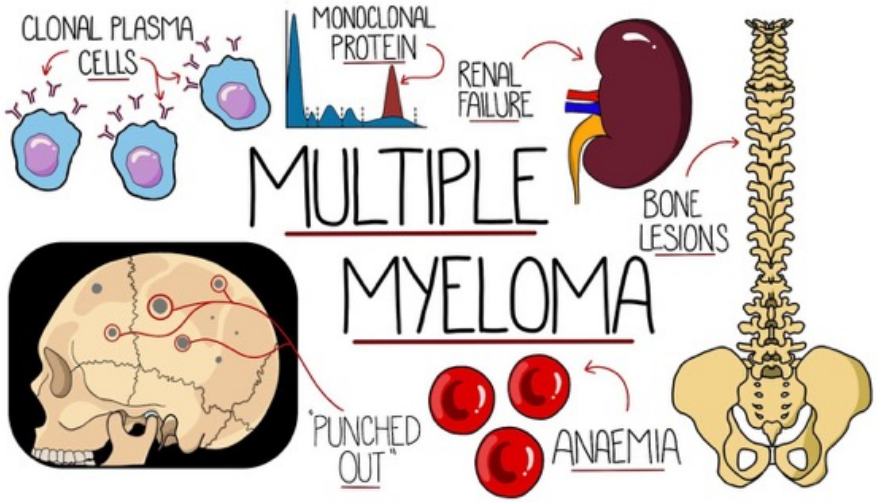

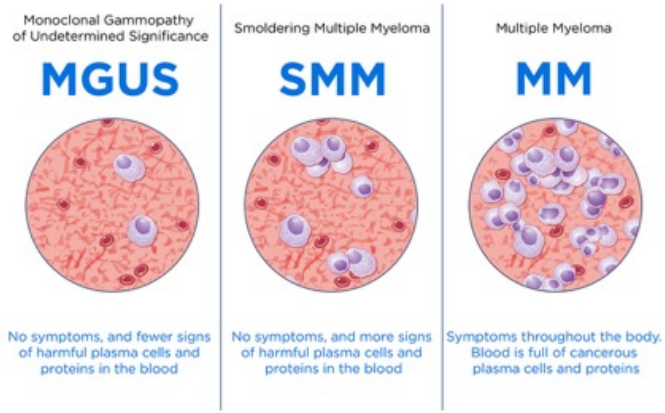

Refractory myeloma is a type of blood cancer that does not respond to treatment or progresses within 60 days of the last therapy. It differs from relapsed, where the cancer returns after a response. It is often managed with new combinations of drugs—such as immunomodulatory drugs, proteasome inhibitors, or BCMA-targeted therapies—to overcome treatment resistance.

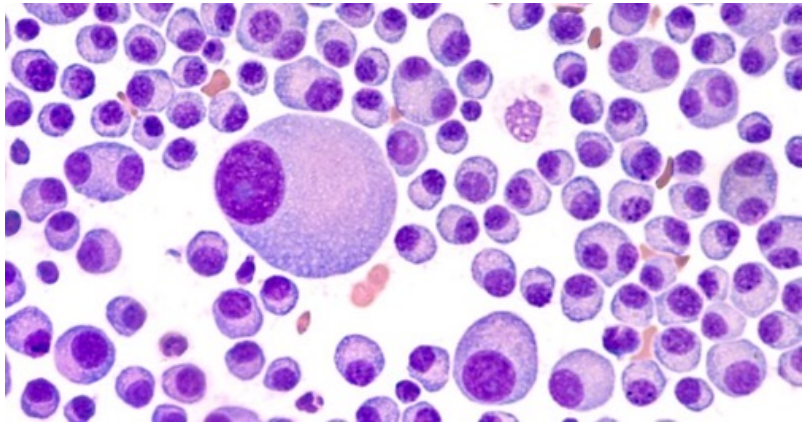

Definition and Types

- **Refractory:** The disease does not respond to treatment, meaning the M-protein level does not decrease, or it continues to grow.
- **Primary Refractory:** The disease fails to achieve at least a minimal response to initial therapy.
- **Relapsed and Refractory (RRMM):** Disease that progresses within 60 days of the last treatment in patients who previously had a response.
- **Double/Triple-Class Refractory:** Disease resistant to a proteasome inhibitor and an immunomodulatory agent, and for triple-class, an anti-CD38 antibody (e.g., daratumumab).

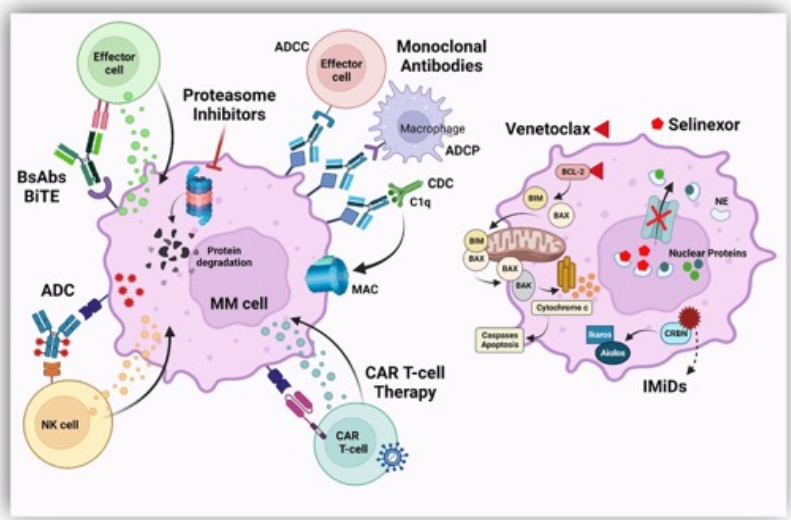

Daratumumab plus teclistamab

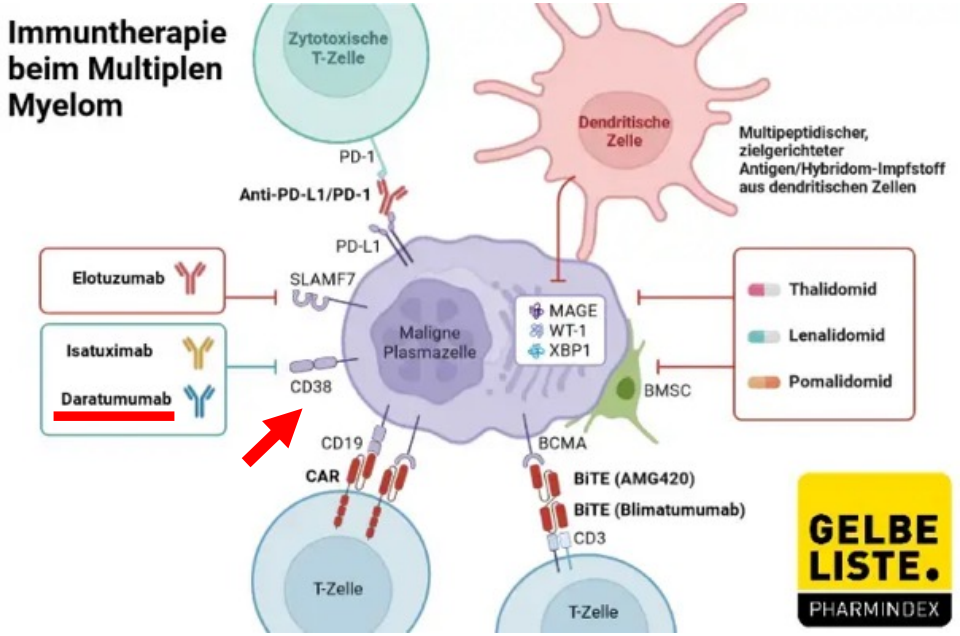

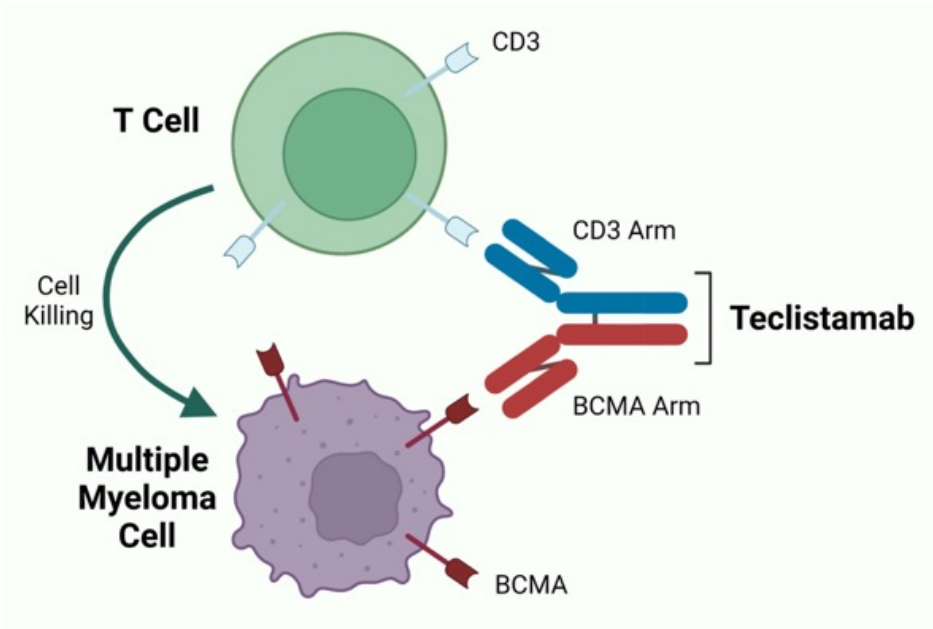

Teclistamab plus Daratumumab in Relapsed or Refractory Multiple Myeloma

In a phase 1–2 trial, teclistamab, a bispecific antibody targeting CD3 on T-cell surfaces and B-cell maturation antigen on myeloma cells, showed durable responses in heavily pretreated patients with relapsed or refractory multiple myeloma. Daratumumab, a monoclonal antibody targeting CD38 protein, has shown survival benefit in patients with multiple myeloma.

In this phase 3 trial, we randomly assigned patients with one to three previous lines of therapy to receive combination therapy with teclistamab–daratumumab or daratumumab combined with dexamethasone plus the investigator's choice of pomalidomide (DPd) or bortezomib (DVd) — the DPd or DVd group. The primary end point was progression-free survival, as assessed by an independent review committee.

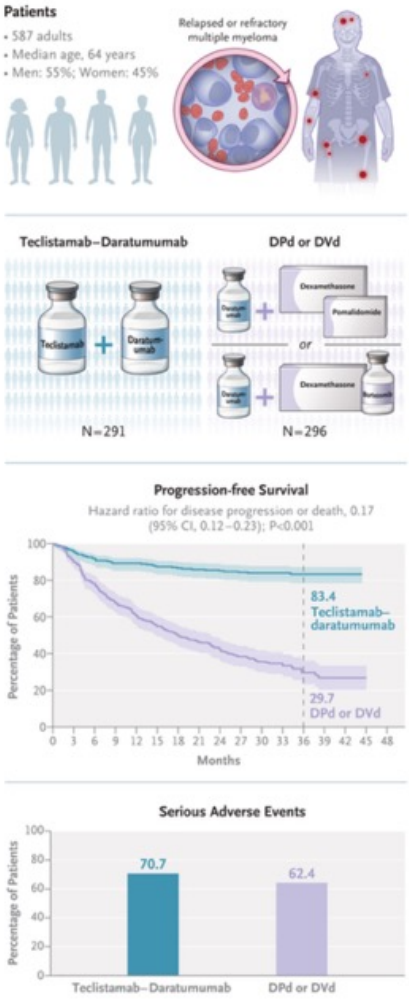

Multiple myeloma is characterized by progressive immune dysfunction and multiple relapses. The treatment of relapsed or refractory multiple myeloma is increasingly challenging because the evolving frontline landscape complicates second-line treatment selection. Challenges are compounded by limited effective salvage treatment options and high attrition. Emerging anti–B-cell maturation antigen (BCMA) treatments, including chimeric antigen receptor T-cell (CAR-T) therapy and antibody drug conjugates, offer promise, with ciltacabtagene autoleucel therapy resulting in a high incidence of minimal residual disease negativity and durable progression-free survival. However, off-the-shelf and highly effective regimens are needed to fully address the needs of individual patients.

In the phase 1–2 MajesTEC-1 trial, teclistamab, a bispecific antibody targeting CD3 on T-cell surfaces and B-cell maturation antigen on myeloma cells and B cells, showed deep and durable responses in heavily pretreated patients with relapsed or refractory multiple myeloma. Daratumumab, an anti-CD38–targeting monoclonal antibody, is a cornerstone of standard treatment regimens for multiple myeloma, with a survival benefit across all lines of therapy

Patients

Eligible patients had received one to three lines of antimyeloma therapy, including a proteasome inhibitor and lenalidomide, with documented disease progression on or after the last therapy line. Patients who had received only one previous line of therapy were required to have lenalidomide-refractory myeloma, according to the criteria of the International Myeloma Working Group. Key exclusion criteria were previous BCMA-directed therapy or refractoriness to anti-CD38 monoclonal antibodies.

Treatments

Patients were randomly assigned in a 1:1 ratio to receive teclistamab–daratumumab or the investigator's choice of standard-care regimens of DPd or DVd — the DPd or DVd group. Patients were stratified according to the investigator's choice of DPd or DVd, the International Staging System disease stage (I, II, or III), previous exposure to monoclonal antibodies against CD38, and the number of previous lines of therapy (one, two, or three).

End Points and Assessments

The primary end point was progression-free survival, as assessed by an independent review committee and defined according to a time-to-event analysis.

Characteristic	Teclistamab–Daratumumab (N=291)	DPd or DVd (N=296)	All Patients (N=587)
Median age (range) — yr	64 (36–88)	63 (25–84)	64 (25–88)
Male sex — no. (%)	156 (53.6)	169 (57.1)	325 (55.4)
Race or ethnic group — no. (%)†			
White	190 (65.3)	194 (65.5)	384 (65.4)
Asian	68 (23.4)	63 (21.3)	131 (22.3)
Black	13 (4.5)	20 (6.8)	33 (5.6)
Other ethnic group	20 (6.9)	19 (6.4)	39 (6.6)
ECOG performance-status score — no. (%)‡			
0	167 (57.4)	160 (54.1)	327 (55.7)
1	108 (37.1)	127 (42.9)	235 (40.0)
2	16 (5.5)	9 (3.0)	25 (4.3)
Stage on International Staging System — no. (%)§			
I	182 (62.5)	185 (62.5)	367 (62.5)
II	85 (29.2)	88 (29.7)	173 (29.5)
III	24 (8.2)	23 (7.8)	47 (8.0)
Previous therapy exposure			
Median number of previous lines of therapy (range)	2 (1–3)	2 (1–3)	2 (1–3)
Medications — no. (%)			
Proteasome inhibitor	290 (99.7)	296 (100)	586 (99.8)
Immunomodulatory drug	291 (100)	296 (100)	587 (100)
Anti-CD38 antibody	15 (5.2)	16 (5.4)	31 (5.3)
Refractory status — no. (%)			
Any proteasome inhibitor	117 (40.2)	104 (35.1)	221 (37.6)
Any immunomodulatory drug	247 (84.9)	253 (85.5)	500 (85.2)
Median time from diagnosis of multiple myeloma to randomization — yr (range)	3.7 (0.4–20.3)	3.9 (0.2–22.3)	3.8 (0.2–22.3)
Cytogenetic risk — no./total no. (%)¶			
Standard	126/285 (44.2)	145/294 (49.3)	271/579 (46.8)
High	104/285 (36.5)	104/294 (35.4)	208/579 (35.9)
Undetermined	55/285 (19.3)	45/294 (15.3)	100/579 (17.3)

Treatment Response and Minimal Residual Disease Negativity (Intention-to-Treat Population).

Variable	Teclistamab–Daratumumab (N=291)	DPd or DVd (N=296)	Risk Ratio (95% CI)*
Overall response — no. (%)†	259 (89.0)	223 (75.3)	1.18 (1.09–1.27)
Response — no. (%)‡			
Stringent complete response§	225 (77.3)	69 (23.3)	—
Complete response	13 (4.5)	26 (8.8)	—
Very good partial response	14 (4.8)	74 (25.0)	—
Partial response	7 (2.4)	54 (18.2)	—
Minimal response	1 (0.3)	13 (4.4)	—
Stable disease	13 (4.5)	46 (15.5)	—
Progressive disease	3 (1.0)	5 (1.7)	—
Not evaluable	15 (5.2)	9 (3.0)	—
Complete response or better	238 (81.8)	95 (32.1)	2.55 (2.14–3.03)
Very good partial response or better	252 (86.6)	169 (57.1)	1.52 (1.36–1.69)
Measure of response			
Median duration — mo (95% CI)	NE (NE–NE)	23.5 (19.8–29.9)	—
Median time until first response — mo (range)	1.2 (0.9–25.0)	1.2 (0.7–6.3)	—
Median time until complete response or better — mo (range)	6.9 (1.0–34.5)	6.9 (1.5–18.8)	—
Minimal residual disease¶			
Patients in sequencing analysis set — no.	262	269	—
Patients with negativity of 10^{-5} — no. (%)	153 (58.4)	46 (17.1)	3.43 (2.58–4.55)

Die Kombination aus Lenalidomid und Bortezomib (oft als RVD/VRd-Schema mit Dexamethason ergänzt) ist ein hocheffektiver Standard in der Erstlinienbehandlung des multiplen Myeloms.

Most Common Adverse Events (Safety Population).

Adverse Event	Teclistamab–Daratumumab (N=283)		DPd or DVd (N=290)	
	Any Grade	Grade 3 or 4	Any Grade	Grade 3 or 4
	number of patients (percent)			
Any adverse event	283 (100)	269 (95.1)	290 (100)	280 (96.6)
Hematologic				
Neutropenia	222 (78.4)	214 (75.6)	240 (82.8)	228 (78.6)
Anemia	111 (39.2)	58 (20.5)	103 (35.5)	50 (17.2)
Thrombocytopenia	103 (36.4)	55 (19.4)	126 (43.4)	68 (23.4)
Lymphopenia	63 (22.3)	59 (20.8)	50 (17.2)	32 (11.0)
Leukopenia	51 (18.0)	30 (10.6)	61 (21.0)	46 (15.9)
Nonhematologic				
Hypogammaglobulinemia	194 (68.6)	16 (5.7)	104 (35.9)	4 (1.4)
Cytokine release syndrome	170 (60.1)	0	0	0
Diarrhea	147 (51.9)	10 (3.5)	89 (30.7)	7 (2.4)
Cough	136 (48.1)	1 (0.4)	66 (22.8)	0
Covid-19	124 (43.8)	17 (6.0)	97 (33.4)	6 (2.1)
Upper respiratory tract infection	115 (40.6)	12 (4.2)	88 (30.3)	7 (2.4)
Pyrexia	104 (36.7)	4 (1.4)	55 (19.0)	1 (0.3)
Pneumonia	65 (23.0)	47 (16.6)	53 (18.3)	43 (14.8)
Covid-19 pneumonia	34 (12.0)	32 (11.3)	12 (4.1)	7 (2.4)

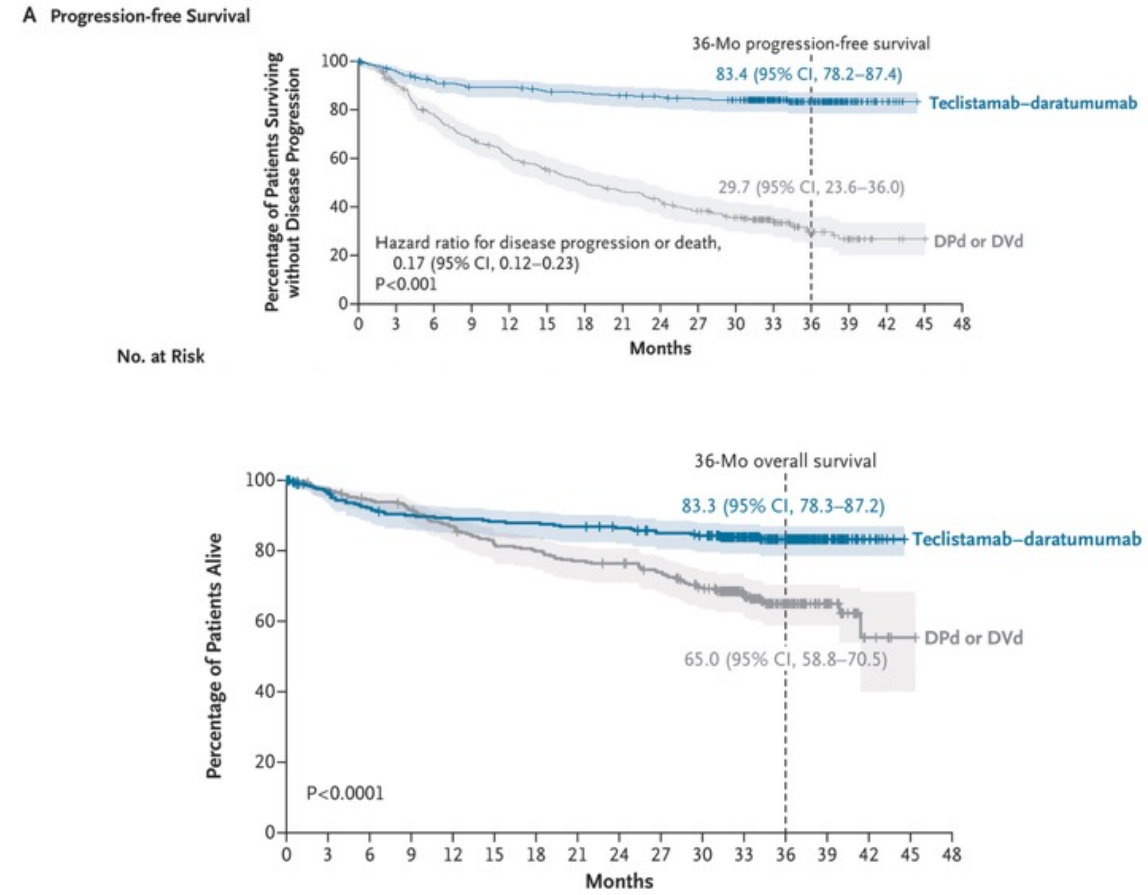

Progression-free Survival.

Panel A shows Kaplan–Meier estimates of progression-free survival at 36 months among patients who were randomly assigned to receive teclistamab in combination with daratumumab (teclistamab–daratumumab) or daratumumab in combination with dexamethasone and the investigator's choice of either pomalidomide or bortezomib (DPd or DVd); shading indicates 95% confidence intervals, and tick marks indicate censored data. At a median follow-up of 34.5 months, the median progression-free survival was not reached in the teclistamab–daratumumab group and was 18.1 months in the DPd or DVd group, therefore favoring teclistamab–daratumumab treatment. Panel B shows the results of a prespecified subgroup analysis of the risk of disease progression or death in the intention-to-treat population. A hazard ratio of less than 1.0 indicates an advantage for teclistamab–daratumumab as compared with DPd or DVd. The International Staging System (ISS) consists of three stages (with a higher stage indicating more severe disease) and is based on levels of serum beta-2-microglobulin and albumin. High cytogenetic risk is defined by fluorescence in situ hybridization or karyotype testing of patients having one or more of the following abnormalities: t(4;14), t(14;16), and del(17p). The performance-status score on Eastern Cooperative Oncology Group (ECOG) scale ranges from 0 to 5, with higher scores indicating greater disability. Baseline soft-tissue plasmacytomas include both extramedullary and paraskeletal plasmacytomas. The widths of the confidence intervals have not been adjusted for multiplicity and may not be used in place of hypothesis testing. Several subgroup analyses — geographic region, previous exposure to anti-CD38 therapy, and refractory status to lenalidomide — were performed post hoc.

B Subgroup Analysis

Subgroup	Teclistamab–Daratumumab	DPd or DVd	Hazard Ratio for Disease Progression or Death (95% CI)
	no. of events/total no. of patients		
Age			
<65 yr	18/147	103/160	0.13 (0.08–0.22)
65 to <75 yr	19/113	71/111	0.17 (0.10–0.29)
≥75 yr	7/31	13/25	0.35 (0.14–0.89)
Sex			
Male	27/156	106/169	0.20 (0.13–0.30)
Female	17/135	81/127	0.13 (0.08–0.23)
Race			
White	33/190	124/194	0.18 (0.12–0.27)
Asian	8/68	43/63	0.11 (0.05–0.24)
Black	1/13	9/20	0.19 (0.02–1.49)
Other	2/20	11/19	0.14 (0.03–0.62)
Geographic region			
North America	4/35	21/46	0.18 (0.06–0.54)
Europe	28/176	101/158	0.18 (0.11–0.27)
Other	12/80	65/92	0.15 (0.08–0.27)
Previous anti-CD38 therapy			
Yes	3/15	12/16	0.19 (0.05–0.67)
No	41/276	175/280	0.17 (0.12–0.23)
Refractory to lenalidomide			
Yes	38/240	162/251	0.17 (0.12–0.24)
No	6/51	25/45	0.17 (0.07–0.41)
Renal function at baseline			
≤60 ml/min	14/56	36/55	0.31 (0.16–0.57)
>60 ml/min	30/235	150/240	0.14 (0.09–0.20)
Baseline ECOG performance-status score			
0	23/167	98/160	0.16 (0.10–0.25)
≥1	21/124	89/136	0.18 (0.11–0.29)
Investigator's choice of DPd or DVd			
DPd	42/267	166/269	0.18 (0.13–0.26)
DVd	2/24	21/27	0.05 (0.01–0.24)
No. of lines of previous therapy			
1	13/108	71/114	0.14 (0.08–0.25)
2 or 3	31/183	116/182	0.18 (0.12–0.27)
ISS disease stage at baseline			
I	19/182	110/185	0.12 (0.07–0.20)
II	19/85	59/88	0.23 (0.13–0.38)
III	6/24	18/23	0.31 (0.12–0.79)
Soft-tissue plasmacytomas at baseline			
No	30/250	158/255	0.13 (0.09–0.20)
Yes	14/41	29/41	0.33 (0.17–0.63)
Cytogenetic risk group			
High-risk	20/104	78/104	0.15 (0.09–0.25)
Standard-risk	15/126	84/145	0.16 (0.09–0.27)
Percent plasma cells in bone marrow			
≤30	31/216	140/234	0.17 (0.11–0.25)
>30 to <60	7/42	24/35	0.17 (0.07–0.39)
≥60	6/28	21/24	0.17 (0.07–0.43)

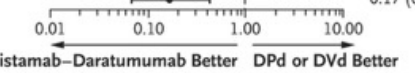

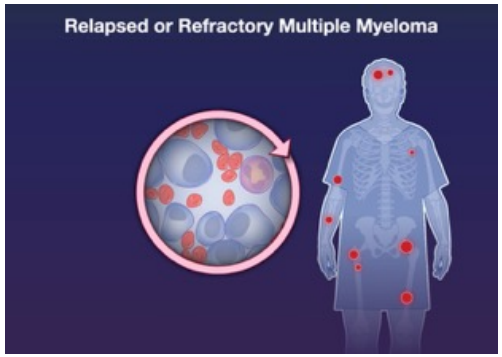
Relapsed or Refractory Multiple Myeloma

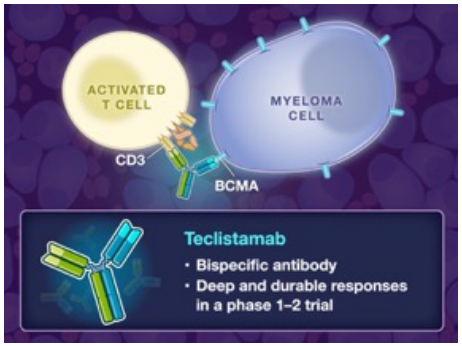
ACTIVATED T CELL
MYELOMA CELL
CD3
BCMA
Teclistamab
• Bispecific antibody
• Deep and durable responses in a phase 1–2 trial

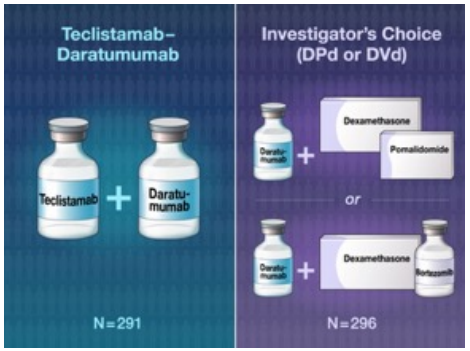
Teclistamab–Daratumumab
Investigator's Choice (DPd or DVd)
Teclistamab
Daratu-mumab
Dexamethasone
Pomalidomide
or
Dexamethasone
N=291
N=296


SAFETY
Serious Adverse Events
Percentage of Patients
70.7%
64.2%
Teclistamab–Daratumumab
DPd or DVd

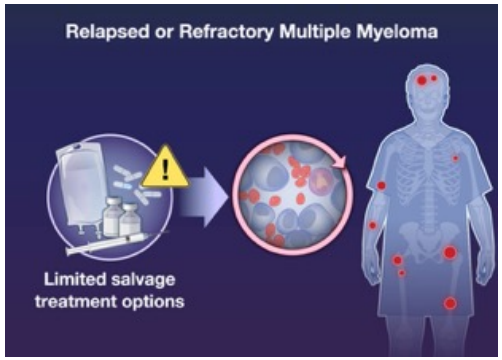
Relapsed or Refractory Multiple Myeloma
Limited salvage treatment options


MajesTEC-3 Trial
Efficacy and Safety?
Teclistamab
Daratu-mumab
Off-the-shelf combination immunotherapy

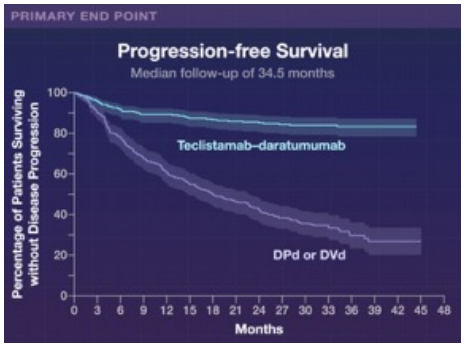
PRIMARY END POINT
Progression-free Survival
Median follow-up of 34.5 months
Percentage of Patients Surviving without Disease Progression
Teclistamab–daratumumab
DPd or DVd
Months

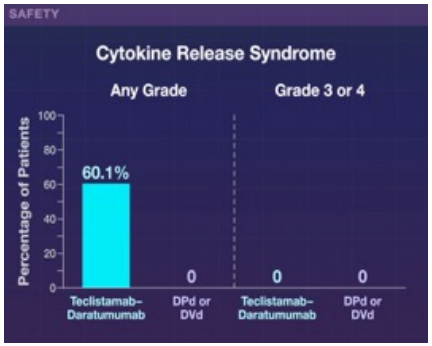
SAFETY
Cytokine Release Syndrome
Any Grade
Grade 3 or 4
Percentage of Patients
60.1%
0
0
0
Teclistamab–Daratumumab
DPd or DVd
Teclistamab–Daratumumab
DPd or DVd

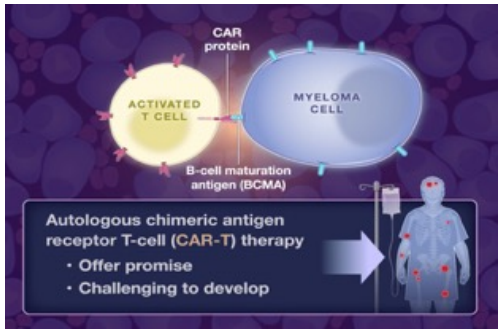
CAR protein
ACTIVATED T CELL
MYELOMA CELL
B-cell maturation antigen (BCMA)
Autologous chimeric antigen receptor T-cell (CAR-T) therapy
• Offer promise
• Challenging to develop


MajesTEC-3 Trial
• Phase 3
• Randomized
• Open-label
• Active-controlled
• Multinational

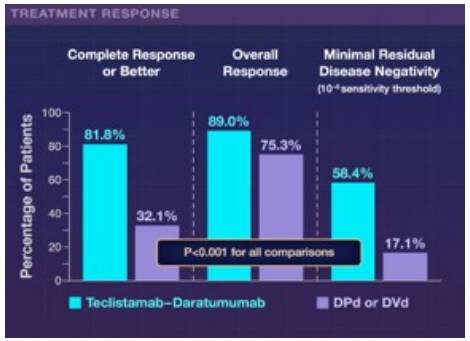
TREATMENT RESPONSE
Complete Response or Better
Overall Response
Minimal Residual Disease Negativity
Percentage of Patients
81.8%
32.1%
89.0%
75.3%
58.4%
17.1%
P<0.001 for all comparisons
Teclistamab–Daratumumab
DPd or DVd

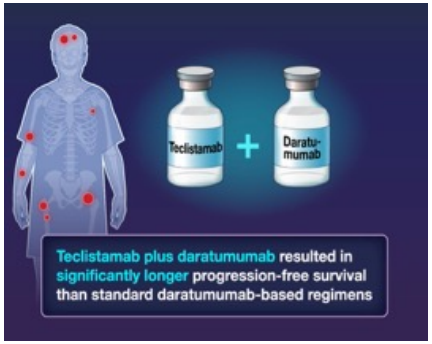
Teclistamab
Daratu-mumab
Teclistamab plus daratumumab resulted in significantly longer progression-free survival than standard daratumumab-based regimens

Cystinosis is a rare, inherited metabolic disorder caused by a genetic *CTNS* mutation that leads to the toxic accumulation of the amino acid cystine within lysosomes, forming crystals that damage cells throughout the body, particularly the kidneys and eyes. It is a life-long condition requiring lifelong treatment with cysteamine, which helps manage crystal buildup and extends kidney function.

Cornea deposits

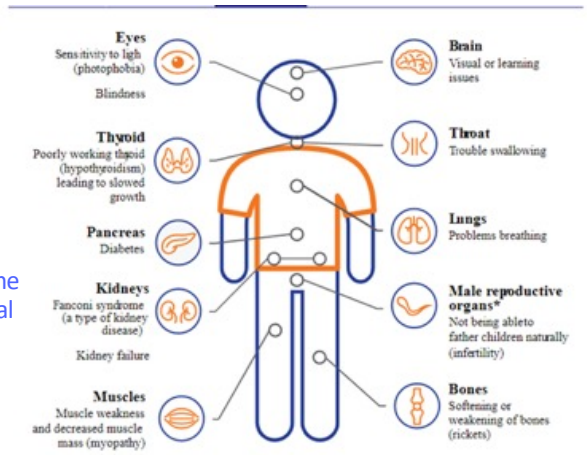

Juvenile Fanconi syndrome and renal failure

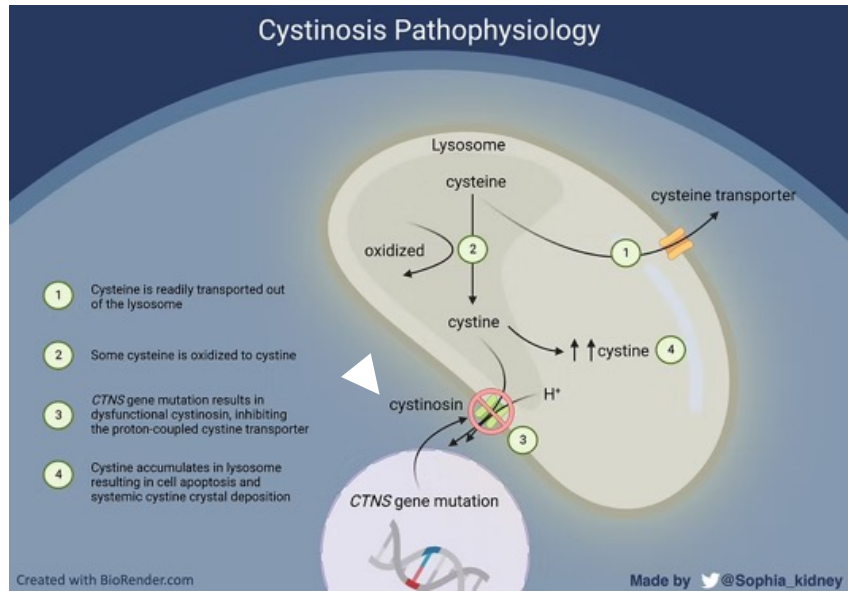

Cystein

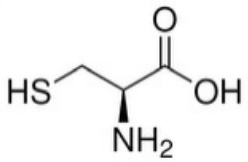

Cystin

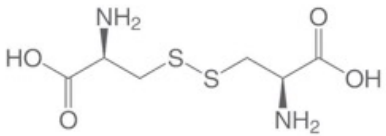

Cystine is a stable, sulfur-containing amino acid formed by two oxidized cysteine molecules, serving as a critical structural component in hair, skin, and nails (keratin).

Mechanism of lysosomal cystine depletion by cysteamine (aminothiol).
Cysteamine enters the lysosome through an unknown transporter and breaks the disulfide bond in cystine. This results in formation of cysteine and a new cysteine-cysteamine mixed disulfide, each of which can exit the lysosome through its own transporter.

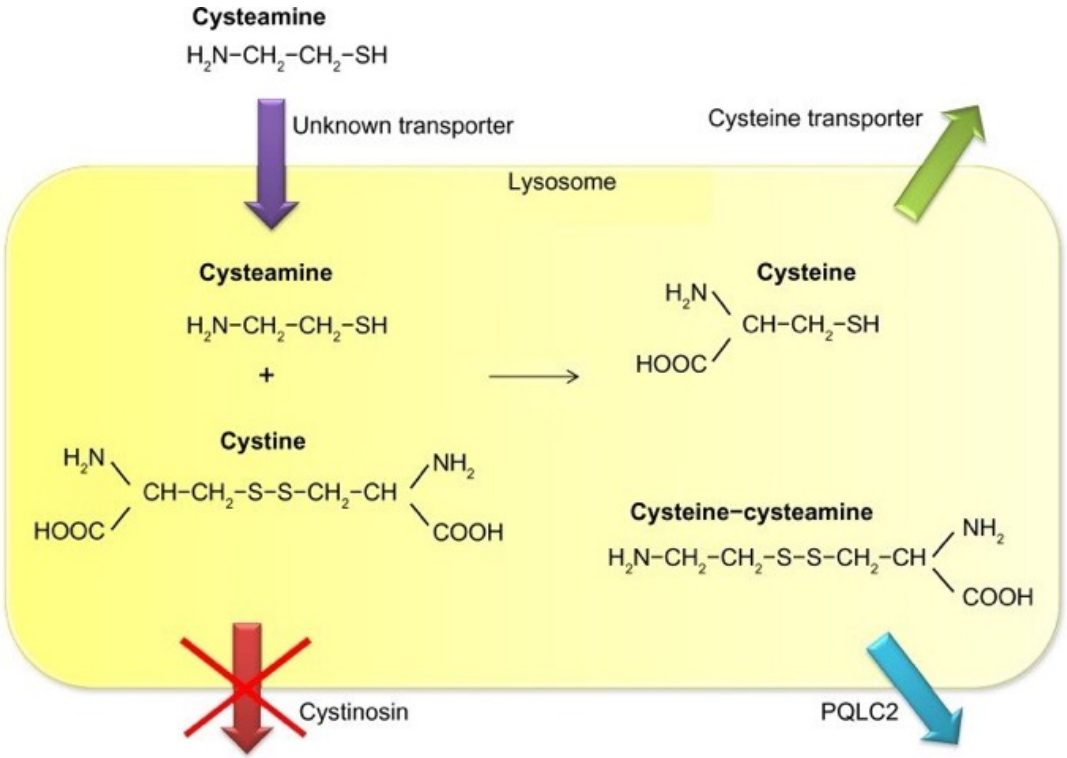

Lentiviraler Gentransfer bezeichnet die Verwendung von modifizierten Lentiviren (meist abgeleitet vom HIV-1) als Vektoren, um genetisches Material in Zielzellen einzuschleusen. Diese Methode zeichnet sich vor allem durch die Fähigkeit aus, Gene stabil in das Wirtsgenom zu integrieren, was eine dauerhafte Expression ermöglicht.

Kernmerkmale und Funktionsweise

Lentivirale Vektoren nutzen den natürlichen Infektionsmechanismus des Virus, wurden jedoch für die Anwendung in Forschung und Klinik weitgehend entkernt, um sie **replikationsdefizient** und damit sicher zu machen.

- **Zielzellen:** Im Gegensatz zu anderen Retroviren können Lentiviren sowohl sich teilende als auch **nicht-teilungsfähige (post-mitotische) Zellen** wie Neuronen oder Stammzellen infizieren.
- **Ablauf (Transduktion):**
    1. **Bindung & Eintritt:** Der Vektor bindet über Oberflächenproteine an die Zellmembran und setzt seine RNA im Zytoplasma frei.
    2. **Reverse Transkription:** Die virale RNA wird durch die mitgelieferte Reverse Transkriptase in DNA umgeschrieben.
    3. **Integration:** Die DNA wird in den Zellkern transportiert und dort durch das Enzym Integrase dauerhaft in das Genom der Wirtszelle eingebaut.
- **Kapazität:** Sie können relativ große Gensequenzen von bis zu **8–10 kb** transportieren.

Viral vector platforms within the gene therapy landscape

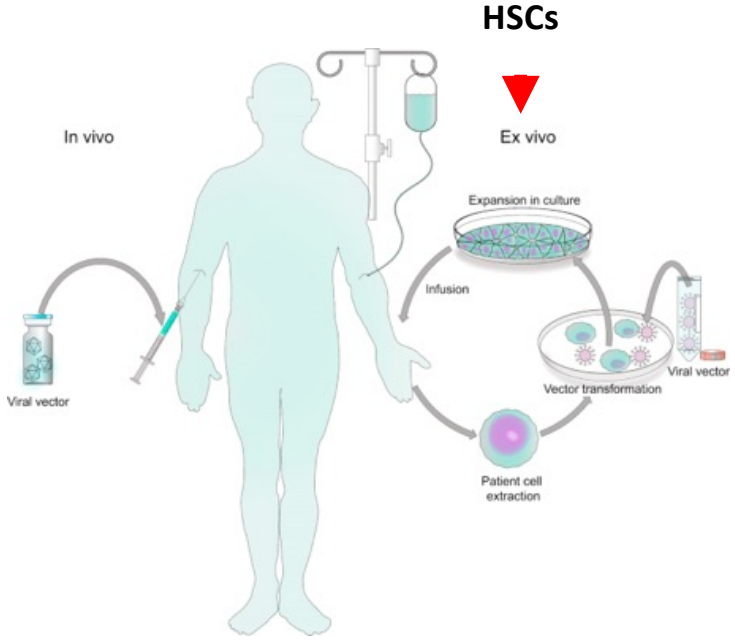

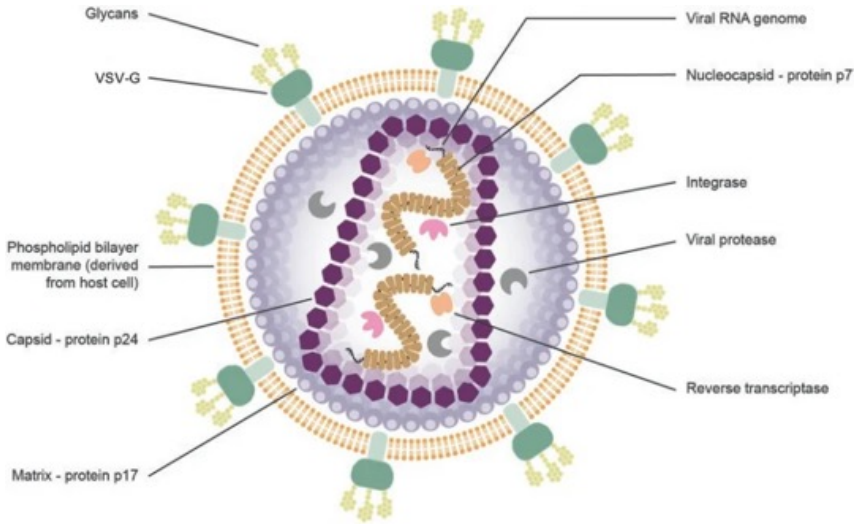

In vivo gene therapy entails the direct administration of vector carrying a therapeutic transgene into the patient. Ex vivo gene therapy involves the extraction of a patient's cells or from an allogenic source, genetic modification by a vector carrying a therapeutic transgene, selection and expansion in culture, and infusion to re-introduce the engineered cells back into the patient.

Expressing the *CTNS* gene in hematopoietic stem cells (HSCs) is designed to cure cystinosis by turning blood-forming stem cells into delivery vehicles that transport a functional cystine transporter (cystinosin) to damaged tissues throughout the body.

The Core Mechanism: Cross-Correction via Macrophages

Cystinosis is caused by a defect in the *CTNS* gene, leading to the accumulation of cystine within lysosomes, which damages tissues, particularly the kidneys and eyes.

- **HSC Differentiation:** Transplanted, gene-modified HSCs engraft in the bone marrow and differentiate into myeloid cells, such as macrophages and microglia.
- **Tissue Migration:** These modified, functional macrophages migrate to tissues suffering from the disease, such as the kidneys, eyes, and brain.
- **Tunneling Nanotubes:** Once in the tissues, these new, healthy cells establish "tunneling nanotubes" (cellular bridges) with the surrounding diseased cells.
- **Lysosomal Transfer:** Through these tubes, the healthy cells transfer functional, *CTNS*-carrying lysosomes to the diseased cells, breaking down the accumulated cystine and "cross-correcting" them.

Hematopoietic Stem-Cell Gene Therapy for Cystinosis

Cystinosis is a multisystemic lysosomal storage disorder caused by pathogenic variants in *CTNS*, the gene encoding cystinosin, a lysosomal transmembrane cystine transporter. In patients with cystinosis, cystine accumulates within lysosomes in all organs. The cystine-depleting agent cysteamine delays but does not prevent disease progression.

Methods

In this phase 1–2, open-label, ongoing clinical study, we performed a preliminary assessment of CTNS-RD-04, which consists of autologous CD34+ cells transduced with lentiviral vectors carrying *CTNS* complementary DNA, in patients with cystinosis. The primary end points were the safety and the side-effect profiles of CTNS-RD-04. Secondary end points were measures of efficacy, including white-cell cystine levels and cystine storage depletion. Oral cysteamine was withdrawn before CTNS-RD-04 infusion, and cysteamine eyedrops were withdrawn 1 month after myeloablation.

Conclusions

In this small study, CTNS-RD-04, an ex vivo gene therapy for cystinosis, had adverse effects that were largely consistent with the myeloablative regimen and underlying disease profile. White-cell cystine levels decreased after therapy.

Cystinosis is a rare autosomal recessive lysosomal storage disease that places a tremendous burden on patients and caregivers and has poor outcomes, despite the availability of cystine-reducing treatment with cysteamine. The disease is caused by pathogenic variants or deletions in the ubiquitous gene *CTNS* (17p13.2), which encodes cystinosin, a lysosomal transmembrane cystine transporter, and leads to the accumulation of cystine within lysosomes and cystine crystals within tissues. Three allelic forms of cystinosis exist, the most severe and most common of which is the infantile form (Online Mendelian Inheritance in Man number, 219800). Renal Fanconi's syndrome develops in affected children by 6 to 18 months of age, and chronic kidney disease (CKD) eventually leads to end-stage kidney disease (ESKD). Nonrenal complications of cystinosis include photophobia and corneal erosion, cardiovascular complications, diabetes mellitus, hypothyroidism, bone deformities and fragility, neurologic defects, and progressive myopathy that can result in life-threatening respiratory dysfunction, dysphagia, and aspiration pneumonia. Intracellular cystine reduction with the cystine-depleting agent cysteamine allows cystine to exit cells and slows the progression of the disease. To reduce corneal cystine crystal accumulation, cysteamine eyedrops are needed every hour during the time the person is awake. Premature death is inevitable, despite these therapies.

Drug-Product Manufacturing and Infusion Procedures

Before the drug-product infusion, patients received conditioning with busulfan with a target area under the curve (AUC) of 85 to 90 mg per liter per hour, a dose selected because it provides an effective level of myeloablation with an acceptable side-effect profile. Oral cysteamine treatment was discontinued 2 weeks before myeloablation conditioning with busulfan, and cysteamine eyedrops were discontinued 1 month after such conditioning; CTNS-RD-04 was infused intravenously.

To obtain CD34+ HSPCs, each patient underwent leukapheresis, and CD34+ HSPCs were selected after mobilization with granulocyte colony-stimulating factor, administered for 4 days, and plerixafor, administered for 1 day. Positive selection of CD34+ cells was performed before lentiviral vector transduction. In the course of this study, two different lentiviral vectors were used to generate a CTNS-RD-04 product, the pCCL-CTNS vector (for use in Patients 1, 2, and 3) and the pCDY-CTNS vector (for use in Patients 4, 5, and 6), the latter to prepare for transition to a commercially compatible vector.

End Points

The patients attended regular follow-up visits at which blood samples were obtained and the patients were assessed for adverse events and disease progression.

Demographics

Characteristic	Patient 1	Patient 2	Patient 3	Patient 4	Patient 5	Patient 6
Age at symptom onset or diagnosis	8 mo	6 mo	4 yr	6 yr	8 mo	2 yr
Age at time of CTNS-RD-04 treatment	20 yr	46 yr	22 yr	33 yr	31 yr	30 yr
Date of CTNS-RD-04 treatment	October 2019	June 2020	November 2020	November 2021	March 2022	October 2022
Sex	Male	Male	Male	Male	Female	Male
Pathogenic variant	57-kb deletion, nt1035(ins C), p.Val233Argfs*63	57-kb deletion, c.473t→C, p.Leu158Pro	c.18_21del, p.Thr7Phefs*7, c.295_298del, p.Val99Ilefs*18	57-kb deletion, c.473T→C, p.Leu158Pro	57-kb deletion, c.414G→A, p.Trp138*	Homozygous 57-kb deletion
Kidney transplantation status (yr)	Stage 3 CKD moderate at enrollment; 1 kidney transplantation 34 months after CTNS-RD-04 treatment (2022)	2 kidney transplantations (1987 and 1999)	1 kidney transplantation (2010)	2 kidney transplantations (2008 and 2017)	No kidney transplantation; stage 3 CKD moderate at enrollment	2 kidney transplantations (2010 and 2019)

Patient 1 has CKD, 2-6 are renal transplant patients

Major Adverse Events.

Category	Attribution and Time Point (No. of Events)	No. of Events	No. of Patients
Gastrointestinal		26	6
Vomiting	Gastric erosions at screening (1), plerixafor mobilization (1), busulfan conditioning (3), appendicitis after infusion (1), immunization reaction at follow-up (2)	8	4
Diarrhea	Plerixafor mobilization (5), busulfan conditioning (2), food poisoning after infusion (1), erythromycin at follow-up (1)	9	5
Constipation	Opioid after infusion (3)	3	2
Oral mucositis	Busulfan conditioning (6)	6	6
Hematologic		20	5
Thrombocytopenia	Busulfan conditioning (7)	7	5
Leukopenia	Busulfan conditioning (4)	4	4
Neutropenic fever	Busulfan conditioning (5)	5	4
Epistaxis	Busulfan conditioning (3), mild trauma at follow-up (1)	4	3
Renal or electrolyte		18	4
Increased creatinine, BUN, chloride and decreased bicarbonate, potassium, phosphorus	CKD at screening (4) and after infusion (2), Fanconi's syndrome at screening (1) and after infusion (1), acyclovir and sulfamethoxazole–trimethoprim after infusion (1), plerixafor mobilization (1), busulfan conditioning (2), tacrolimus after infusion (2)	14	4
Hypomagnesemia	Apheresis mobilization (3), tacrolimus after infusion (1)	4	3
Endocrine		15	6
Azoospermia	Cystinosis at screening (5)	5	5
Gonadal failure	Busulfan conditioning (6)	6	6
Hypothyroidism	Cystinosis after infusion (1), cystinosis at follow-up (3)	4	4
Constitutional		14	5
Anorexia	Eosinophilic esophagitis at screening (1), busulfan conditioning (1), appendicitis after infusion (1), constipation after infusion (1), immunization reaction at follow-up (1)	5	2
Fatigue or lethargy	Apheresis mobilization (1), stress and anxiety at mobilization (1), busulfan conditioning (4)	6	5
Unintentional weight loss	Eosinophilic esophagitis at screening (1), appendicitis at follow-up (1), Covid-19 at follow-up (1)	3	2
Dermatologic		13	6
Alopecia	Busulfan conditioning (6)	6	6
Rash	Tape sensitivity at mobilization (1), PICC dressing after infusion (1), folliculitis after infusion (2), dermatitis after infusion (1), sulfamethoxazole–trimethoprim after infusion (1), vancomycin after infusion (1)	7	6
Swelling		5	2
Edema	Renal insufficiency after infusion (2)	2	2
Swelling of leg, arm, or knee	Popliteal cyst after infusion (1), intravenous infiltration at follow-up (1), mild trauma at follow-up (1)	3	2
Infection		3	3
Covid-19	Covid-19 after infusion (1), Covid-19 at follow-up (2)	3	3
Cardiac		1	1
Mitral-valve surgery†	Manifestation of preexisting valvular calcification at follow-up (1)	1	1

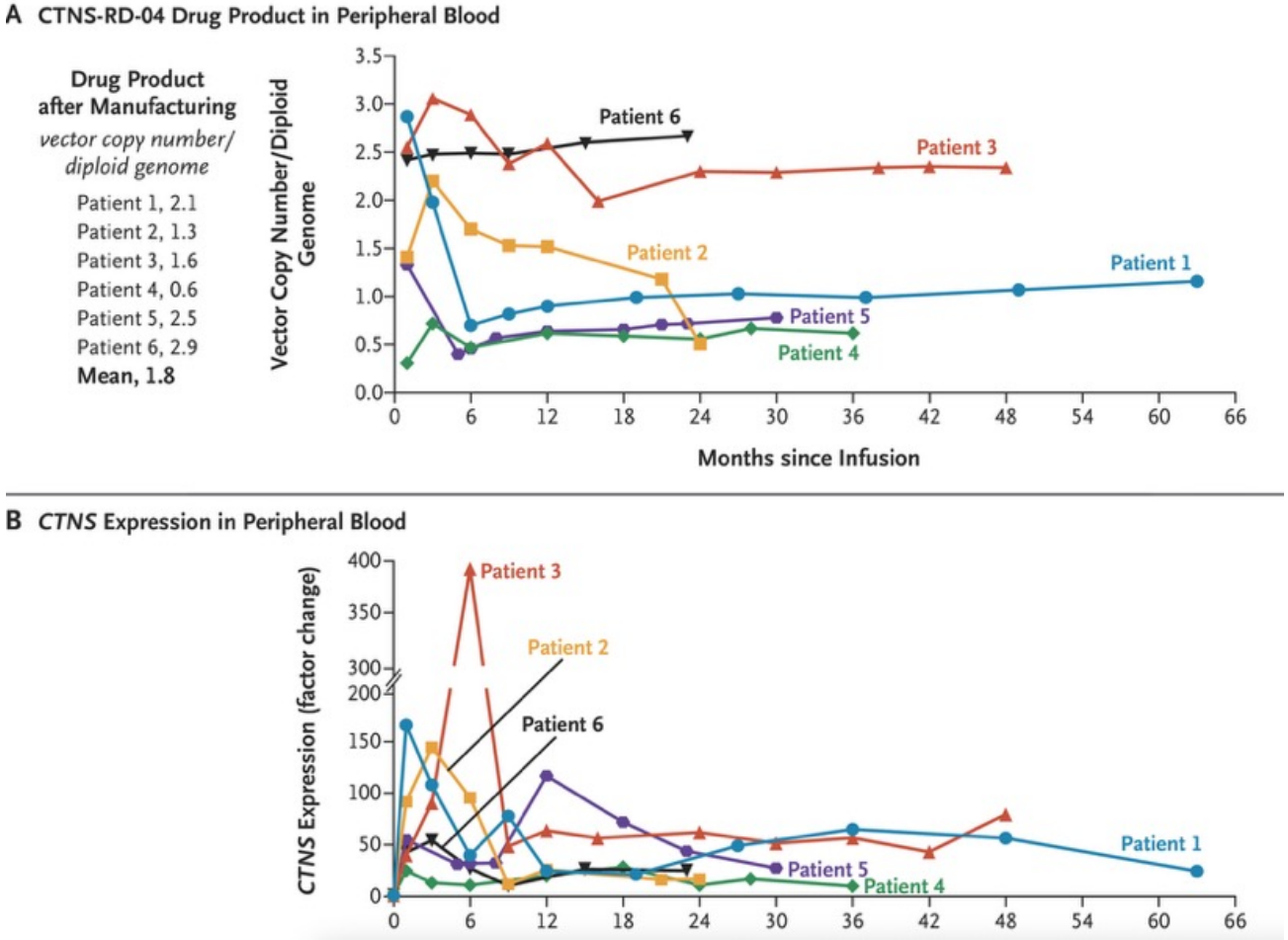

Vector Copy Number and *CTNS* Expression in Peripheral Blood over Time after Infusion.

Panel A shows the vector copy number in the CTNS-RD-04 drug product at the time of infusion and in peripheral blood at various times after infusion in each of the six patients. Patient 6 received two separate drug-product infusions, and the reported vector copy number represents the average of the two drug products. Panel B shows *CTNS* expression in the peripheral blood for each of the six patients at various times after infusion of CTNS-RD-04. For comparison, the mean *CTNS* expression in peripheral blood from three healthy donors was a factor change (±SD) of 2.97±0.65.

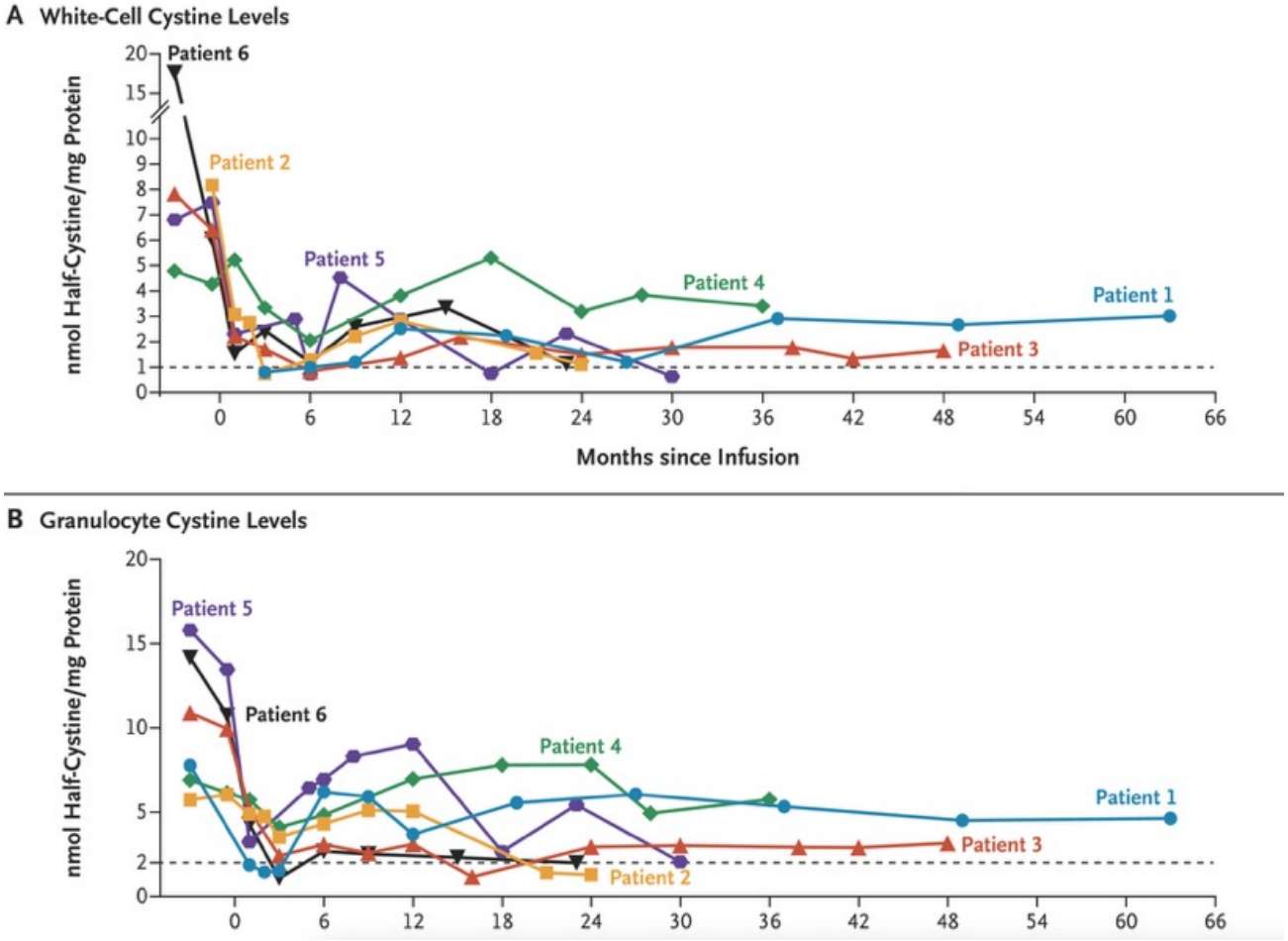

White-Cell Cystine Levels and Granulocyte Cystine Levels.

Panel A shows the white-cell cystine level at baseline and at various times after infusion. The white-cell cystine level was not measured at baseline in Patient 1. The therapeutic upper limit is indicated by the dotted line. Panel B shows the granulocyte cystine level at baseline and at various times after infusion. Patient 4 restarted oral cysteamine (150 mg per day) at 36 months after infusion. Patient 5 restarted oral cysteamine (450 mg per day) at 14 months after infusion.

Discussion

The interim analysis of this study involving six patients with cystinosis supports the safety of gene-modified autologous CD34+ cell transplantation, with findings that suggest an acceptable risk–benefit profile and support continued clinical development of CTNS-RD-04 for the treatment of cystinosis. Evidence of sustained donor-cell engraftment was observed during follow-up (>5 years in one patient) with stable gene marking and *CTNS* expression in peripheral blood and tissues after infusion of CTNS-RD-04. None of the adverse events appeared to be related to CTNS-RD-04, and no fatal or life-threatening adverse events, clonal expansions, or leukoproliferative complications were reported. We interpret the results of our study to suggest that this approach may provide a therapeutic advance for patients with nephropathic cystinosis and suggest a need for additional study.

The peripheral-blood white-cell cystine level is an established surrogate marker for the diagnosis and therapeutic monitoring of cystinosis. A decrease in cystine levels was observed by both the classic mixed white-cell cystine assay and purified granulocyte cystine determination, and results were associated with the vector copy number in the hematopoietic cell progeny. These results, along with those from longer follow-up periods, will be necessary to assess the therapeutic threshold of CTNS-RD-04 more completely.

Cystine crystal levels in the intestinal mucosa–biopsy samples, estimated with the method described previously by Dohil and colleagues, were lower after gene therapy in three patients. A decrease from baseline in cystine crystals in the skin, as assessed by the intradermal confocal microscopy method, occurred in four patients.

Myotonic dystrophy type 1 (DM1), or Steinert disease, is a genetic disorder characterized by progressive muscle wasting, weakness, and myotonia (inability to relax muscles). It affects muscles in the face, neck, and limbs, along with the heart, eyes, and brain. Caused by a triplet repeat expansion in the *DMPK gene* on chromosome 19, it is an autosomal dominant condition with symptoms often appearing in adulthood.

Key Aspects of Myotonic Dystrophy Type 1

- **Symptoms:** Muscle weakness (especially in the face/jaw, causing a "hatchet-faced" appearance) and stiffness (myotonia), which often manifests as difficulty releasing a grip. Other common symptoms include early-onset cataracts, cardiac arrhythmias (heart rhythm issues), daytime sleepiness, and digestive issues, as well as insulin-resistant diabetes.
- **Inheritance:** Inherited in an autosomal dominant pattern, meaning a 50% chance of passing the gene to children. It displays "genetic anticipation," where the disease often becomes more severe and appears earlier in successive generations due to expansion of the repeat.

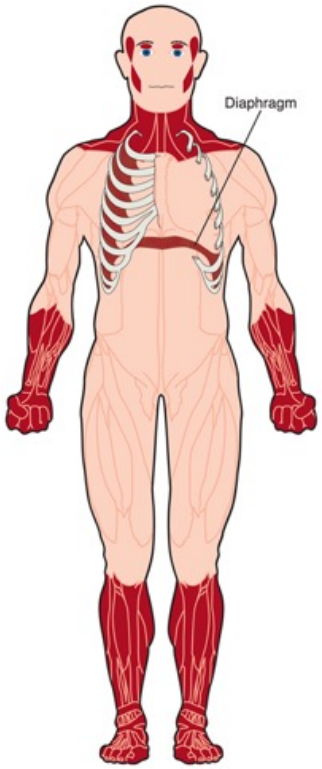

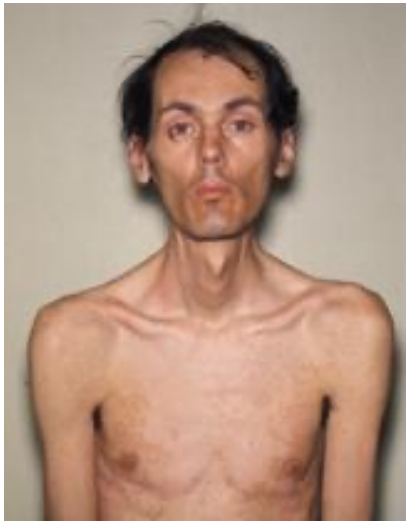

Das **DMPK-Gen** (Dystrophia Myotonica Protein Kinase) kodiert für ein Enzym, das eine entscheidende Rolle bei der Aufrechterhaltung der Struktur und Funktion von Skelettmuskeln, Herz und Gehirnzellen spielt. Mutationen in diesem Gen sind die Ursache für die **Myotone Dystrophie Typ 1 (DM1)**, die häufigste Form der Muskeldystrophie bei Erwachsenen.

In der Genetik und Zellbiologie steht DMPK für die **Dystrophia Myotonica Protein Kinase**. Dies ist ein Enzym (eine Serin/Threonin-Kinase), das vom gleichnamigen *DMPK*-Gen auf Chromosom 19 kodiert wird.

- **Funktion**: Es spielt eine entscheidende Rolle bei der Kommunikation innerhalb von Zellen, insbesondere in **Muskel-, Herz- und Gehirnzellen**.
- **Muskelsteuerung**: Das Enzym reguliert Strukturen in Muskelzellen, indem es andere Proteine beeinflusst. Beispielsweise "schaltet" es die **Myosin-Phosphatase** aus, ein Enzym, das für das Anspannen und Entspannen von Muskeln zuständig ist.
- **Krankheitsbezug**: Mutationen in diesem Gen (speziell CTG-Wiederholungen) verursachen die **Myotone Dystrophie Typ 1 (Steinert-Erkrankung)**, eine Form des Muskelschwunds

Dystrophia Myotonica

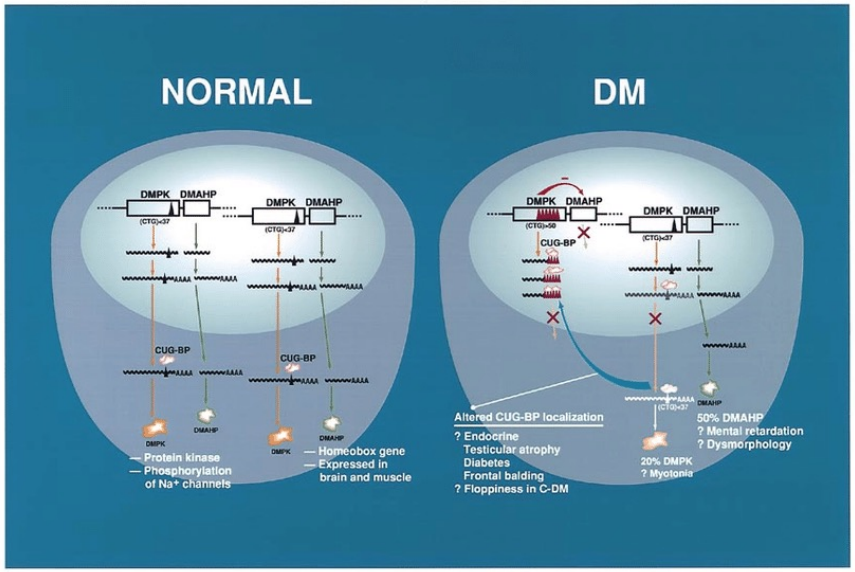

CTG triplet expansion

A toxic mRNA that needs to be destroyed

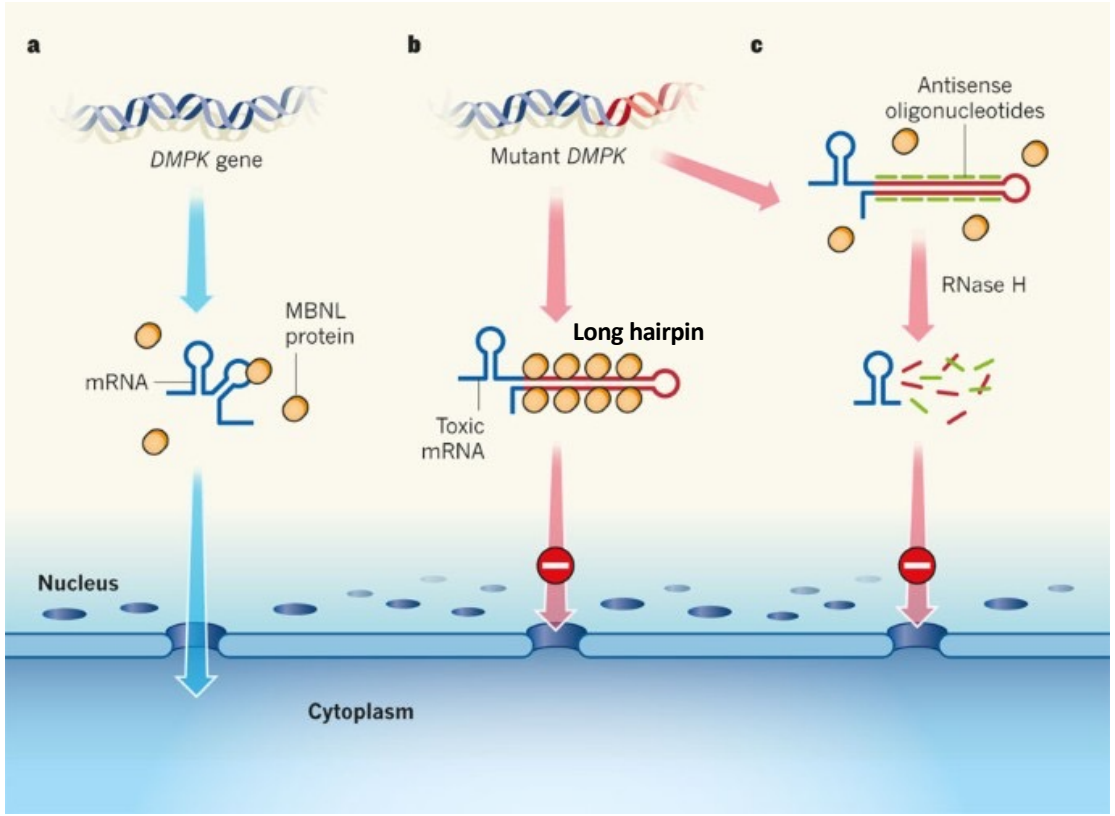

Muscleblind-like (MBNL) Proteine sind eine evolutionär konservierte Familie von RNA-bindenden Proteinen (RBPs), die eine zentrale Rolle bei der Regulation des RNA-Metabolismus spielen.

Antibody vector connected to an oligonucleotide

Delpacibart-Etedesiran (Del-Desiran, ehemals AOC 1001) ist ein neuartiges Antikörper-Oligonukleotid-Konjugat (AOC) zur Behandlung der Myotonen Dystrophie Typ 1 (DM1), entwickelt von Avidity Biosciences. Es reduziert die toxische DMPK-mRNA im Muskelgewebe, um die Ursache der Erbkrankheit zu bekämpfen. Die FDA hat den Wirkstoff als "Breakthrough Therapy" eingestuft.

Wichtige Fakten zu Delpacibart-Etedesiran:

- **Wirkmechanismus:** Es kombiniert einen monoklonalen Antikörper, der an den Transferrinrezeptor 1 (TfR1) bindet, mit einer siRNA, die den Abbau der DMPK-mRNA induziert. Dies ermöglicht die gezielte Abgabe der siRNA in Muskelzellen.
- **Indikation:** Behandlung der myotonen Dystrophie Typ 1 (DM1), einer seltenen, progressiven Muskelerkrankung.
- **Klinische Entwicklung:** Der Wirkstoff wird in der Phase-3-Studie HARBOR™ untersucht.
- **Ergebnisse:** Daten der MARINA-Studie zeigten eine Verbesserung der Handmuskelfunktion (vHOT), Muskelkraft und der Aktivitäten des täglichen Lebens.
- **Status:** Die FDA hat den Status „Breakthrough Therapy“, „Orphan Drug“ und „Fast Track“ erteilt, zudem gibt es den „Orphan“-Status in Europa und Japan.

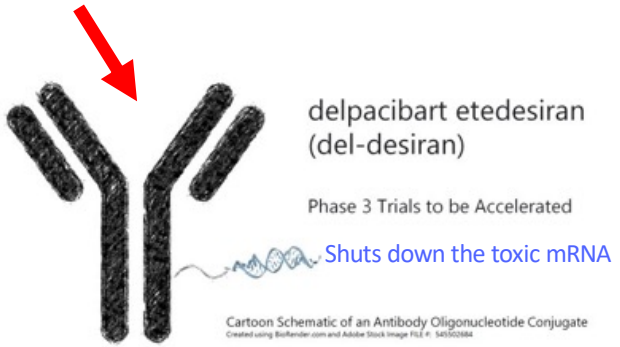

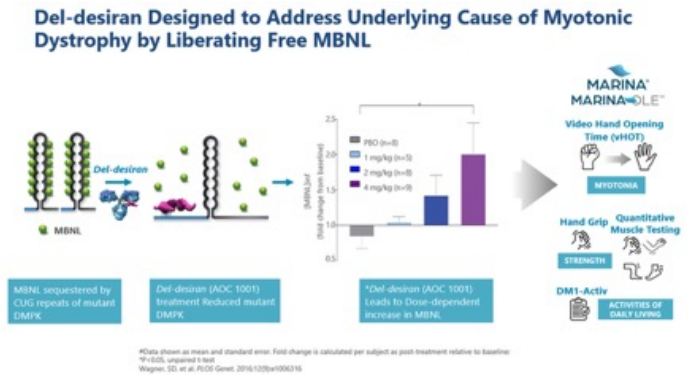

An Antibody–Oligonucleotide Conjugate for Myotonic Dystrophy Type 1

Myotonic dystrophy type 1 is a rare, dominantly inherited, progressive, disabling, neuromuscular disease that leads to decreased life expectancy and has no approved therapies. The disease is caused by a trinucleotide repeat expansion in *DMPK*, which encodes myotonic dystrophy type 1 protein kinase and imparts a toxic gain of function to the transcribed messenger RNA (mRNA), resulting in dysregulated alternative splicing (missplicing). Delpacibart etedesiran (del-desiran [AOC 1001]) is a monoclonal antibody–oligonucleotide conjugate. The antibody component targets transferrin receptor 1, and the oligonucleotide component targets *DMPK* mRNA.

In this phase 1–2, multicenter, double-blind, randomized, placebo-controlled trial, we assigned participants with myotonic dystrophy type 1 to receive del-desiran intravenously in a single dose (1 mg per kilogram of body weight) or three doses (2 mg or 4 mg per kilogram) or placebo. The primary end point was safety, and secondary end points were the pharmacokinetic and pharmacodynamic profiles of del-desiran and changes in downstream aberrant splicing patterns at 43 days in the 1-mg group and at 92 days (49 days after the second dose) in the 2-mg and 4-mg groups.

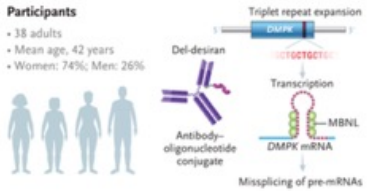

Muscleblind-like protein

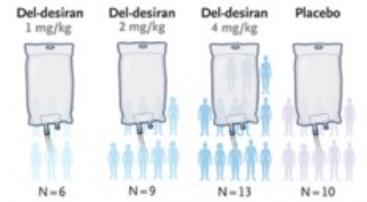

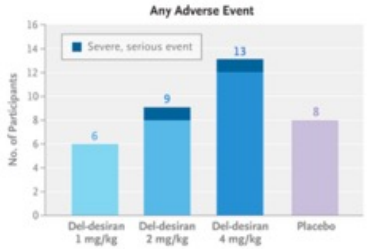

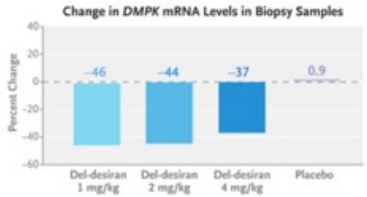

Myotonic dystrophy type 1 is a rare, autosomal-dominant, progressive disorder that affects multiple organ systems, primarily skeletal and smooth muscle and the cardiac conduction system, resulting in decreased life expectancy. Adult-onset myotonic dystrophy type 1 is characterized by myotonia and progressive muscle weakness leading to deficits in hand function, impaired mobility, respiratory insufficiency, dysarthria, dysphagia, and gastrointestinal motility disorders. Currently there are no disease-modifying therapies for myotonic dystrophy type 1.

The disorder is caused by a CTG expansion in the 3′-untranslated region of the myotonic dystrophy type 1 protein kinase gene (*DMPK*) that results in a toxic gain-of-function transcript through the formation of hairpin–loop structures. These sequester RNA-regulating proteins, including muscleblind-like proteins, and result in global splicing defects that lead to diverse disease manifestations. Several therapeutic approaches have aimed at reducing levels of toxic *DMPK* messenger RNA (mRNA), including antisense oligonucleotides and gene therapy; however, effective delivery of these agents to muscle has remained a challenge.

Delpacibart etedesiran (del-desiran [AOC 1001]) is an antibody–oligonucleotide conjugate developed to treat the underlying cause of myotonic dystrophy type 1 by delivering a small interfering RNA (siRNA) that induces degradation of *DMPK* mRNA through the endogenous RNA-induced silencing complex, thereby reducing the sequestration of muscleblind-like proteins and other splicing factors.

Because siRNAs are approximately 12 kDa and water soluble, siRNA uptake by extrahepatic cells has been problematic. Del-desiran delivers siRNA to muscle through conjugation of the siRNA to a monoclonal antibody targeting transferrin receptor 1 (TfR1), which allows for TfR1-mediated internalization of the antibody–oligonucleotide conjugate. In mice and monkey models, antibody–oligonucleotide conjugates were shown to deliver oligonucleotides to skeletal and cardiac (striated) muscle tissue at concentrations that were 15 times as high as concentrations of oligonucleotides delivered by unconjugated siRNA. The MARINA trial was a phase 1–2 clinical trial involving adults with myotonic dystrophy type 1 that was designed to evaluate single and multiple doses of del-desiran for safety, delivery to muscle, and activity.

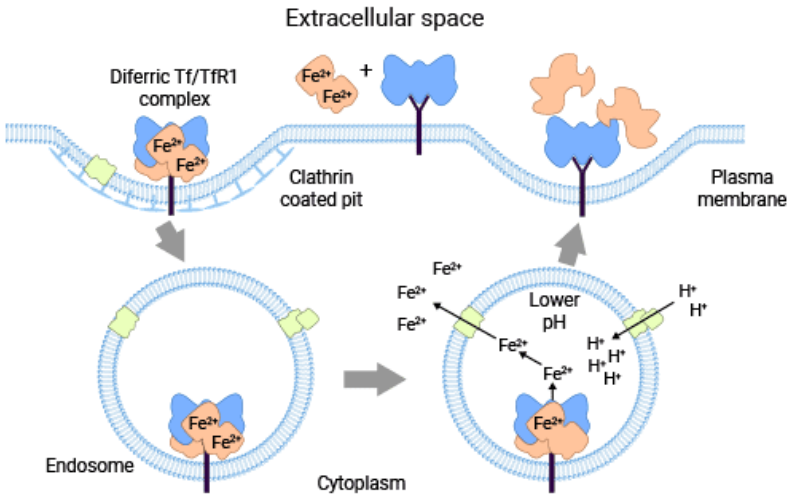

Methods

Trial Design and Treatments

MARINA was a multicenter, 6-month, two-part, double-blind, randomized, placebo-controlled trial. In Part A, participants received del-desiran in a single infusion at a dose of 1 mg per kilogram of body weight or placebo (saline). Part B had a nested single-dose and multiple-ascending-dose design; participants received three infusions of del-desiran at a dose of 2 mg or 4 mg per kilogram or placebo at approximately 6-week intervals. Both parts included a 3-month follow-up period.

The siRNA component of del-desiran was designed to hybridize with the 3′ untranslated region of the *DMPK* mRNA transcript upstream from the CUG expansion. The nucleotides that comprise the siRNA are modified to enhance its metabolic stability. The linker connecting the siRNA moiety to the antibody targeting TfR1 is conjugated to the 5′ terminus of the siRNA passenger strand.

Participant Selection

Participants were recruited from eight centers in the United States.

Objectives and End Points

The primary objective of the trial was to evaluate the safety and side-effect profile of single and multiple doses of del-desiran.

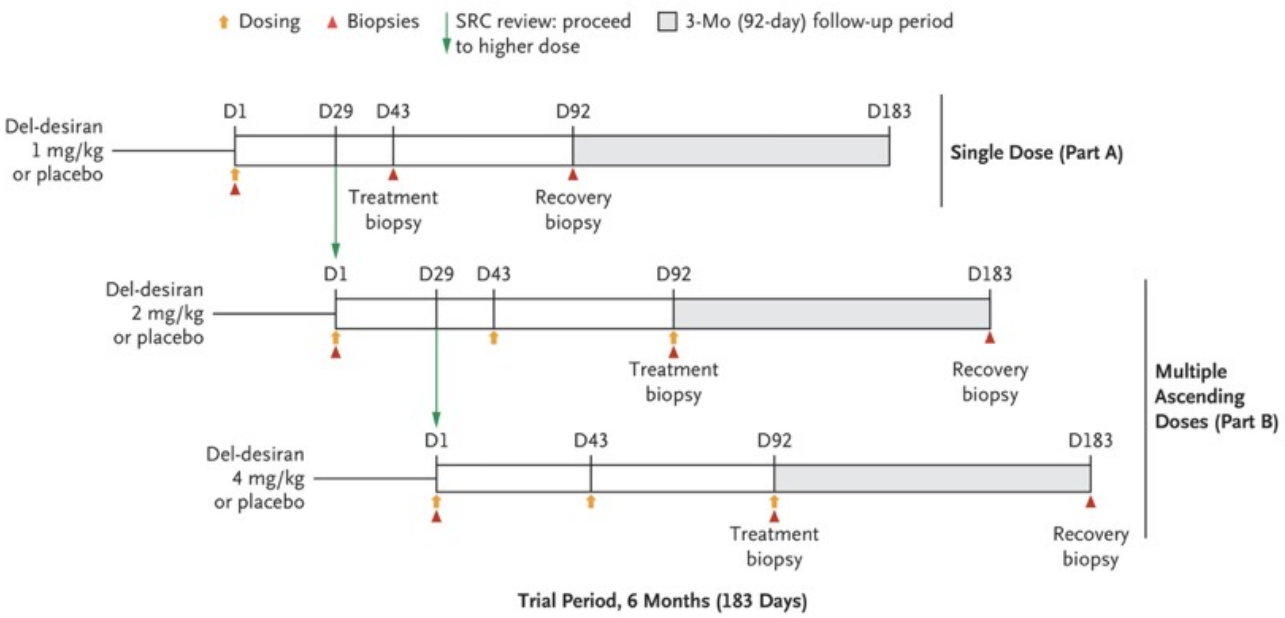

Trial Timeline.

Shown is the timeline for randomization and for the treatment and follow-up periods. Randomization to del-desiran or placebo was performed in a 3:1 ratio within each trial part. For Part A, day 43 corresponded to 6 weeks after the single dose and day 92 corresponded to 13 weeks after the single dose. For Part B, day 92 corresponded to 7 weeks after the second dose and day 183 corresponded to 13 weeks after the third of three doses. D denotes day, and SRC safety review committee.

Demographic and Clinical Characteristics of the Participants at Baseline.

Characteristic	Part A		Part B			Total (N=38)
	Placebo (N=2)	Del-desiran, 1 mg/kg (N=6)	Placebo (N=8)†	Del-desiran, 2 mg/kg (N=9)	Del-desiran, 4 mg/kg (N=13)	
Age — yr	40.5±9.2	37.0±18.0	48.0±8.5	37.6±13.6	44.0±12.4	42.0±12.9
Female sex — no. (%)	1 (50)	5 (83)	4 (50)	9 (100)	9 (69)	28 (74)
DMPK CTG repeat length — no. (%)						
≥100 to <500	0	3 (50)	4 (50)	1 (11)	6 (46)	14 (37)
≥500 to <1000	2 (100)	3 (50)	2 (25)	7 (78)	7 (54)	21 (55)
≥1000	0	0	2 (25)	1 (11)	0	3 (8)
Muscular Impairment Rating Scale score — no. (%)‡						
1	0	0	0	0	0	0
2	0	3 (50)	0	0	0	3 (8)
3	1 (50)	0	3 (38)	1 (11)	3 (23)	8 (21)
4	1 (50)	3 (50)	5 (62)	7 (78)	8 (62)	24 (63)
5	0	0	0	1 (11)	2 (15)	3 (8)
10-m walk–run test — sec	6.92±0.24	5.23±3.19	6.76±3.19	6.69±3.09	7.67±3.09	6.82±3.02
Video-assessed hand-opening time — sec§	5.11±3.60	6.81±5.34	11.34±20.80	8.04±6.36	10.20±8.41	9.13±11.01
DM1-Activ^{c} score¶	71.5±23.3	73.0±15.3	77.6±15.3	55.6±9.9	64.1±18.1	67.0±16.9
Composite QMT — % of predicted normal‖	41.1±7.6	56.3±13.3	54.1±17.2	50.1±12.0	41.6±19.3	48.5±16.4

Adverse events

Event	Part A		Part B		
	Placebo (N=2)	Del-desiran, 1 mg/kg (N=6)	Placebo (N=8)*	Del-desiran, 2 mg/kg (N=9)	Del-desiran, 4 mg/kg (N=13)
	number of participants (percent)				
Any adverse event	1 (50)	6 (100)	7 (88)	9 (100)	13 (100)
Related to trial regimen	0	1 (17)	2 (25)	3 (33)	10 (77)
Related to trial procedure	1 (50)	0	1 (12)	6 (67)	6 (46)
Any severe adverse event	0	0	0	1 (11)	1 (8)†
Related to trial regimen	0	0	0	0	1 (8)
Related to trial procedure	0	0	0	0	0
Any serious adverse event	0	0	0	1 (11)	1 (8)
Related to trial regimen	0	0	0	0	1 (8)
Related to trial procedure	0	0	0	0	0
Adverse event leading to discontinuation	0	0	0	0	1 (8)
Adverse event with fatal outcome	0	0	0	0	0

Treatment was stopped in one patient. The severe, serious adverse event in the participant in the 4-mg group was deemed to be related to del-desiran; it was reported as symptoms of memory loss and visual impairment during the 24-hour post-treatment observation period after the first infusion of 4 mg per kilogram of del-desiran.

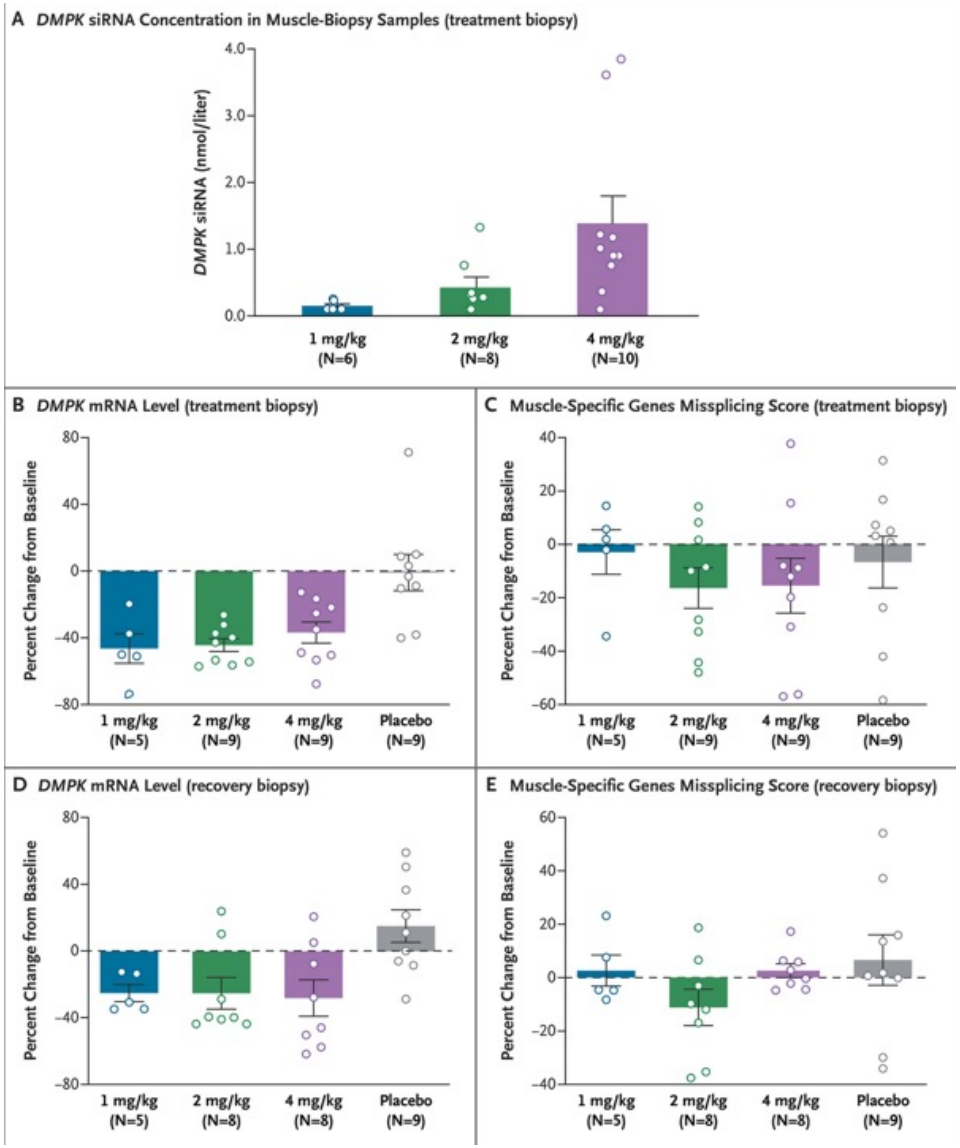

Pharmacokinetic and Pharmacodynamic Characterization of Del-desiran in Tibialis Anterior Muscle–Biopsy Samples (Secondary End Point).

Panel A shows the mean concentrations (in nanomoles per liter) of *DMPK* small interfering RNA (siRNA) in muscle at the treatment biopsy (obtained at 6 to 7 weeks). Panel B shows the change from baseline in the mean expression of *DMPK* messenger RNA (mRNA) in muscle at the treatment biopsy. Panel C shows change in the mean composite missplicing score of four muscle-specific genes (*ATP2A1*, *BIN1*, *CACNA1S*, and *CLCN1*) at the treatment biopsy. The number of patients in each group may be smaller than the full group because of biopsy samples that could not be evaluated. Data from the full 22-gene panel are presented in Figure S2. Panel D shows change in the mean expression of *DMPK* mRNA in muscle at the recovery biopsy (obtained at 13 weeks). Panel E shows the change in the mean composite missplicing score of the same four muscle-specific genes at the recovery biopsy. Sample sizes may be smaller than the group size because of biopsy samples that could not be evaluated. I bars indicate standard errors. The widths of the confidence intervals have not been adjusted for multiplicity, and the confidence intervals should not be used in place of hypothesis testing. In Part B, data from the placebo groups were pooled. Table S7 in the Supplementary Appendix shows the data that were used to calculate the baseline levels for all panels.

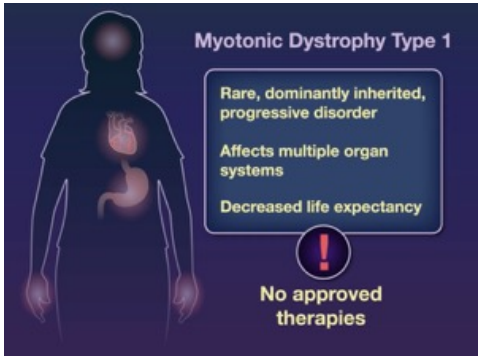
Myotonic Dystrophy Type 1
Rare, dominantly inherited, progressive disorder
Affects multiple organ systems
Decreased life expectancy
No approved therapies

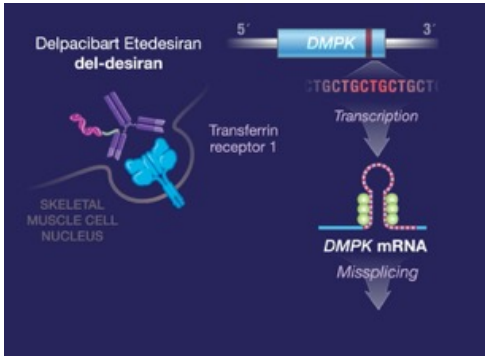
Delpacibart Etedesiran
del-desiran
5′
DMPK
3′
CTGCTGCTGCTGCT
Transcription
Transferrin receptor 1
SKELETAL MUSCLE CELL NUCLEUS
DMPK mRNA
Missplicing

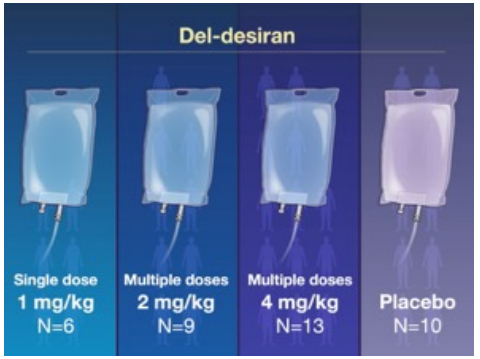
Del-desiran
Single dose 1 mg/kg N=6
Multiple doses 2 mg/kg N=9
Multiple doses 4 mg/kg N=13
Placebo N=10

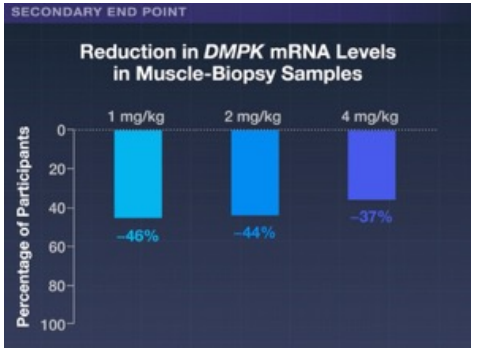
SECONDARY END POINT
Reduction in DMPK mRNA Levels in Muscle-Biopsy Samples
1 mg/kg
2 mg/kg
4 mg/kg
Percentage of Participants
0
20
40
60
80
100
−46%
−44%
−37%

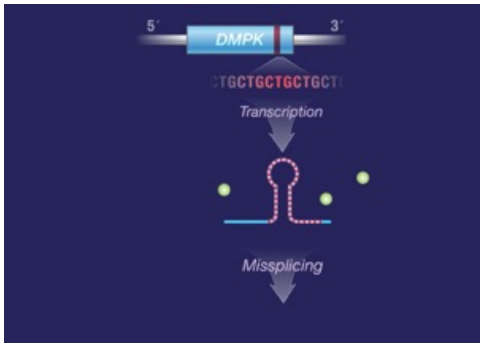
5′
DMPK
3′
CTGCTGCTGCTGCT
Transcription
Missplicing

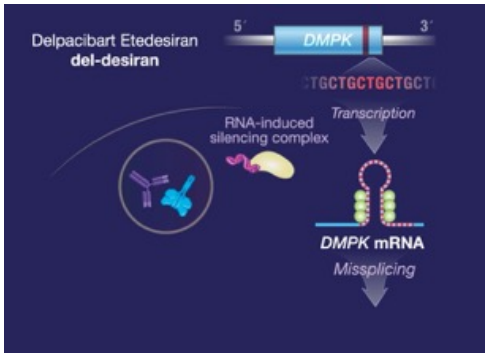
Delpacibart Etedesiran
del-desiran
5′
DMPK
3′
CTGCTGCTGCTGCT
Transcription
RNA-induced silencing complex
DMPK mRNA
Missplicing

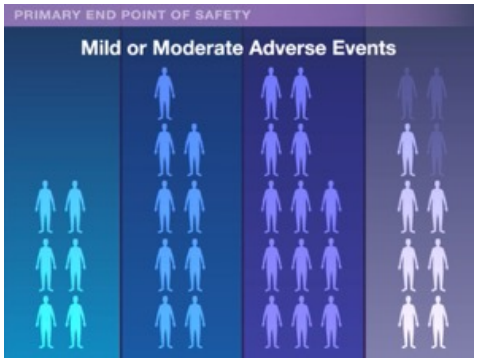
PRIMARY END POINT OF SAFETY
Mild or Moderate Adverse Events

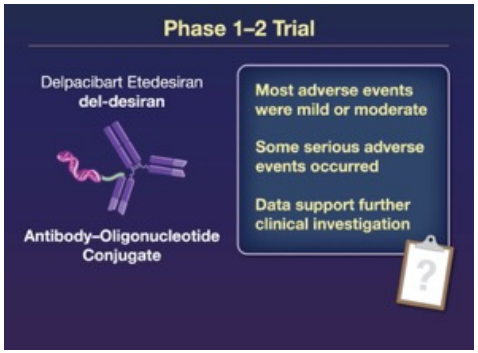
Phase 1–2 Trial
Delpacibart Etedesiran
del-desiran
Antibody–Oligonucleotide Conjugate
Most adverse events were mild or moderate
Some serious adverse events occurred
Data support further clinical investigation
?

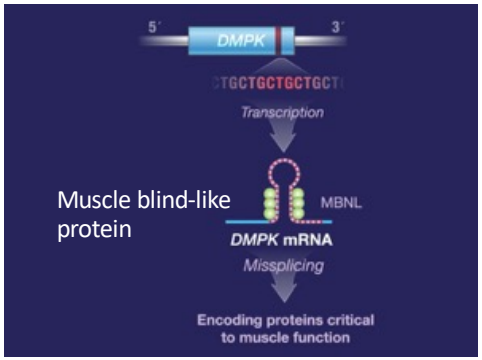
5′
DMPK
3′
CTGCTGCTGCTGCT
Transcription
Muscle blind-like protein
MBNL
DMPK mRNA
Missplicing
Encoding proteins critical to muscle function

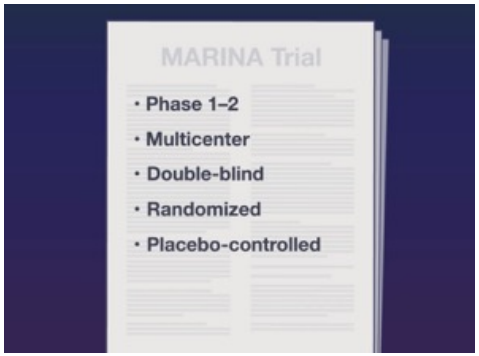
MARINA Trial
• Phase 1–2
• Multicenter
• Double-blind
• Randomized
• Placebo-controlled

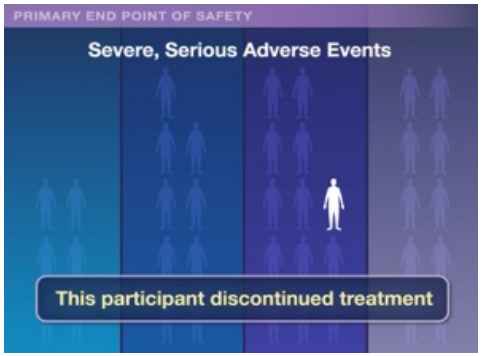
PRIMARY END POINT OF SAFETY
Severe, Serious Adverse Events
This participant discontinued treatment

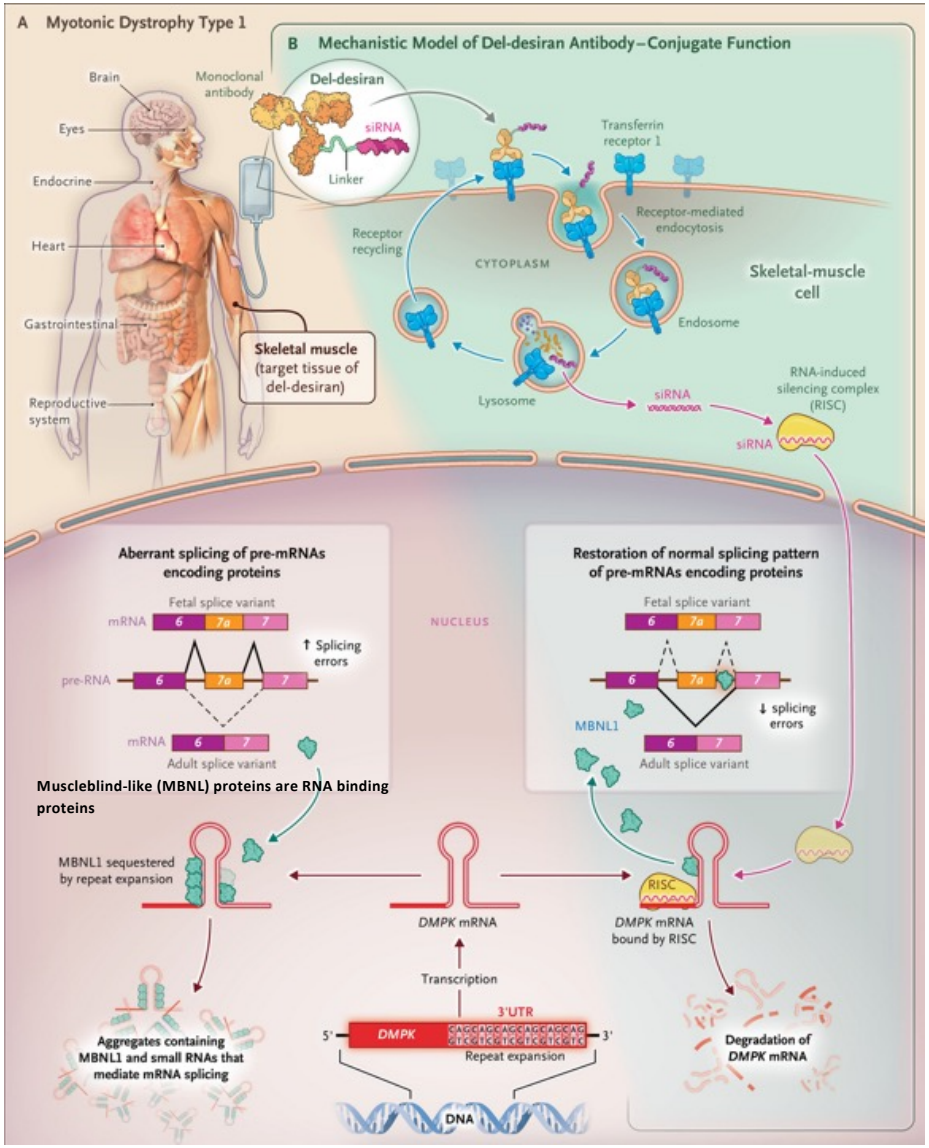

An Antibody–Oligonucleotide Conjugate for Myotonic Dystrophy Type 1.

Myotonic dystrophy type 1 is a multisystemic disease that affects multiple organ systems (left side of human figure) as well as skeletal muscle (highlighted on right side of human figure) (Panel A). Delpacibart etedesiran (del-desiran [AOC1001]) is a conjugate of a monoclonal antibody that binds the transferrin receptor 1 (which is highly expressed in skeletal muscle) and a small interfering RNA (siRNA) targeting *DMPK* messenger RNA (mRNA) (Panel B). In a phase 1 trial, Johnson et al. delivered del-desiran intravenously to patients with myotonic dystrophy type 1. After receptor-mediated endocytosis, the siRNA component of del-desiran is released and incorporated into the RNA-induced silencing complex (RISC). RISC guides the siRNA to its complementary sequence in *DMPK* mRNA, which promotes the cleavage and degradation of the *DMPK* mRNA. Although RISC-mediated *DMPK* mRNA degradation is illustrated here in the nucleus where mutant *DMPK* mRNA is trapped into hallmark nuclear foci, the precise location is unclear because RISC-mediated mRNA degradation typically occurs primarily in the cytoplasm. Johnson et al. reported a reduction in *DMPK* mRNA levels and correction of downstream splicing defects in the muscle tissue of trial participants.

Implications for Myotonic Dystrophy and Beyond

Johnson et al. have shown siRNA uptake by skeletal muscle, dose-dependent reductions in *DMPK* mRNA, and the amelioration of missplicing of myotonic dystrophy–relevant mRNA transcripts. These findings validate the concept that reducing toxic RNA can restore splicing regulation. Findings for exploratory functional end points are consistent with improvements in hand-opening time and quantitative muscle strength. However, the occurrence of a bilateral thalamic brain hemorrhage in one of the participants represents a safety signal and underscores the importance of careful safety monitoring in future trials.

Although the RNA gain-of-function mechanism in myotonic dystrophy type 1 has been well studied, other mechanisms mediated by the *DMPK* CTG repeat expansion have been reported. These include bidirectional transcription and repeat-associated non-AUG translation: it would be important to understand how they are affected by del-desiran. In addition, there are substantial neurologic and multisystemic components to myotonic dystrophy type 1 that will not be addressed by targeting skeletal muscle. Adapting the antibody–oligonucleotide approach to target the central nervous system and other tissues would be a major endeavor and require preclinical assessments of safety, neurotoxicity, and strategies for penetrating the blood–brain barrier.

The antibody-targeted delivery of siRNAs described by Johnson et al. shows strong potential to address the skeletal-muscle spliceopathy of myotonic dystrophy type 1. More generally, the trial represents an advance in the field of pathogenic repeat expansions and neuromuscular disorders.

Der transkatheter Aortenklappenersatz (TAVR oder TAVI) ist ein minimalinvasives Verfahren zur Behandlung einer verengten Aortenklappe (Aortenstenose), bei dem eine neue Klappe via Katheter – meist über die Leiste – eingeführt wird, ohne den Brustkorb zu öffnen. Es eignet sich für Patienten mit hohem, mittlerem oder geringem Operationsrisiko, ermöglicht eine schnelle Genesung und wird oft als Alternative zur offenen Herzoperation (SAVR) eingesetzt.

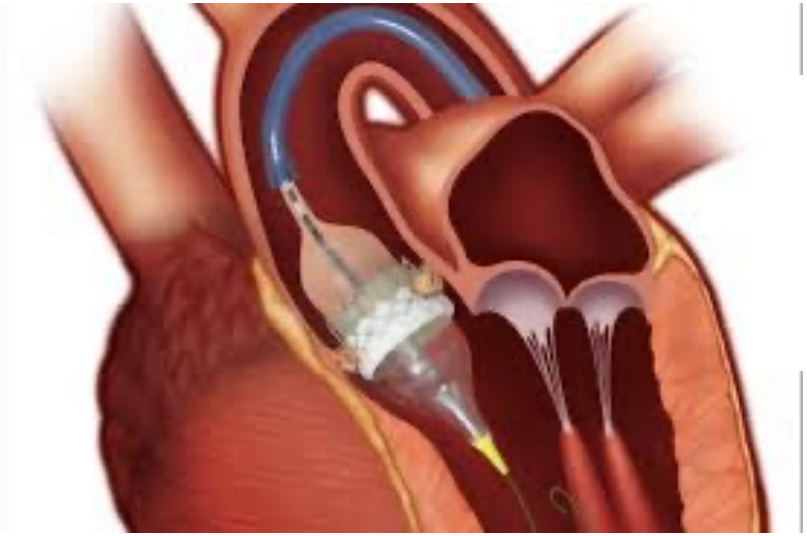

Sapiens valve

Transcatheter or Surgical Aortic-Valve Replacement in Low-Risk Patients at 7 Years

Five-year data from the PARTNER 3 trial showed that among low-risk patients with severe, symptomatic aortic stenosis, outcomes were similar among patients who had undergone transcatheter aortic-valve replacement (TAVR) and those who had undergone surgical aortic-valve replacement. Longer-term assessments of clinical outcomes and valve durability are needed.

Patients were randomly assigned in a 1:1 ratio to undergo transfemoral TAVR or surgery. The first primary end point was a nonhierarchical composite of death, stroke, or rehospitalization related to the procedure, the valve, or heart failure. The second primary end point was a hierarchical composite of death, disabling stroke, nondisabling stroke, and the number of rehospitalization days related to the procedure, the valve, or heart failure, analyzed with the use of a win ratio analysis.

Clinical, echocardiographic, valve-durability, and health-status end points were assessed through 7 years.

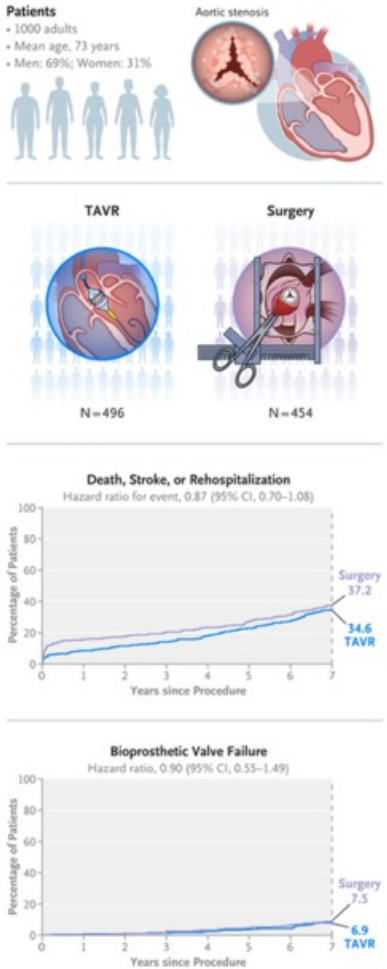

Transcatheter aortic-valve replacement (TAVR) has been increasingly used as an alternative to surgery for treating patients with severe, symptomatic aortic stenosis. Randomized trials have shown that in patients at low, intermediate, or high surgical risk, TAVR was superior or similar to surgical aortic-valve replacement through 5 years of follow-up. As reported previously, the Placement of Aortic Transcatheter Valves (PARTNER) 3 trial showed that the incidence of death, stroke, or rehospitalization (the primary composite end point) at 1, 2, and 5 years after TAVR was lower than or was not different from that with surgery in younger, low-risk patients. Late bioprosthesis failure after aortic-valve implantation remains an important consideration in lifelong patient-care decisions. Here, we describe the 7-year clinical and echocardiographic results of the PARTNER 3 trial.

Patients

Patients were eligible for inclusion if they had symptomatic, severe aortic stenosis and were considered to have low surgical risk on the basis of an evaluation by the heart team, including a score of less than 4% on the Society of Thoracic Surgeons Predicted Risk of Mortality (STS-PROM; scores range from 0 to 100%, with higher scores indicating a greater risk of death within 30 days after the procedure).

Key Clinical End Points

End Point	Baseline to 1 Yr			1 Yr to 7 Yr			Baseline to 7 Yr		
	TAVR (N=496)	Surgery (N=454)	Hazard Ratio (95% CI)	TAVR (N=490)	Surgery (N=441)	Hazard Ratio (95% CI)	TAVR (N=496)	Surgery (N=454)	Hazard Ratio (95% CI)
	no. of patients with event (Kaplan–Meier %)			*no. of patients with event (Kaplan–Meier %)*			*no. of patients with event (Kaplan–Meier %)*		
Death, stroke, or rehospitalization related to procedure, valve, or heart failure†	42 (8.5)	71 (15.8)	0.51 (0.35–0.75)	123 (28.5)	85 (25.4)	1.15 (0.87–1.52)	165 (34.6)	156 (37.2)	0.87 (0.70–1.08)‡
Death from any cause with data from vital-status sweep	5 (1.0)	11 (2.4)	0.41 (0.14–1.19)	89 (18.7)	62 (14.7)	1.31 (0.94–1.81)	94 (19.5)	73 (16.8)	1.17 (0.86–1.59)§
Death from any cause without data from vital-status sweep	5 (1.0)	11 (2.5)	0.41 (0.14–1.17)	86 (18.6)	49 (12.8)	1.52 (1.07–2.16)	91 (19.4)	60 (14.9)	1.32 (0.95–1.83)§
Death from cardiovascular causes	4 (0.8)	9 (2.0)	0.40 (0.12–1.30)	42 (9.5)	22 (5.9)	1.65 (0.99–2.77)	46 (10.3)	31 (7.8)	1.29 (0.82–2.04)§
Death from noncardiovascular causes¶	1 (0.2)	2 (0.5)	0.44 (0.04–4.87)	44 (10.0)	27 (7.3)	1.41(0.88–2.28)	45 (10.2)	29 (7.7)	1.35 (0.85–2.15)§
Stroke	6 (1.2)	15 (3.3)	0.36 (0.14–0.92)	32 (7.3)	18 (5.0)	1.52 (0.85–2.70)	38 (8.5)	33 (8.1)	1.00 (0.62–1.59)
Disabling	1 (0.2)	5 (1.1)	0.18 (0.02–1.54)	21 (4.9)	9 (2.5)	2.02 (0.93–4.42)	22 (5.1)	14 (3.6)	1.37 (0.70–2.68)
Nondisabling	5 (1.0)	10 (2.2)	0.45 (0.15–1.32)	12 (2.7)	9 (2.4)	1.13 (0.48–2.68)	17 (3.7)	19 (4.6)	0.78 (0.40–1.50)
Death or disabling stroke†	5 (1.0)	14 (3.1)	0.32 (0.11–0.89)	97 (20.9)	54 (14.1)	1.56 (1.12–2.18)	102 (21.7)	68 (16.8)	1.31 (0.96–1.78)§
Rehospitalization related to procedure, valve, or heart failure	36 (7.3)	51 (11.5)	0.62 (0.41–0.95)	57 (14.4)	44 (13.5)	1.05 (0.71–1.56)	93 (20.6)	95 (23.5)	0.82 (0.62–1.10)
Aortic-valve reintervention¶	4 (0.8)	2 (0.5)	1.78 (0.33–9.71)	24 (5.9)	20 (5.5)	1.04 (0.58–1.89)	28 (6.7)	22 (6.0)	1.11 (0.63–1.94)
Endocarditis	1 (0.2)	2 (0.5)	0.44 (0.04–4.88)	11 (2.7)	9 (2.4)	1.05 (0.44–2.54)	12 (2.9)	11 (2.8)	0.94 (0.42–2.14)
Clinically significant valve thrombosis‖	2 (0.4)	0 (0.0)	NA	11 (2.4)	2 (0.5)	4.80 (1.06–21.64)	13 (2.8)	2 (0.5)	5.70 (1.29–25.25)
New left bundle-branch block¶	99 (20.0)	35 (7.7)	2.68 (1.83–3.95)	5 (1.4)	9 (2.4)	0.55 (0.18–1.64)	104 (21.1)	44 (9.9)	2.25 (1.58–3.20)
New onset atrial fibrillation¶	34 (8.2)	150 (40.9)	0.17 (0.12–0.24)	35 (10.4)	8 (4.3)	2.42 (1.12–5.21)	69 (17.7)	158 (43.5)	0.30 (0.23–0.41)
New permanent pacemaker¶	38 (7.9)	25 (5.8)	1.41 (0.85–2.33)	40 (10.3)	26 (7.4)	1.36 (0.83–2.23)	78 (17.3)	51 (12.8)	1.38 (0.97–1.97)
Serious bleeding¶**	24 (4.8)	46 (10.2)	0.45 (0.28–0.74)	47 (11.3)	31 (9.2)	1.27 (0.81–2.00)	71 (15.6)	77 (18.5)	0.79 (0.57–1.09)
Myocardial infarction¶	4 (0.8)	8 (1.8)	0.45 (0.14–1.49)	21 (5.2)	14 (3.8)	1.29 (0.65–2.53)	25 (6.0)	22 (5.6)	0.99 (0.56–1.75)
Revascularization¶	5 (1.0)	13 (2.9)	0.34 (0.12–0.96)	26 (6.4)	18 (5.0)	1.23 (0.68–2.25)	31 (7.3)	31 (7.7)	0.86 (0.53–1.42)
Percutaneous coronary intervention	5 (1.0)	8 (1.8)	0.56 (0.18–1.71)	23 (5.6)	18 (4.9)	1.10 (0.59–2.04)	28 (6.6)	26 (6.6)	0.94 (0.55–1.60)
Coronary-artery bypass grafting	1 (0.2)	5 (1.1)	0.18 (0.02–1.55)	3 (0.8)	1 (0.3)	2.60 (0.27–24.97)	4 (1.0)	6 (1.4)	0.59 (0.17–2.10)

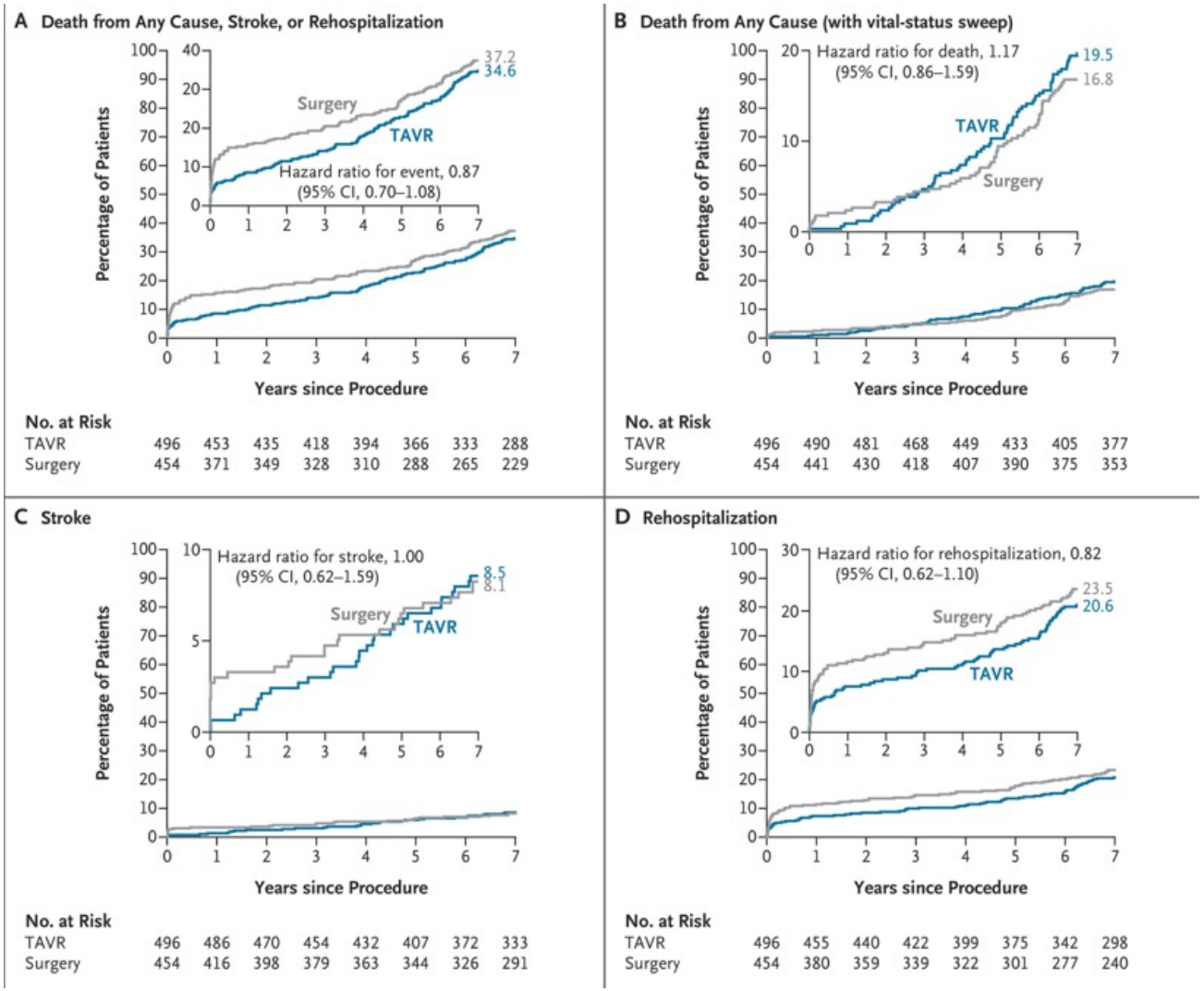

Kaplan–Meier Curves for the First Primary End Point and Its Components.

Panel A shows the Kaplan–Meier estimates for death from any cause, stroke, or rehospitalization related to the procedure, the valve, or heart failure (the first composite primary end point); these data do not include those obtained from the vital-status sweep. Panels B, C, and D show the estimates for the components of the end point. In accordance with the statistical analysis plan, the prespecified analysis of the composite primary end point involved the difference in the Kaplan–Meier estimates between transcatheter aortic-valve replacement (TAVR) and surgery, calculated with the Wald test (difference, −2.61%; 95% CI, −8.95% to 3.74%). To provide the most complete follow-up available, the analysis of death alone includes data obtained from the vital-status sweep. Additional details can be found in Table S3 in the Supplementary Appendix. Because some evidence was observed of nonproportionality of hazards over time for the component of death, the odds ratio was also assessed and was 1.20 (95% CI, 0.86 to 1.67). The inset in each panel shows the same data on an enlarged y axis. All analyses were performed in the as-treated population, which included the patients who underwent randomization and began to undergo the index procedure.

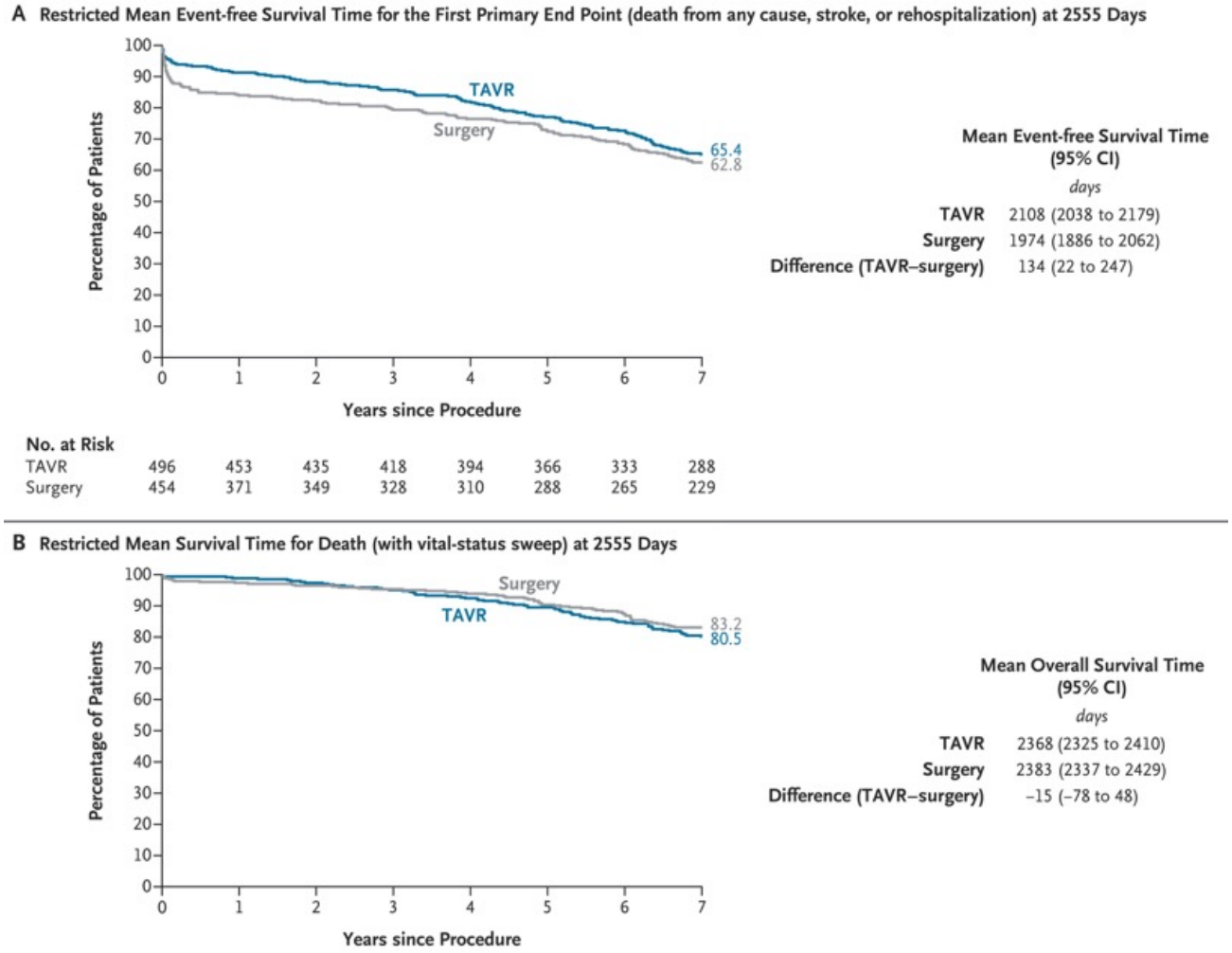

Restricted Mean Event-free Survival Time for the First Primary End Point and Death from Any Cause.

Panel A shows the restricted mean event-free survival time for the first primary end point, which is a composite of death from any cause, stroke, or rehospitalization related to the procedure, the valve, or heart failure; these data do not include those obtained from the vital-status sweep. Panel B shows the restricted mean survival time for death from any cause, including data obtained from the vital-status sweep. Additional details can be found in Table S3. In both analyses, event-free days are defined according to Gregson et al.[24] Additional details can be found in the Supplementary Appendix. All analyses were performed in the as-treated population.

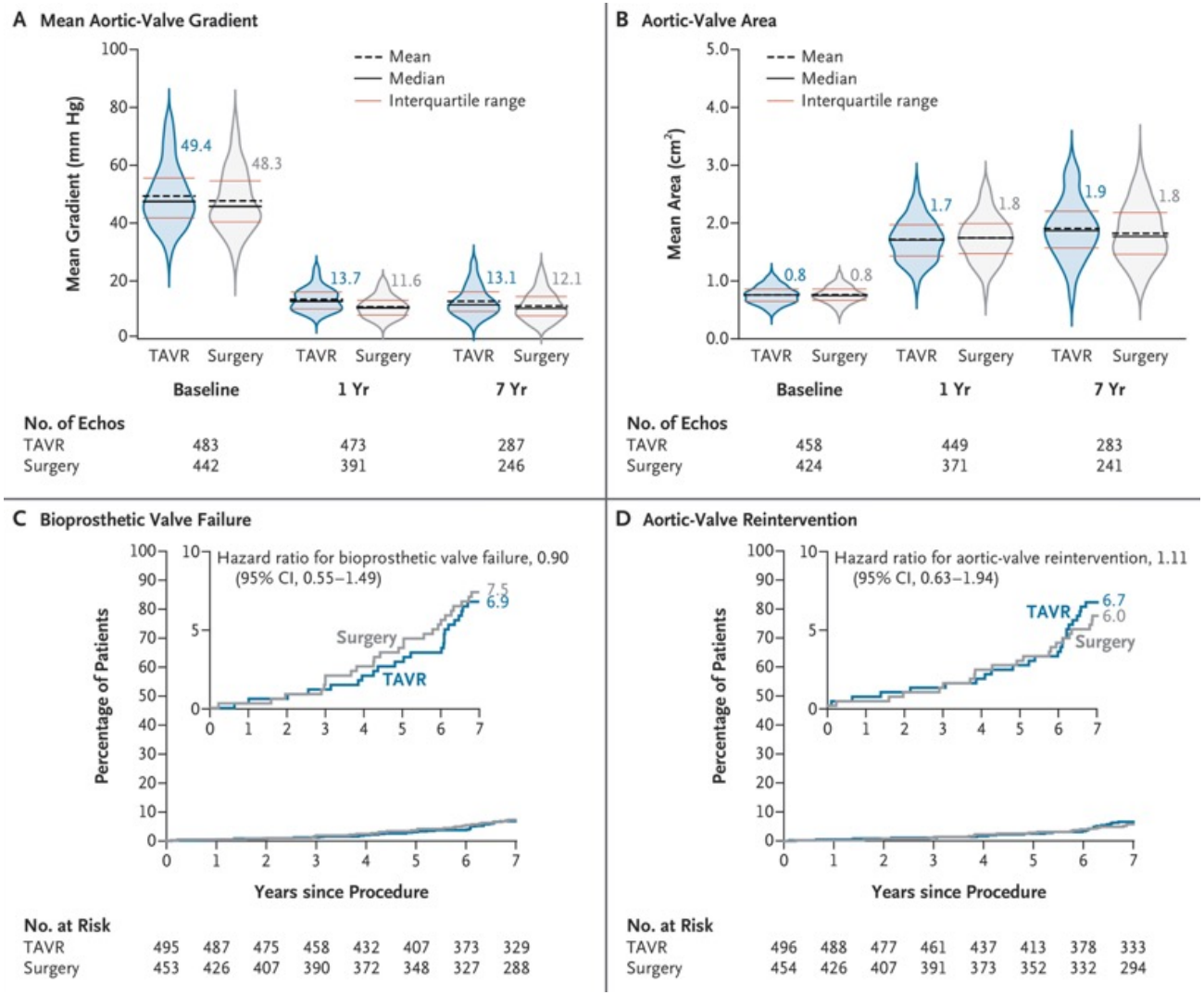

Valve Hemodynamics and Durability.

The mean aortic-valve gradients and mean aortic-valve areas as assessed by echocardiography at a core laboratory are shown in Panels A and B, respectively. Analyses were performed in the valve-implant population, which included the patients who received the intended valve. Data from patients who had their valve explanted or who received a valve-in-valve procedure were censored after reintervention. The cumulative incidence of bioprosthetic valve failure, adjudicated according to Valve Academic Research Consortium 3 criteria, is shown in Panel C; the hazard ratio for bioprosthetic valve failure was estimated with the Fine and Gray method, and the analysis was performed in the valve-implant population. Kaplan–Meier estimates for site-reported aortic-valve reintervention are shown in Panel D; the analysis was performed in the as-treated population. The insets in Panels C and D show the same data on an enlarged y axis.

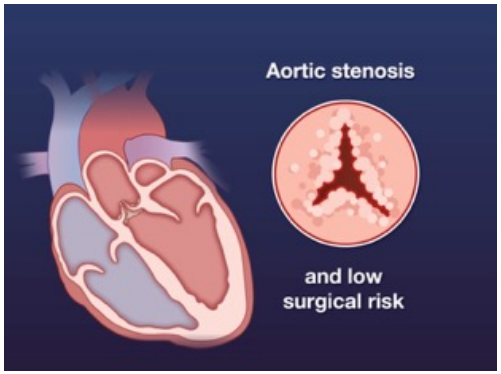
Aortic stenosis
and low
surgical risk

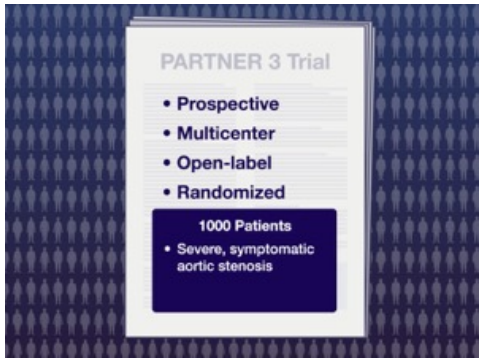
PARTNER 3 Trial
• Prospective
• Multicenter
• Open-label
• Randomized
1000 Patients
• Severe, symptomatic aortic stenosis

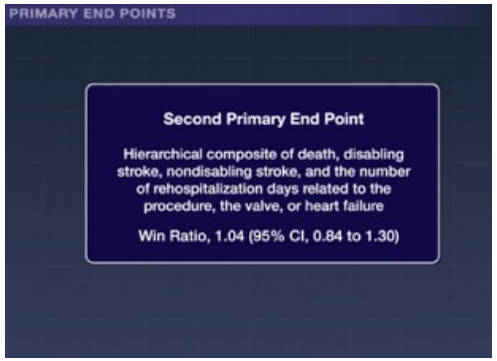
PRIMARY END POINTS
Second Primary End Point
Hierarchical composite of death, disabling stroke, nondisabling stroke, and the number of rehospitalization days related to the procedure, the valve, or heart failure
Win Ratio, 1.04 (95% CI, 0.84 to 1.30)


PARTNER 3 Trial
TAVR
≈
Surgical aortic-valve replacement
at 5 years
YEAR 5

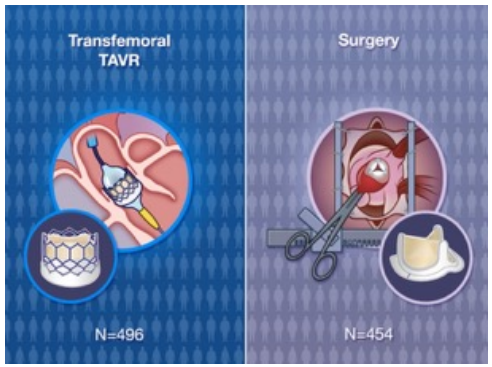
Transfemoral TAVR
Surgery
N=496
N=454

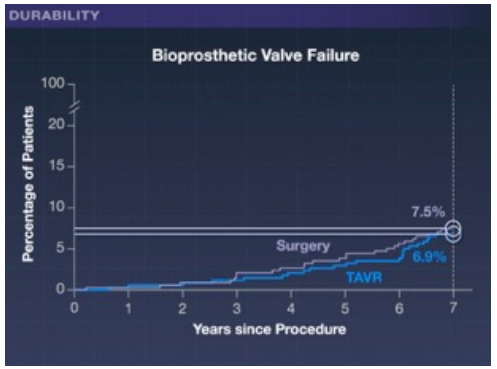
DURABILITY
Bioprosthetic Valve Failure
Percentage of Patients
100
20
15
10
5
0
7.5%
Surgery
6.9%
TAVR
0 1 2 3 4 5 6 7
Years since Procedure

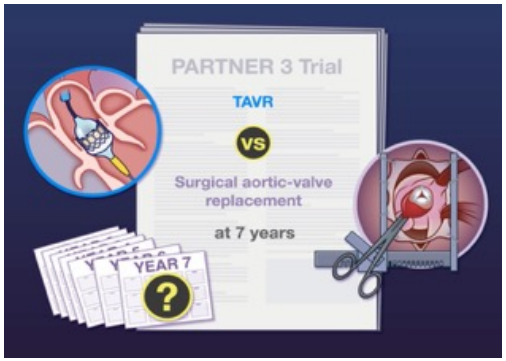
PARTNER 3 Trial
TAVR
VS
Surgical aortic-valve replacement
at 7 years
YEAR 7
?

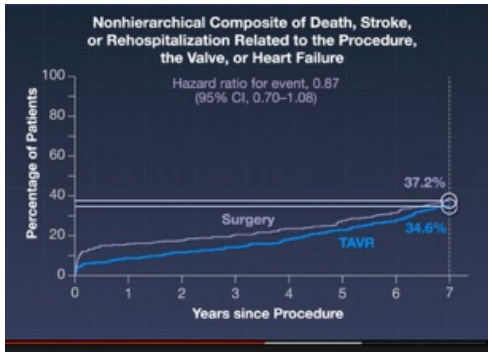
Nonhierarchical Composite of Death, Stroke, or Rehospitalization Related to the Procedure, the Valve, or Heart Failure
Hazard ratio for event, 0.87
(95% CI, 0.70–1.08)
Percentage of Patients
100
80
60
40
20
0
37.2%
Surgery
34.6%
TAVR
0 1 2 3 4 5 6 7
Years since Procedure

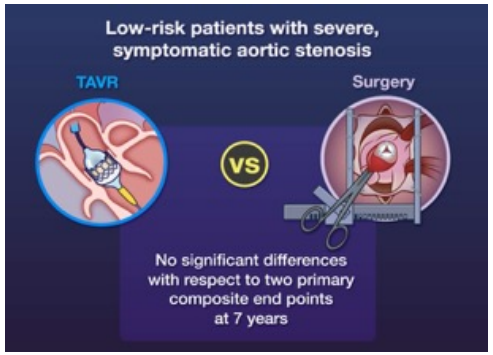
Low-risk patients with severe, symptomatic aortic stenosis
TAVR
Surgery
VS
No significant differences with respect to two primary composite end points at 7 years

Secondary Prevention after Ischemic Stroke

A 74-year-old man was transported to the emergency department by ambulance for sudden onset of weakness in the right side of his face and in his right arm and leg and slurred speech, which had begun 6 hours earlier. The National Institutes of Health Stroke Scale score was 4 (on a scale of 0 to 42, with higher scores indicating more severe neurologic impairment), and he had mild facial and upper and lower limb weakness and dysarthria on examination. A computed tomographic (CT) scan of the head was unremarkable, and a CT angiogram of the head and neck showed no stenosis or large-vessel occlusion. A magnetic resonance imaging (MRI) scan of the head later revealed a 1-cm infarct in the left posterior limb of the internal capsule, with hyperintensity on diffusion-weighted sequences. The patient has hypertension and hyperlipidemia treated with daily lisinopril (10 mg) and atorvastatin (10 mg), and his most recent glycated hemoglobin level was 6.5%. He is a nonsmoker, drinks alcohol occasionally, and maintains a healthy diet, but he has been less active in recent years because of joint pain. His body-mass index (the weight in kilograms divided by the square of the height in meters) is 32. How would you treat this patient to reduce his risk of another ischemic stroke?

KEY POINTS

Secondary Prevention after Ischemic Stroke

- After ischemic stroke, the risk of recurrence can be reduced by modifying risk factors related to the specific mechanism of stroke.
- Diagnostic studies help identify the mechanism of stroke and provide targets for intervention.
- Strategies for secondary prevention should be instituted as early as possible to improve adherence to therapy and prevent recurrence.
- Poststroke monitoring of risk metrics, lifestyle behaviors, and medication recommendations is of key importance.

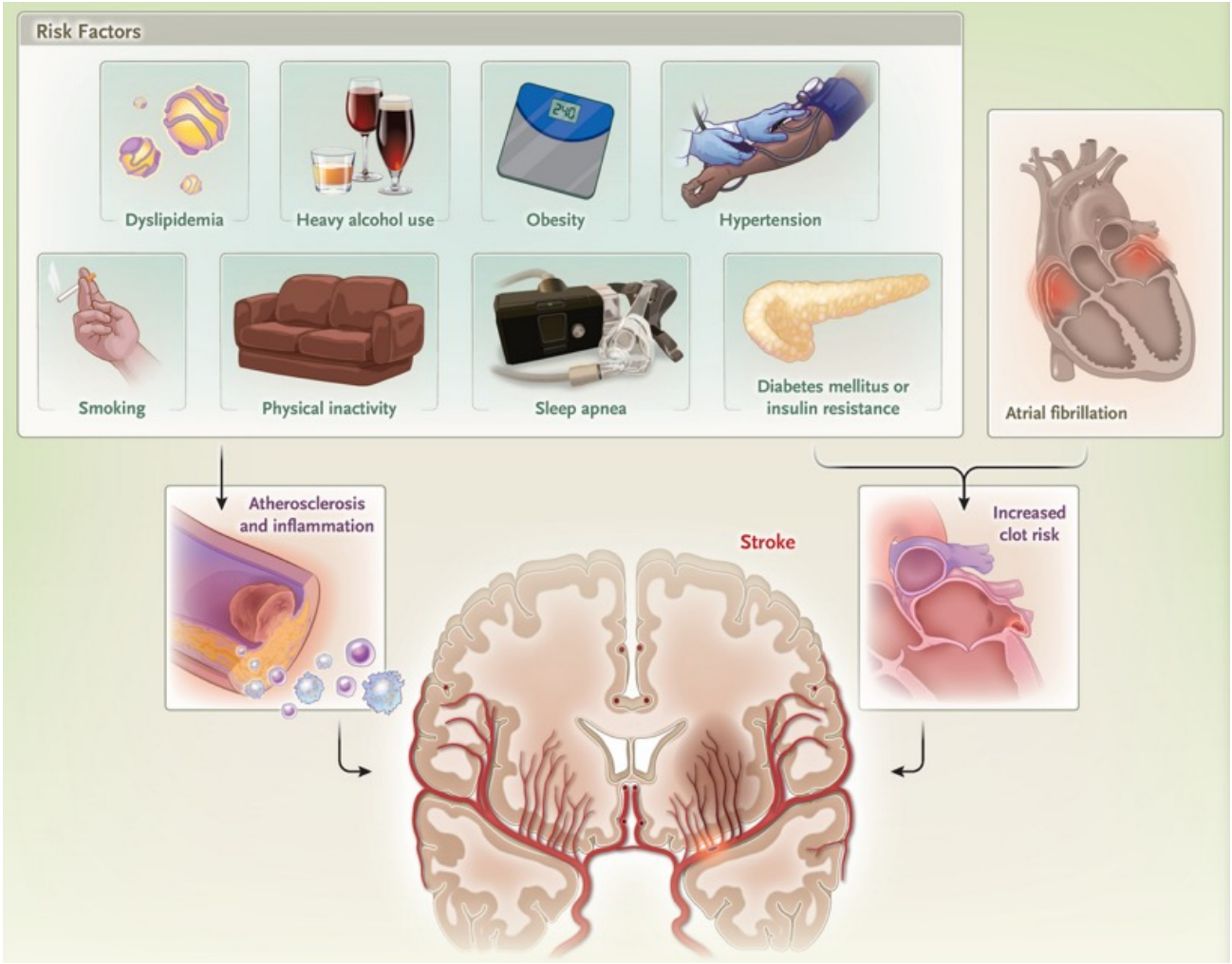

Pathophysiological Contributors to Stroke.

Interactions among vascular endothelium, flow dynamics, the inflammatory and coagulation systems, and structural cardiac disease contribute to stroke risk. Dyslipidemia, heavy alcohol use, obesity, hypertension, smoking, physical inactivity, sleep apnea, and diabetes mellitus or insulin resistance are all risk factors for stroke.

Mechanisms of Ischemic Stroke.

Large-artery atherosclerosis

Infarction in the territory of a stenotic (>50%) artery supplying the brain, attributed to atherosclerosis

- Extracranial
- Intracranial

Cardioembolism

Detection of a high- or medium-risk embolic source from the heart

- Atrial fibrillation
- Valvular disease (e.g., mechanical prosthetic valve or mitral stenosis)
- Left ventricular thrombus
- Cardiac myxoma
- Endocarditis (infectious or marantic)
- Patent foramen ovale or other intracardiac shunts

Small-vessel occlusion or lacunar stroke

Occlusion of a lenticulostriate, thalamogeniculate, basilar, or other perforator artery. Large-artery atherosclerosis and a cardioembolic source must be ruled out. CT scan or MRI may be normal, but a small (<1.5 cm) subcortical infarct supports the diagnosis.

Stroke of undetermined cause, including cryptogenic stroke or embolic stroke of undetermined source

No mechanism identified despite adequate investigation. Accounts for 30–40% of ischemic strokes. Potential causes include the following:

- Aortic-arch atheroma
- Atrial myopathy
- Nonstenosing atherosclerotic plaque

Other determined cause of stroke

Less common conditions that may cause stroke include the following:

- Dissection
- Hypercoagulable state
- Vasculitis
- Migraine
- Reversible cerebral vasoconstrictive syndrome
- Genetic disorders (e.g., CADASIL or CARASIL)
- Fabry's disease

Common Diagnostic Studies to Aid in Secondary Stroke Prevention.

Cardiovascular imaging

CT angiography, magnetic resonance angiography, or ultrasonography (carotid duplex ultrasonography and transcranial Doppler ultrasonography) to evaluate patency of the large arteries

High-resolution vascular-wall imaging, if indicated

Laboratory assessment

Total cholesterol, low-density and high-density lipoprotein cholesterol, and triglyceride levels; consider lipoprotein(a) level

Glycated hemoglobin

Glucose

Thrombophilia screen (in selected patients)

Imaging of the head

MRI

CT

Cardiac testing

12-Lead electrocardiogram

Telemetry

Prolonged ambulatory monitoring if embolism is suspected but the source is not identified

Transthoracic echocardiography

Transesophageal echocardiography or cardiac CT or MRI for suspected endocarditis, left atrial appendage thrombus, or aortic-arch atheroma

Conclusions and Recommendations

The patient described in the vignette has a lacunar ischemic stroke with multiple cardiovascular risk factors and evidence of insulin resistance. We would prescribe aspirin and clopidogrel for 21 days, followed by aspirin at a dose of 81 mg daily thereafter, and would intensify his blood-pressure treatment with indapamide to reach a blood pressure of less than 130/80 mm Hg. We would also favor increasing his lipid-lowering therapy to meet an LDL cholesterol goal of less than 70 mg per deciliter, initially with the dose of atorvastatin increased to 80 mg per day. We would counsel the patient on lifestyle management, including a structured weight-loss program. Ongoing monitoring of adherence to therapy and prevention goals is important.

Hb A1C below 5.7%,
I would add an
SGLT2 inhibitor

Peritoneal Coccidioidomycosis

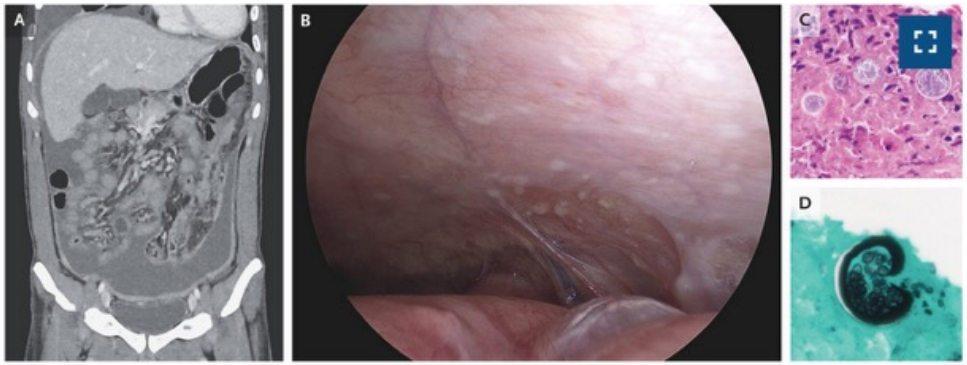

A previously healthy 23-year-old man presented to the emergency department with a 2-month history of unintentional weight loss and worsening abdominal pain and distention. The patient had recently moved to Arizona from a remote Pacific island. Physical examination was notable for a firm abdomen with diffuse tenderness to palpation. A computed tomographic scan of the chest, abdomen, and pelvis showed diffuse peritoneal thickening and nodularity with ascites (Panel A, coronal view), as well as mediastinal and hilar lymphadenopathy and a large pleural effusion on the right side. Diagnostic laparoscopy revealed peritoneal nodules and inflammatory adhesions throughout the abdomen (Panel B). Histopathological analysis of a peritoneal-biopsy specimen showed necrotizing granulomas with large, thick-walled spherules (Panel C, hematoxylin and eosin stain), some of which had ruptured and released endospores (Panel D, Grocott's methenamine silver stain). Fungal culture of peritoneal tissue grew coccidioides. A diagnosis of peritoneal coccidioidomycosis was made. Owing to concern for other sites of extrapulmonary infection in the context of an elevated coccidioides serum complement fixation titer of 1:512, a lumbar puncture was performed, which ruled out meningitis. Testing for human immunodeficiency virus infection was also negative. Treatment with a prolonged course of fluconazole was initiated. At 1-month follow-up after discharge, the patient's symptoms had resolved.

Majocchi's Granuloma

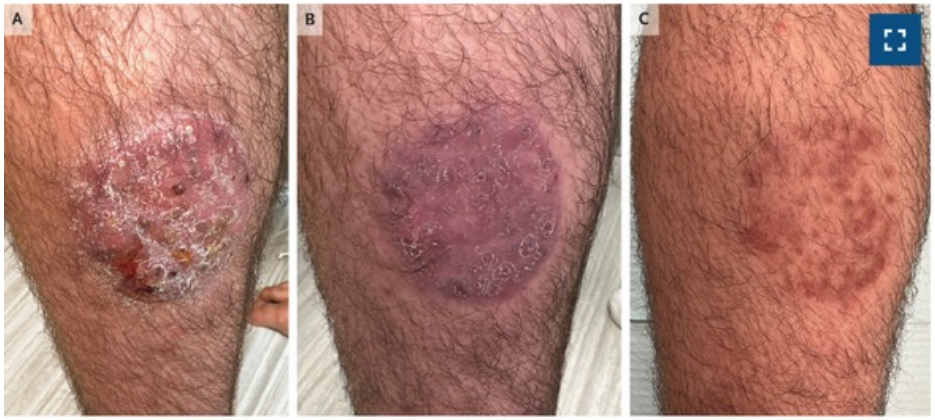

A previously healthy 17-year-old high-school wrestler presented to the dermatology clinic with a 6-week history of an itchy rash on his calf. One month earlier, a superficial shave biopsy of the lesion performed by another provider had shown fungal hyphae in the stratum corneum. A topical antifungal agent and high-potency topical glucocorticoid had been prescribed, but the lesion had subsequently worsened. On physical examination, a circular, red, scaly plaque 6 cm in diameter with papules, nodules, and pustules was seen on the posterior left calf (Panel A). Fungal culture of a skin scraping grew *Trichophyton tonsurans*. A diagnosis of Majocchi's granuloma was made. Majocchi's granuloma is a localized deep fungal infection of hair follicles that may occur in immunocompromised patients or when topical glucocorticoids are applied to superficial fungal infections. Unlike superficial dermatophyte infections, Majocchi's granuloma is treated with systemic medications. Although the diagnosis typically requires visualization of perifollicular granulomatous inflammation on histopathological examination, a probable diagnosis was made in this case on the basis of the clinical presentation, the presence of dermal nodules, and the preceding use of a potent topical glucocorticoid in the context of histologically proven superficial fungal infection. Oral terbinafine was prescribed, and the lesion abated (Panel B, after 1 month of treatment; Panel C, 6 months after completion of treatment).

Case 6-2026: A 91-Year-Old Man with Shortness of Breath, Weight Loss, and Eosinophilia

Presentation of Case

A 91-year-old man presented to the emergency department of this hospital because of worsening dyspnea on exertion, weight loss, and eosinophilia.

The patient had been in his usual state of health, with the ability to walk on level ground and ascend stairs and hills without limitations, until 8 months before the current admission, when progressive dyspnea on exertion developed, along with new difficulty walking up hills and stairs. These symptoms were accompanied by sinus congestion, rhinorrhea, and anosmia. A physical examination performed by his primary care physician showed no murmurs, wheezing, or peripheral edema. A complete blood count showed a normal hemoglobin level and a normal platelet count and total white-cell count; the absolute eosinophil count was elevated, at 1280 per microliter (reference range, 0 to 500). Treatment with umeclidinium was started.

Umeclidiniumbromid ist ein langwirksamer Muskarinrezeptor-Antagonist (LAMA), der als inhalative Erhaltungstherapie (meist 1-mal täglich 55 µg) zur Symptomlinderung bei chronisch-obstruktiver Lungenerkrankung (COPD) bei Erwachsenen eingesetzt wird

On the day of the current admission, the patient noticed progressive dyspnea while descending stairs, which prompted him to seek care with his primary care physician, who was affiliated with this hospital. At the time of initial evaluation, the oxygen saturation, obtained after ambulation while the patient was breathing ambient air, was 70%. He was immediately referred to the emergency department of this hospital. On his arrival at the emergency department, the oxygen saturation was 95% while he was at rest and breathing ambient air; other vital signs were normal.

A chest radiograph obtained in the emergency department showed a decrease in the size of the opacities in the right lower lobe and no change in the size of the opacities in the left lower lobe, as compared with the findings seen on radiography 2 months earlier. New small bilateral pleural effusions were present. The fluctuating size of the lung opacities, in association with pleural fluid, suggests a recurrent or persistent process rather than a single acute event.

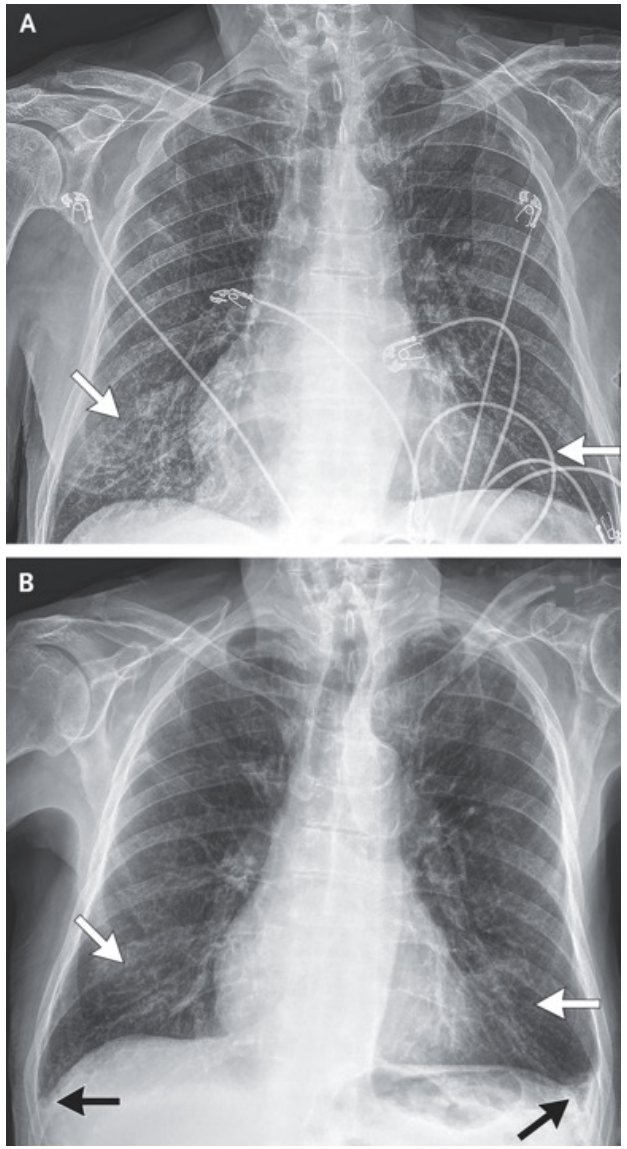

On examination, the oral temperature was 35.6°C, the blood pressure 98/54 mm Hg, the pulse 71 beats per minute, the respiratory rate 20 breaths per minute, and the oxygen saturation 93% while the patient was breathing ambient air. No jugular venous distention or murmur was detected, but the heart rhythm was irregularly irregular. Diffuse wheezing was present on auscultation, without crackles or diminished breath sounds. He had no rash, palpable organomegaly, or lymphadenopathy.

The white-cell count was 37,780 per microliter (reference range, 4000 to 11,000), with an absolute eosinophil count of 27,390 per microliter. The platelet count was normal, and the hemoglobin level was 12.8 mg per deciliter (reference range, 13.5 to 17.5). Examination of a peripheral-blood smear revealed an elevated number of mature eosinophils along with normal red-cell and platelet morphologic features. The blood levels of vitamin B_{12}, alanine aminotransferase, aspartate aminotransferase, bilirubin, alkaline phosphatase, electrolytes, urea nitrogen, and creatinine were all within normal limits. The N-terminal pro–B-type natriuretic peptide (NT-proBNP) level was 4300 pg per milliliter (age-adjusted reference range, 0 to 1800). Serial measurements of the high-sensitivity troponin T level were elevated, at 56 ng per liter (reference range, 0 to 14), without a change over time.

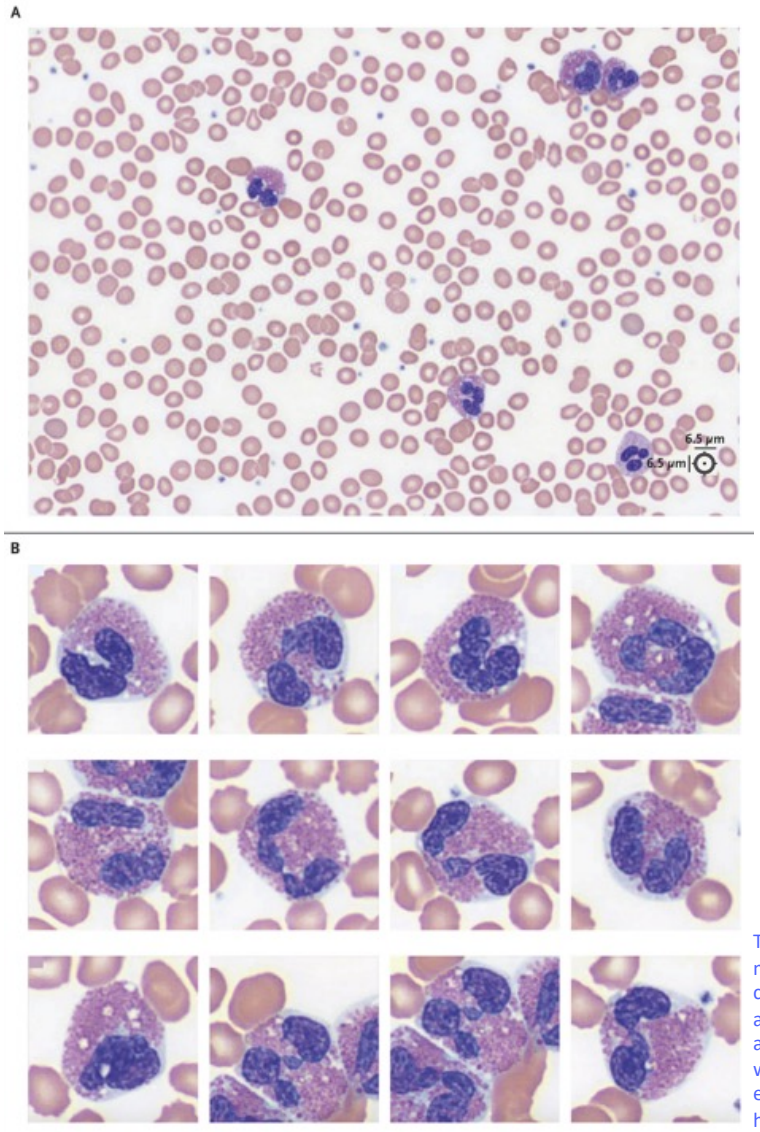

Peripheral-Blood Specimen.

Wright–Giemsa staining of a peripheral-blood smear (Panel A) shows mild anisopoikilocytosis with rare red-cell fragments but no morphologic abnormalities. The platelets appear normal in number and appearance. The white cells that are present in the sample are mostly eosinophils, which appear mature and reactive. At higher magnification (Panel B), mature-appearing eosinophils with bilobed nuclei and vacuolization, which is suggestive of reactivity, are seen. No premature or blast forms were observed on examination of the total white-cell population in the sample.

Tryptase is measured primarily as a diagnostic marker for mast cell activation, specifically to confirm anaphylaxis (severe allergic reactions) and diagnose mastocytosis or mast cell activation syndrome (MCAS). It acts as a "silent witness" to mast cell degranulation, with elevated blood levels indicating that these cells have released mediators into the circulation

Variable	Reference Range, Adults†	On Admission
Hemoglobin (g/dl)	13.5–17.5	12.8
Hematocrit (%)	41.0–53.0	38.2
White-cell count (per μl)	4000–11,000	37,780
Differential count (per μl)		
Neutrophils	1800–7700	8080
Lymphocytes	1000–4800	570
Monocytes	200–1200	1440
Eosinophils	0–900	27,390
Basophils	0–300	300
Immature granulocytes	0–100	0
Platelet count (per μl)	150,000–400,000	248,000
Sodium (mmol/liter)	135–145	139
Potassium (mmol/liter)	3.4–5.0	4.4
Chloride (mmol/liter)	98–108	106
Carbon dioxide (mmol/liter)	23–32	26
Urea nitrogen (mg/dl)	8–25	15
Creatinine (mg/dl)	0.60–1.50	0.74
Calcium (mg/dl)	8.5–10.5	8.5
Glucose (mg/dl)	70–110	88
Aspartate aminotransferase (U/liter)	10–40	21
Alanine aminotransferase (U/liter)	10–55	10
Alkaline phosphatase (U/liter)	15–115	113
Total bilirubin (mg/dl)	0.0–1.2	0.9
Albumin (g/dl)	3.3–5.0	3.6
Globulin (g/dl)	1.9–4.1	4.1
High-sensitivity troponin T (ng/liter)	0–14	56
N-terminal pro–B-type natriuretic peptide (pg/ml)	0–1800	4300
IgG (mg/dl)	614–1295	3099
IgA (mg/dl)	69–309	196
IgM (mg/dl)	53–334	203
IgE (IU/ml)	0–100	266
Free kappa light chain (mg/liter)	3.3–19.4	45.6
Free lambda light chain (mg/liter)	5.7–26.3	36.2
Ratio of kappa to lambda free light chains	0.30–1.70	1.26
Serum protein electrophoresis	Negative for monoclonal component	Negative for monoclonal component
Aspergillus fumigatus, IgE (kU/liter)	<0.10	2.99
Lactate dehydrogenase (U/liter)	110–210	397
Vitamin B_{12} (pg/ml)	>231	912
Tryptase (ng/ml)	<11.5	6.3
Erythrocyte sedimentation rate (mm/hr)	0–19	49
C-reactive protein (mg/liter)	<8.0	28.0

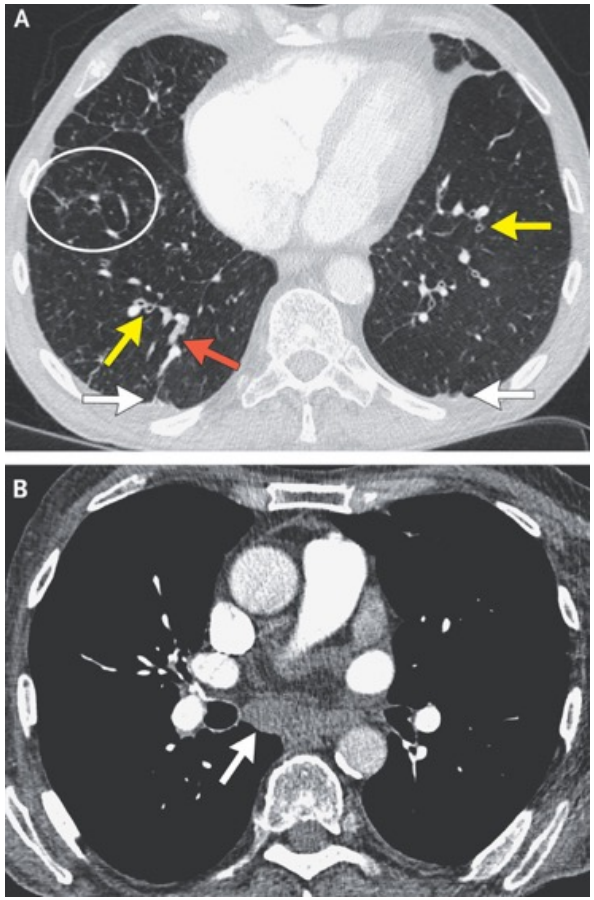

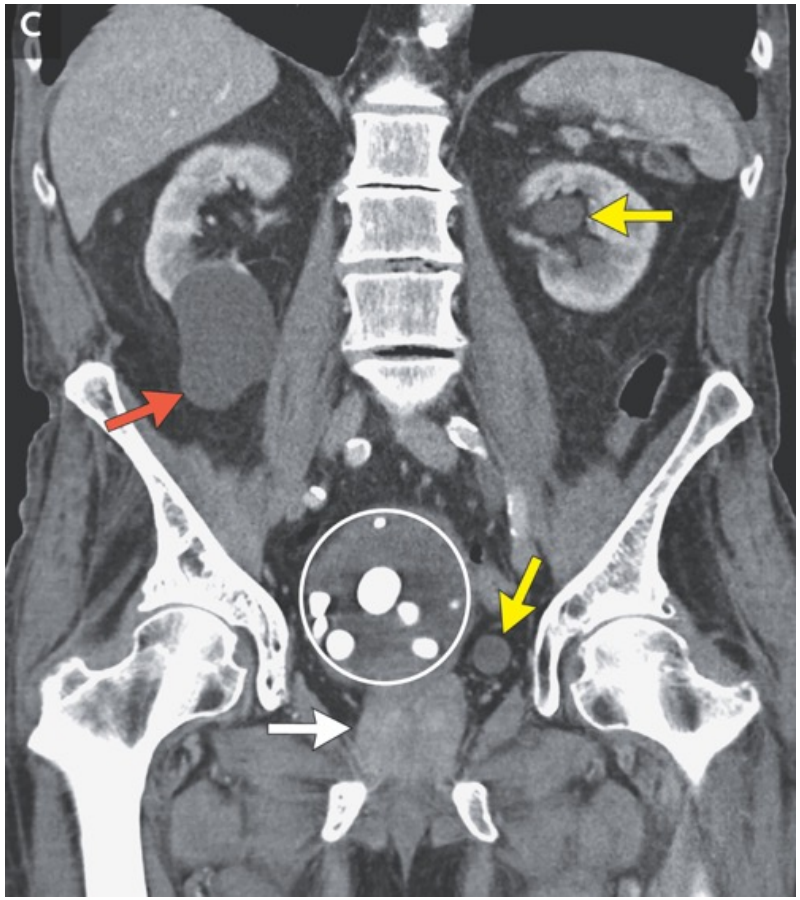

CT of the Chest, Abdomen, and Pelvis.

Contrast-enhanced computed tomography (CT) was performed during the current admission. An axial image of the chest in the lung window (Panel A) shows diffuse bronchial-wall thickening (yellow arrows), mucus plugging (red arrow), and tree-in-bud opacities (circle) in the right lower lobe, along with small areas of bilateral subsegmental atelectasis (white arrows), findings that are collectively suggestive of bronchiolitis, aspiration, or both. An axial image of the chest in the soft-tissue window (Panel B) shows mediastinal subcarinal lymphadenopathy, with nodes measuring up to 1.8 cm in diameter (arrow). A coronal image of the abdomen and pelvis in the soft-tissue window (Panel C) shows an enlarged prostate (white arrow), bladder stones (circle), hydroureteronephrosis of the left ureter and kidney (yellow arrows), and a cortical cyst in the right kidney (red arrow).

Die Hydronephrose und Blasensteine sind ein Nebenbefund.

Eosinophilia

Eosinophilia, defined as an absolute eosinophil count of at least 1500 per microliter, is associated with a broad range of diseases and requires a methodical diagnostic approach. Moreover, the mechanisms underlying hypereosinophilic syndromes remain poorly understood, with a plurality of cases characterized as idiopathic. Competing classification systems of hypereosinophilic syndromes can be confusing and reflect the difficulty in defining discrete disease subtypes and the clinically significant overlap among subtypes. No single set of definitions fits all clinical settings. For the purpose of constructing a differential diagnosis in this case, I will focus on a modified version of the classification system proposed by Klion, which I think best aligns with the perspective of the consulting hematologist in this case.

The first step in evaluating a patient with eosinophilia is to rule out all secondary (nonhematologic) causes. Then, the eosinophilia is categorized into one of the five major classes of hypereosinophilic syndrome, which we consider to be primary hematologic forms of hypereosinophilia.

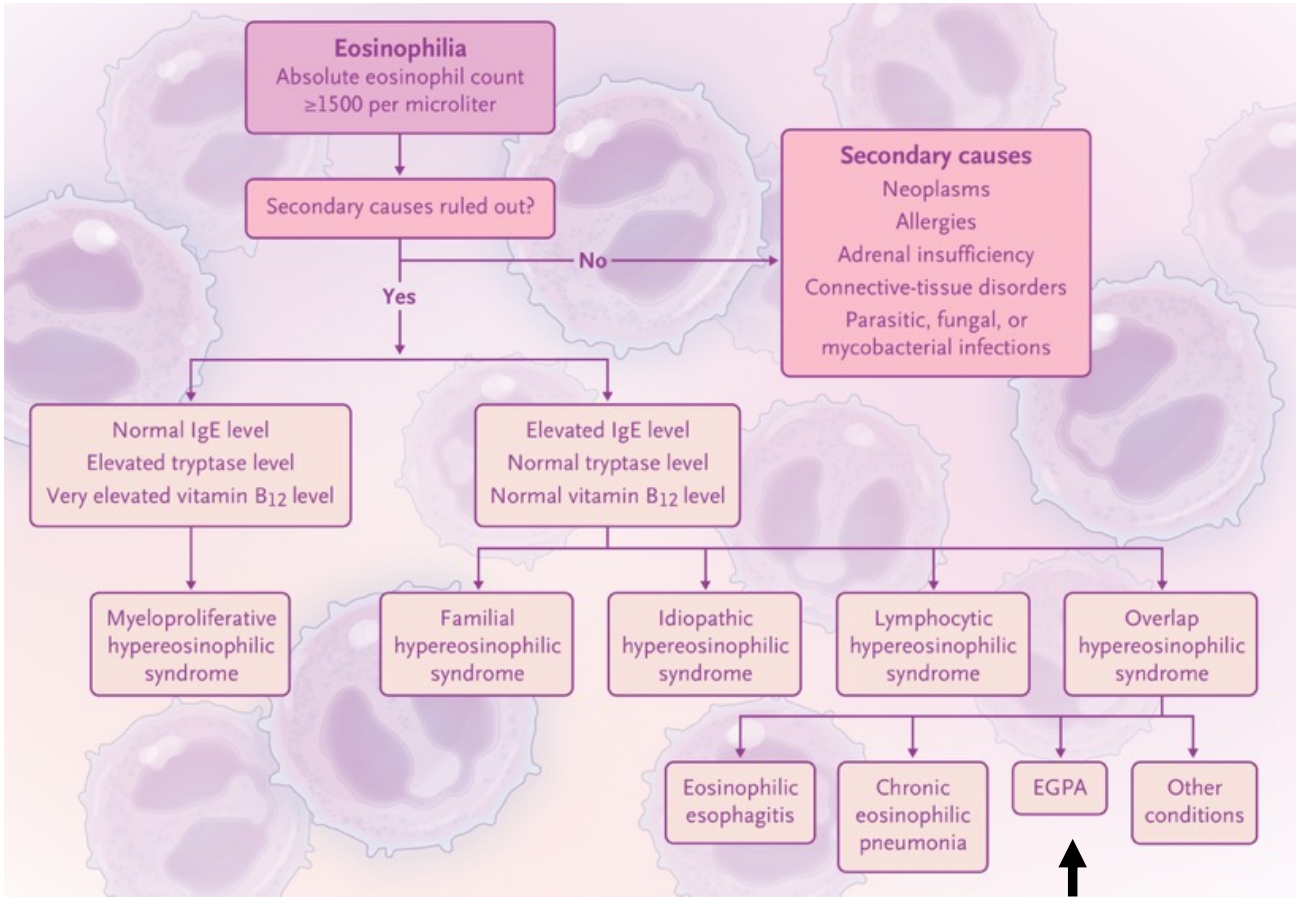

Earlier, Churg-Strauss

Suggested Diagnostic Approach to Disorders Associated with Eosinophilia (Modified Klion Classification).

The first responsibility of the evaluating physician is to rule out secondary (nonhematologic) causes of eosinophilia. Then, eosinophilia is categorized into one of five primary forms of hypereosinophilic syndrome: myeloproliferative, familial, idiopathic, lymphocytic, or overlap. Measurement of IgE, tryptase, and vitamin B_{12} levels helps distinguish myeloproliferative hypereosinophilic syndrome from other forms of hypereosinophilic syndrome. Overlap hypereosinophilic syndrome includes eosinophilic disorders characterized by single end-organ involvement (e.g., eosinophilic esophagitis) and clinically defined eosinophilia syndromes, including eosinophilic granulomatosis with polyangiitis (EGPA). This approach is based on a modification of the classification system proposed by Klion.[6]

Overlap Hypereosinophilic Syndrome

Overlap hypereosinophilic syndrome includes eosinophilic disorders that are restricted to a single organ system (e.g., eosinophilic esophagitis, eosinophilic fasciitis, and eosinophilic pneumonia), as well as clinically defined eosinophilic syndromes that have features that overlap with other forms of hypereosinophilic syndromes. An important subtype of overlap hypereosinophilic syndrome is eosinophilic granulomatosis with polyangiitis (EGPA), formerly known as the Churg–Strauss syndrome. EGPA is a mixed allergic and vasculitic disorder that is classically associated with a prodrome of allergic rhinitis, chronic sinusitis, and adult-onset asthma that can persist for years. The second phase is characterized by eosinophilia and end-organ involvement, followed by a third phase, in which small-vessel vasculitis causes clinical manifestations. Other commonly observed features of EGPA include pulmonary involvement with eosinophil infiltration that causes waxing and waning opacities on radiography, peripheral neuropathy, and signs of cardiac involvement such as cardiomyopathy, pericardial effusion, and valvular insufficiency.

The pathogenesis of EGPA remains unclear. Although overproduction of interleukin-5 appears to be a crucial mediator of the disease process, EGPA is not typically associated with an aberrant clonal T-cell population. EGPA is also not associated with a risk of malignant transformation, as is seen with lymphocytic hypereosinophilic syndrome. Nevertheless, the central role of interleukin-5 in EGPA is evidenced by the high incidence of response that occurs with anti–interleukin-5 therapy.

Approximately 30 to 40% of patients with EGPA have detectable circulating antineutrophil cytoplasmic antibodies (ANCA), and thus, EGPA is classified as an ANCA-associated vasculitis.

Diagnostic Testing

The following tests were ordered: an ANCA assay to establish the diagnosis of EGPA, flow cytometry to rule out clonal T-cell aberrations as a cause of eosinophilia, and nucleic acid testing for specific somatic gene fusions: the *FIP1L1–PDGFRA* and *BCR–ABL1* fusions and the fusion of *FGFR1* with other genes. A rapid heme panel was performed to rule out myeloproliferative or myelodysplastic states that cause eosinophilia.

This patient had a c-ANCA pattern on immunofluorescence staining, and an ELISA for antibodies against PR3 was positive at a titer of more than 100 U per milliliter (reference value, <20). Approximately 60 to 80% of patients with microscopic polyangiitis have a p-ANCA pattern on immunofluorescence staining, whereas 80 to 90% of patients with granulomatosis with polyangiitis have a c-ANCA pattern. ANCA is less predictable in patients with EGPA, with 50% of patients having a negative test for ANCA and 30 to 40% having a p-ANCA pattern on immunofluorescence staining. Only 5% of patients with EGPA have a c-ANCA pattern — the pattern that was seen in this patient. ANCA positivity in this patient's presentation is consistent with a diagnosis of EGPA. Interestingly, EGPA is unique within the ANCA-associated vasculitis spectrum because it is manifested by both hematologic (eosinophilia) and atopic (allergic airway disease) features before vasculitic features develop.

This patient was treated with both systemic glucocorticoids and, benralizumab (anti IL-5), which resulted in a marked abatement of his symptoms. Dyspnea decreased substantially during the subsequent 4 weeks. The absolute eosinophil count decreased to 0 per microliter 6 weeks after treatment initiation. With glucocorticoid tapering and continued benralizumab treatment, the patient's absolute eosinophil count remains between 20 and 30 per microliter 4 months after the initiation of treatment. The level of PR3 antibodies decreased and became undetectable after 3 months of treatment. The erythrocyte sedimentation rate and C-reactive protein level have normalized after 4 months of treatment. The patient has not had any signs or symptoms of cardiac involvement associated with EGPA. His kidney function remains within the normal range. He has persistent microscopic hematuria without proteinuria, which is thought to be due to nephrolithiasis and is being monitored by a urologist. The patient continues to undergo a slow glucocorticoid taper, with a goal of discontinuation of glucocorticoid therapy within 6 months after the start of treatment.

Final Diagnosis

Eosinophilic granulomatosis with polyangiitis.

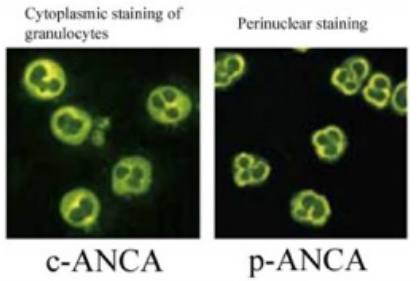

THE LANCET

Posterior stroke

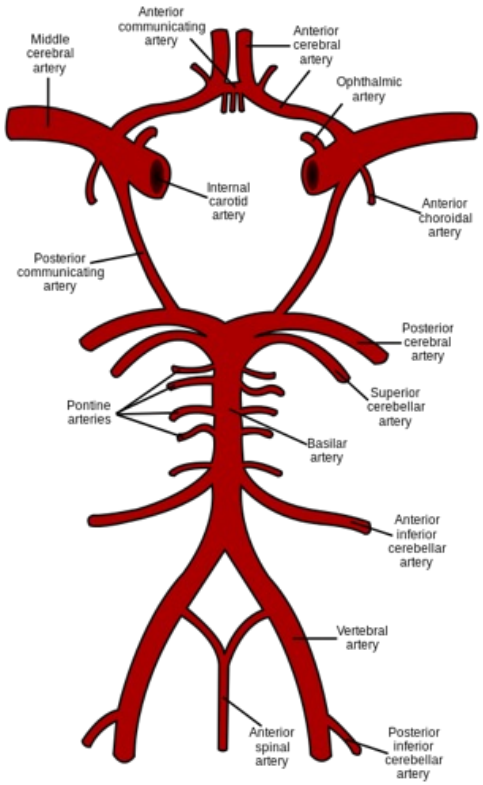

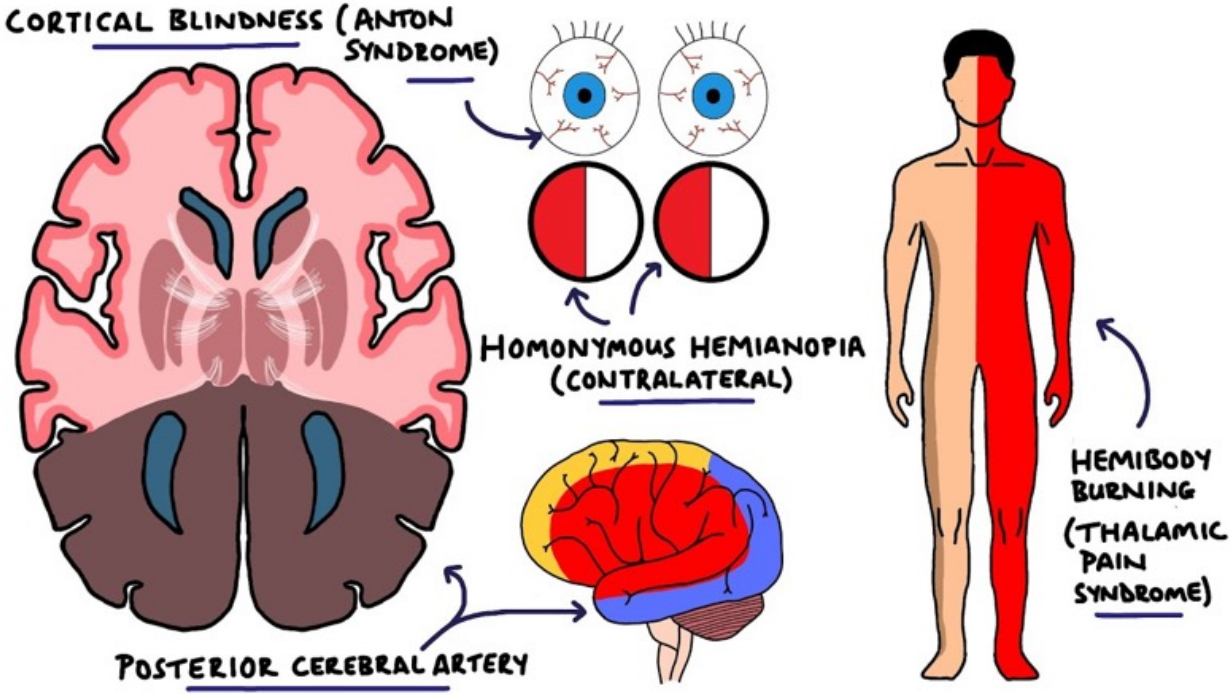

Tenecteplase versus standard medical treatment for basilar artery occlusion within 24 h (TRACE-5): a multicentre, prospective, randomised, open-label, blinded-endpoint, superiority, phase 3 trial

Summary

Background The efficacy and safety of intravenous thrombolysis with tenecteplase within 24 h after stroke onset due to basilar artery occlusion are not well studied. We aimed to assess whether intravenous tenecteplase administered within 24 h after symptom onset improved functional outcome compared with standard medical treatment in patients with basilar artery occlusion.

Methods TRACE-5 was a prospective, randomised, open-label, blinded-endpoint, superiority, phase 3 trial conducted at 66 stroke centres in China. We included patients aged 18 years or older with stroke due to basilar artery occlusion who were eligible for intravenous thrombolytics within 24 h of stroke onset or the time they were last known to be well and had a pre-stroke modified Rankin scale (mRS) score of 3 or less (scores range from 0 to 6, with higher scores indicating greater disability). Patients were randomly assigned to receive a single intravenous bolus of tenecteplase (0·25 mg/kg; maximum 25 mg) within 24 h after symptom onset or standard medical treatment (which could include intravenous alteplase at 0·9 mg/kg, maximum 90 mg, within 4·5 h of symptom onset; anticoagulation; or antiplatelets), with or without endovascular thrombectomy. The primary outcome was a score of 0–1 on the mRS or return to the baseline mRS score (if the baseline pre-stroke mRS score was 2–3) at 90 days. Safety outcomes were symptomatic intracranial haemorrhage and death. The primary outcome and safety outcomes were assessed in all randomly assigned participants included in their originally assigned groups. This trial is registered with ClinicalTrials.gov, NCT06196320.

Findings Between Jan 24, 2024, and June 20, 2025, 452 patients were enrolled (mean age 66·4 years [SD 11·2], 321 [71%] males, and 131 [29%] females), of whom 222 (49%) subsequently underwent thrombectomy; 221 were randomly assigned to receive tenecteplase and 231 to receive standard medical treatment. Alteplase was used in 80 (35%) of the patients in the standard medical treatment group. An mRS score of 0–1 or return to the baseline mRS score occurred in 83 (38%) patients in the tenecteplase group and 66 (29%) patients in the standard medical treatment group (adjusted relative rate 1·50 [95% CI 1·09–2·08], p=0·014). Symptomatic intracranial haemorrhage within 36 h occurred in four (2%) patients in the tenecteplase group and seven (3%) patients in the standard medical treatment group (adjusted relative rate 0·58 [95% CI 0·17–1·99]). All-cause mortality at 90 days was similar between groups (65 [29%] patients in the tenecteplase group and 71 [31%] patients in the standard medical treatment group; adjusted relative rate 0·87 [95% CI 0·62–1·22]), as was the proportion of patients with an mRS score of 5–6 at 90 days (82 [37%] *vs* 89 [39%]; 0·87 [0·65–1·18]).

Interpretation In this trial involving Chinese patients with ischaemic stroke due to basilar artery occlusion, tenecteplase within 24 h after stroke onset improved functional outcome compared with standard medical treatment. The incidence of symptomatic intracranial haemorrhage and death was similar.

Funding Noncommunicable Chronic Diseases-National Science and Technology Major Project, Beijing Municipal Science Fund for Distinguished Young Scholars, National Natural Science Foundation of China, and China Shijiazhuang Pharmaceutical Company Recomgen Pharmaceutical (Guangzhou).

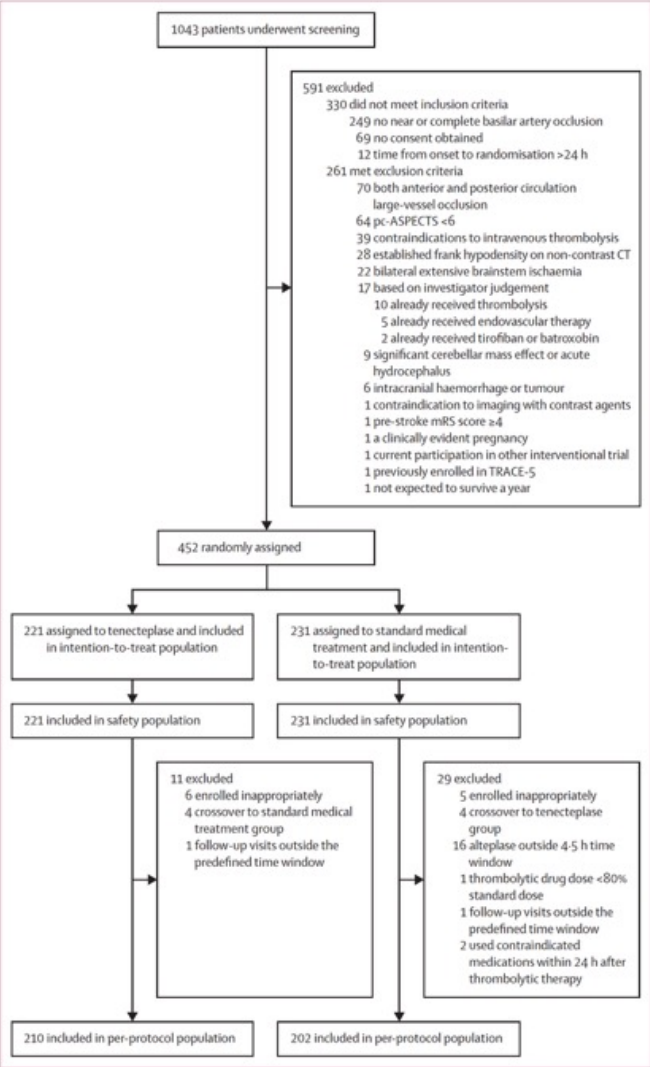

Figure 1: **Trial profile**
mRS=modified Rankin scale. pc-ASPECTS=posterior circulation Acute Stroke Prognosis Early CT Score.

	Tenecteplase group (n=221)	Standard medical treatment group (n=231)
Age, years	66·5 (10·9)	66·2 (11·6)
Sex		
Male	159 (72%)	162 (70%)
Female	62 (28%)	69 (30%)
Hypertension	165 (75%)	170 (74%)
Diabetes	55 (25%)	58 (25%)
Atrial fibrillation	16 (7%)	21 (9%)
mRS score before stroke*		
0–1	211 (95%)	220 (95%)
2–3	10 (5%)	11 (5%)
Baseline NIHSS score†	13 (7–25)	11 (6–21)
<10	86 (39%)	99 (43%)
≥10	135 (61%)	132 (57%)
Basilar artery occlusion‡		
Complete occlusion	208/218 (95%)	220/230 (96%)
Near-complete occlusion	10/218 (5%)	10/230 (4%)
Basilar artery occlusion site		
Proximal	126/218 (58%)	125/230 (54%)
Mid	64/218 (29%)	74/230 (32%)
Distal	28/218 (13%)	31/230 (13%)
pc-ASPECTS§	8 (6–8)	8 (7–8)
≤7	91 (41%)	88 (38%)
8–10	130 (59%)	143 (62%)
TOAST classification		
Large-artery atherosclerosis	191 (86%)	190 (82%)
Cardioembolism	29 (13%)	40 (17%)
Embolic stroke of undetermined source	1 (<1%)	1 (<1%)
Time from symptom onset to randomisation, h	6·1 (3·8–11·3)	6·5 (3·4–11·6)
<4·5	70 (32%)	85 (37%)
4·5–24	113 (51%)	102 (44%)
Wake-up stroke	38 (17%)	44 (19%)
Intravenous alteplase¶	1 (<1%)	80 (35%)
Intention at time of randomisation to perform endovascular thrombectomy	130 (59%)	125 (54%)
Endovascular thrombectomy	112 (51%)	110 (48%)

Data are mean (SD), n (%), or median (IQR). mRS=modified Rankin scale. NIHSS=National Institutes of Health Stroke Scale. pc-ASPECTS=posterior circulation Acute Stroke Prognosis Early CT Score. TOAST=Trial of Org 10172 in Acute Stroke Treatment. *Scores on the mRS range from 0 to 6, with higher scores indicating greater disability. †Scores on the NIHSS range from 0 to 42, with higher scores indicating a greater deficit. ‡Four patients did not have near-complete or complete basilar artery occlusion on core laboratory assessment. §Scores on the pc-ASPECTS were assessed on baseline CT angiography source images, non-contrast CT brain images, or diffusion weighted imaging, ranging from 0 to 10, with higher scores indicating fewer early ischaemic changes. ¶Four patients assigned to tenecteplase crossed over to control (one received alteplase and three received no intravenous thrombolysis) but were analysed in the tenecteplase group as per the intention-to-treat principle.

Table 1: **Baseline characteristics**

	Tenecteplase group (n=221)	Standard medical treatment group (n=231)	Adjusted effect size* (95% CI)†	p value
Primary outcome				
mRS score 0–1 or return to baseline mRS score at 90 days‡	83 (38%)	66 (29%)	1·50 (1·09–2·08)	0·014
Secondary outcomes				
mRS score of 0–2 or return to baseline mRS score at 90 days	98 (44%)	99 (43%)	1·16 (0·88–1·54)	0·29
mRS score of 0–3 at 90 days	114 (52%)	123 (53%)	1·06 (0·82–1·37)	0·66
Ordinal distribution of mRS scores at 90 days	..	..	1·51 (1·06–2·15)	0·022
0	36 (16%)	30 (13%)	..	..
1	43 (19%)	34 (15%)	..	..
2	17 (8%)	34 (15%)	..	..
3	18 (8%)	25 (11%)	..	..
4	25 (11%)	19 (8%)	..	..
5–6§	82 (37%)	89 (39%)	..	..
Early clinical improvement¶	65 (29%)	64 (28%)	1·08 (0·76–1·52)	0·68
Substantial reperfusion at initial angiogram‖	34/141 (24%)	16/126 (13%)	1·90 (1·04–3·49)	0·038
Safety outcomes				
Symptomatic intracranial haemorrhage within 36 h**	4 (2%)	7 (3%)	0·58 (0·17–1·99)	0·39
All-cause mortality within 90 days	65 (29%)	71 (31%)	0·87 (0·62–1·22)	0·41
mRS score 5–6 at 90 days	82 (37%)	89 (39%)	0·87 (0·65–1·18)	0·38

Data are n (%) or n/N (%) unless otherwise stated. mRS=modified Rankin scale. NIHSS=National Institutes of Health Stroke Scale. *The common odds ratio is shown for the ordinal score on the mRS, and the relative rate is shown for other outcomes. †The primary, secondary, and safety outcomes were adjusted for age, baseline NIHSS score, and onset-to-randomisation time (dichotomised as <6 h *vs* 6–24 h). ‡Scores on the mRS range from 0 to 6, with higher scores indicating greater disability; the primary outcome also included patients who returned to their baseline mRS score (if the baseline pre-stroke mRS score was 2–3) at 90 days. §mRS scores 5–6 were prespecified to be merged in ordinal analysis to avoid counting a shift from death (mRS score 6) to severe disability requiring constant nursing care (mRS score 5) as a treatment success. ¶Early clinical improvement defined by a reduction on NIHSS score of ≥8 compared with the initial deficit or a score of 0–1 at 72 h. ‖Proportion of patients with complete occlusion at baseline who reached the expanded Treatment in Cerebral Infarction grade of 2B–3 (reperfusion of ≥50% of the affected territory) on initial digital subtraction angiography run before thrombectomy. Two patients did not go for digital subtraction angiography due to significant improvement of NIHSS scores, and repeated CT angiography showed complete recanalisation of occlusion (Arterial Occlusive Lesion score of 3). **Symptomatic intracranial haemorrhage within 36 h (defined as local or remote parenchymal haemorrhage type 2, combined with a neurological deterioration of ≥4 NIHSS points, or leading to death).

Table 2: **Efficacy and safety outcomes**

Don‘t forget to give minocycline

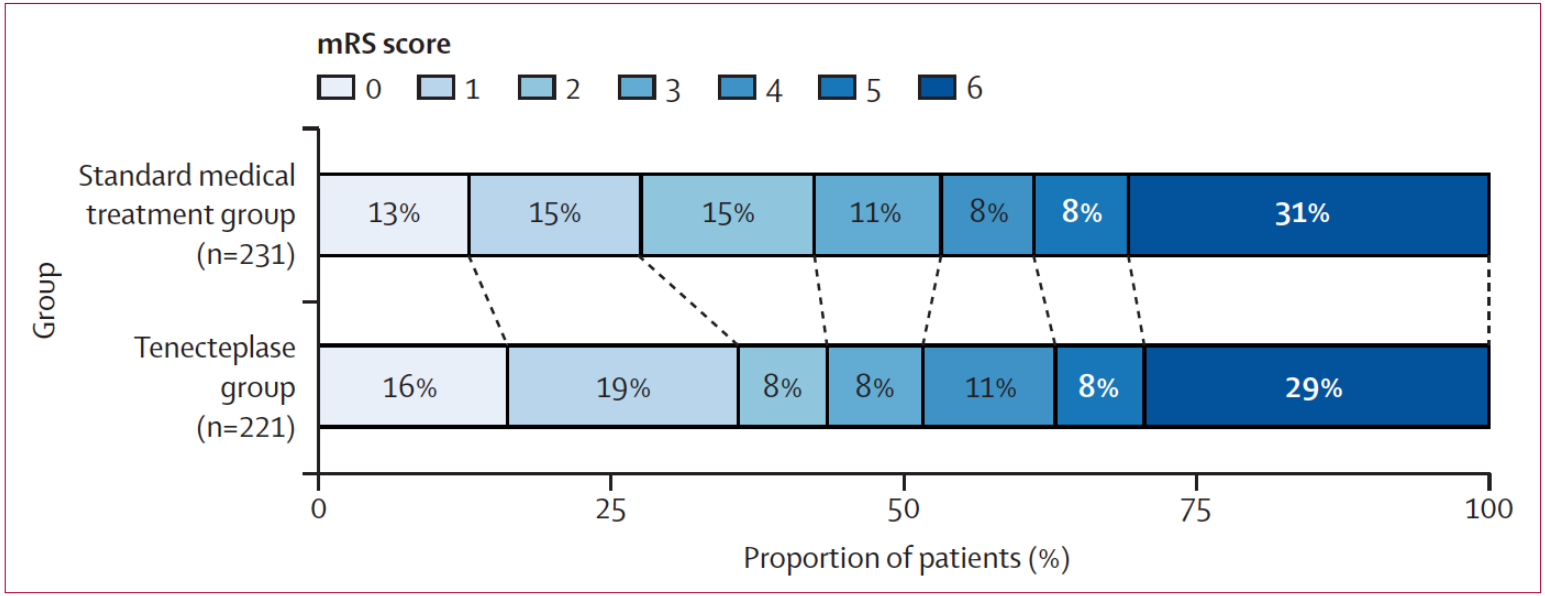

Figure 2: **Distribution of scores on the mRS at 90 days in the intention-to-treat population**
Scores on the modified Rankin scale range from 0 to 6, with 0 indicating no symptoms, 1 indicting symptomatic but not disabled, 2 indicating disabled but independent, 3 indicating dependent but ambulatory, 4 indicating not ambulatory or capable of body self-care, 5 indicating requiring constant nursing care, and 6 indicating death. Percentages might not total 100 because of rounding. mRS=modified Rankin scale.

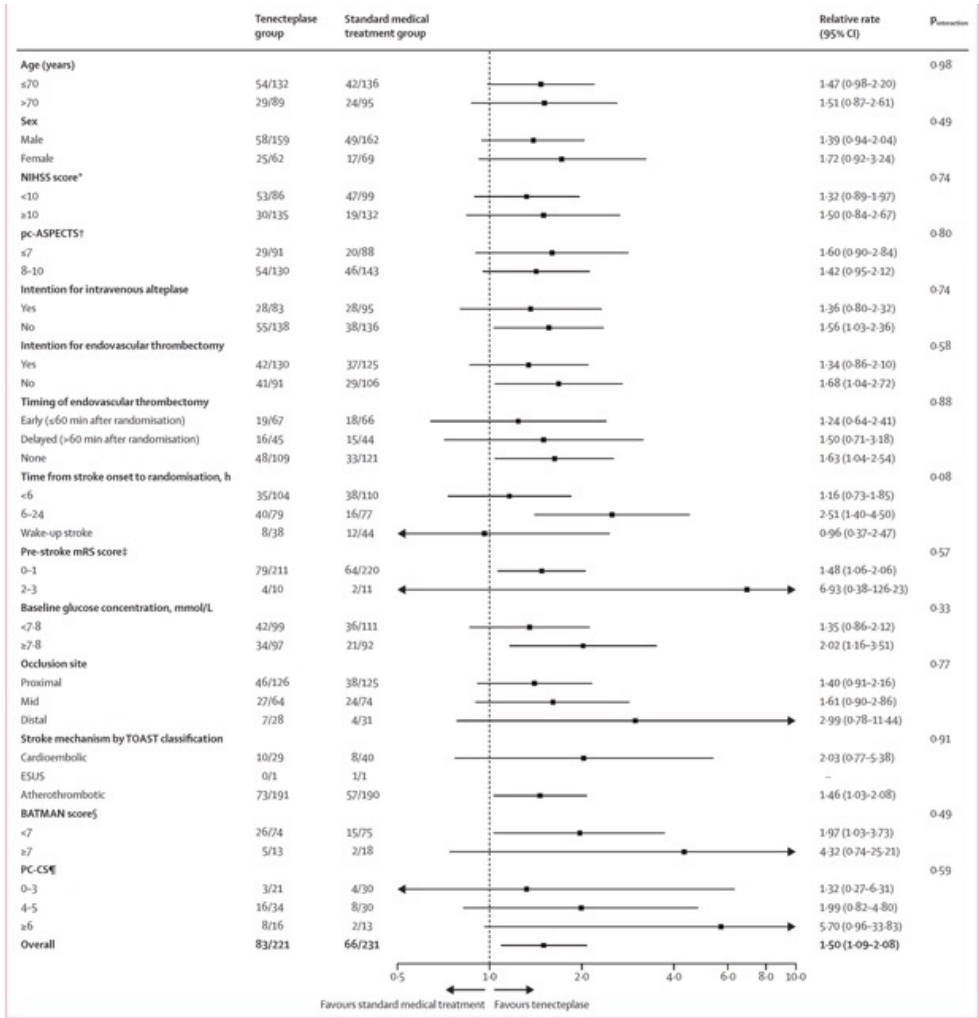

Figure 3: **Subgroup analyses for the primary outcome of mRS score of 0–1 or return to baseline mRS score at 90 days**

BATMAN=Basilar Artery Tomography Angiography. ESUS=embolic stroke of undetermined source. mRS=modified Rankin scale. NIHSS=National Institutes of Health Stroke Scale. pc-ASPECTS=posterior circulation Acute Stroke Prognosis Early CT Score. PC-CS=Posterior Circulation Collateral Score. TOAST=Trial of Org 10172 in Acute Stroke Treatment. *Scores on the NIHSS range from 0 to 42, with higher scores indicating greater deficit. †The pc-ASPECTS was determined by use of baseline CT angiogram source images, non-contrast CT brain images, or diffusion weighted imaging, and ranges from 0 to 10, with higher scores indicating fewer early ischaemic changes. ‡Scores on the mRS range from 0 to 6, with higher scores indicating greater disability. §BATMAN scores were evaluated on baseline CT angiography, ranging from 0 to 10, with higher scores indicating better vascular perfusion and collateral circulation. ¶The PC-CS was calculated on baseline CT angiography, ranging from 0 to 10, with higher scores indicating better collateral blood flow.

Research in context

Evidence before this study

Endovascular thrombectomy is established as an effective treatment for basilar artery occlusion within 24 h of stroke onset according to four phase 3 randomised controlled trials. However, access to endovascular thrombectomy remains limited worldwide, particularly in low-income and middle-income countries. As the first-line therapy for ischaemic stroke within 4·5 h, intravenous thrombolysis is widely used and might offer additional benefits for patients with basilar artery occlusion presenting within 24 h after onset, especially with the use of the newer-generation thrombolytic, tenecteplase.
We searched PubMed and MEDLINE for randomised trials published between Jan 1, 2000, and Oct 31, 2025, using the terms "tenecteplase", "basilar artery occlusion", and "study" or "clinical trial". To date, no phase 3 randomised controlled trial has been published evaluating the efficacy and safety of tenecteplase in patients with confirmed basilar artery occlusion within 24 h of symptom onset. One phase 3 trial compared alteplase with control, administered between 4·5 h and 24 h in patients with posterior circulation stroke, but it mainly included patients with mild strokes, did not require basilar artery occlusion, and excluded patients intended for thrombectomy.

Added value of this study

TRACE-5 is the first phase 3 trial to compare tenecteplase with standard medical treatment in patients with basilar artery occlusion presenting within 24 h of symptom onset. Our findings showed that tenecteplase administered within 24 h of symptom onset improved excellent functional outcomes without increased safety concerns for patients with basilar artery occlusion. This pragmatic trial allowed the use of alteplase in the control group and thrombectomy in both groups, closely reflecting real-world clinical practice.

Implications of all the available evidence

The TRACE-5 trial supports tenecteplase as an effective option for treating basilar artery occlusion within 24 h, both in centres that can provide endovascular thrombectomy and those that cannot. Using single-bolus tenecteplase to complement endovascular thrombectomy without advanced imaging for patient selection enhances its feasibility for future implementation.

Intracerebral hemorrhage

Catheter to remove hematoma

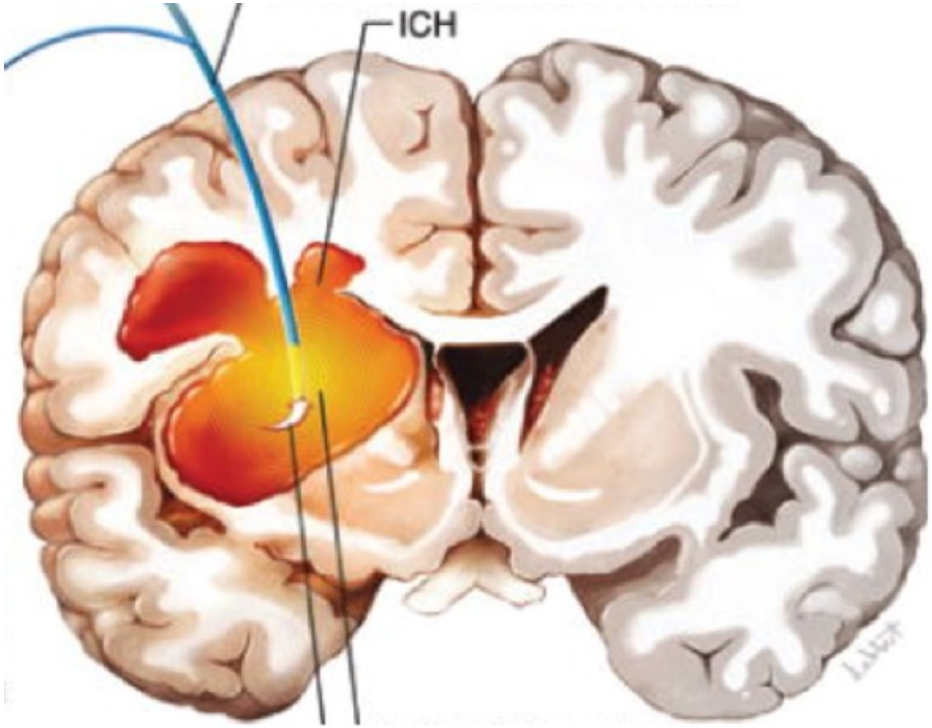

Recombinant factor VIIa versus placebo for spontaneous intracerebral haemorrhage within 2 h of symptom onset (FASTEST): a multicentre, double-blind, randomised, placebo-controlled, phase 3 trial

Summary

Background Recombinant factor VIIa has been shown to slow bleeding in patients with intracerebral haemorrhage (ICH), but no haemostatic agent has been shown to improve clinical outcomes. We aimed to evaluate the safety, clinical efficacy, and effect on growth of ICH and intraventricular haemorrhage (IVH) of recombinant factor VIIa in patients with acute spontaneous ICH who were most likely to benefit from treatment with this agent.

Methods We conducted a multicentre, prospective, double-blind, randomised, placebo-controlled, adaptive, phase 3 trial (FASTEST) at 93 sites across the USA, Japan, Canada, Spain, Germany, and the UK. Adults aged 18–80 years with a spontaneous ICH of 2–60 mL, IVH in less than two-thirds of one lateral ventricle or in less than a third of both lateral ventricles, a Glasgow Coma Scale score of at least 8, no evidence of recent ischaemic stroke or myocardial infarction, no recent use of anticoagulation medication or other structural cause of ICH, and who had been treated with study medication within 2 h of stroke onset or last known well were eligible for inclusion. Patients were randomly assigned (1:1) by a simple randomisation scheme to either 80 µg/kg recombinant factor VIIa (intervention group) or an identical placebo (placebo group), administered intravenously over 2 min. All investigators and participants were masked to allocated group assignment. The primary outcome was functional outcome at 180 days, measured by modified Rankin Scale (mRS; score 0–2, 3, and 4–6) and analysed by intention to treat in all randomly assigned patients. The primary safety outcome was life-threatening thromboembolic events during the first 4 days, assessed in all randomly assigned participants. The secondary aim was change in ICH volume and ICH plus IVH volume between baseline and 24 h of treatment administration. We performed an ordinal logistic regression, adjusted for age, baseline ICH volume, baseline IVH volume, and pre-stroke mRS. Preplanned interim analyses, including adaptive sample size re-estimation and enrichment to a younger subgroup (aged ≤70 years), were also conducted. This trial is registered with ClinicalTrials.gov (NCT03496883) and is closed to new participants.

Findings Between Dec 3, 2021, and Oct 1, 2025, we screened 3288 patients, of whom 626 participants were randomly assigned and included in the intention-to-treat analyses: 298 (48%) in the placebo group and 328 (52%) in the intervention group. 216 (35%) participants were female and 410 (65%) were male, with a mean age of 61 years (SD 12). Mean time from stroke onset to administration of study drug was 100 min (SD 22). The trial met the prespecified stopping criteria for futility at the second interim analysis. There was no differential effect in the primary clinical outcome measure of mRS at 180 days between the intervention group and placebo group (adjusted common odds ratio 1·09 [95% CI 0·79–1·51]; p=0·61). Life-threatening thromboembolic complications within 4 days occurred in 15 (<5%) participants in the intervention group and in four (1%) in the placebo group (relative risk 3·41 [95% CI 1·14–10·15]; p=0·020). Compared with placebo, recombinant factor VIIa was associated with decreased growth of ICH (–3·7 mL [95% CI –5·4 to –1·9]) and of ICH plus IVH growth (–5·2 mL [–7·6 to –2·8]) between baseline and CT scan at 24 h.

Interpretation Recombinant factor VIIa administered within 2 h of ICH onset slowed haematoma growth, but did not improve functional outcomes and showed a small increased risk of life-threatening thromboembolic complications. Further testing of recombinant factor VIIa in patients with the greatest risk of continued bleeding is ongoing.

Funding National Institute of Neurological Diseases and Stroke, Japan Agency for Medical Research and Development, and Novo Nordisk.

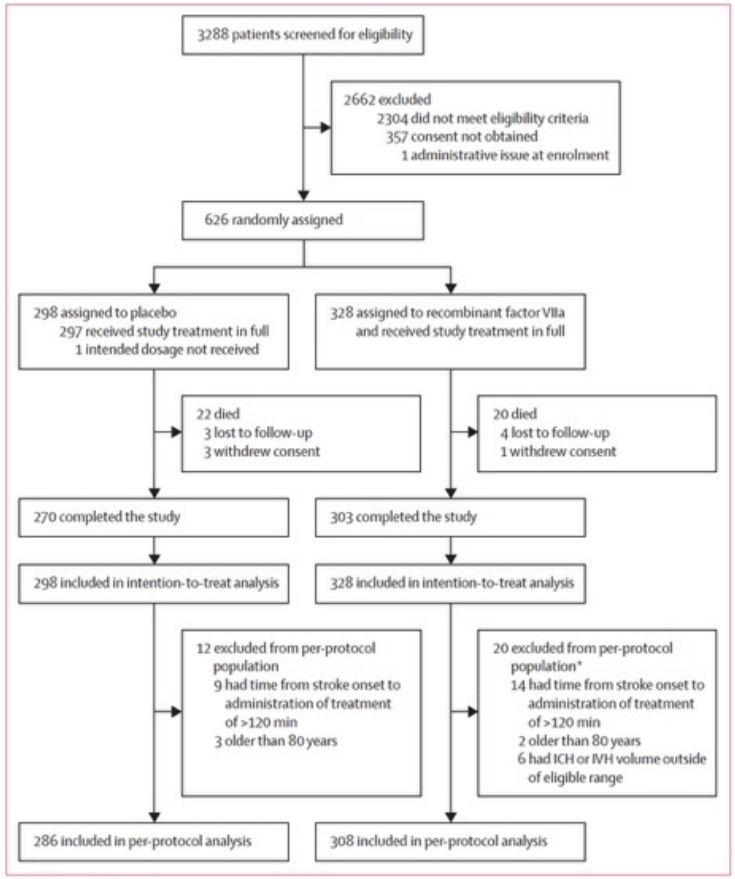

Figure 1: **Trial profile**
ICH=intracerebral haemorrhage. IVH=intraventricular haemorrhage. *Some participants were excluded for multiple reasons.

	Placebo group (n=298)	Intervention group (n=328)
Age, years	60 (12)	61 (12)
Age group, years		
≤70	232 (78%)	241 (73%)
>70	66 (22%)	87 (27%)
Sex		
Female	105 (35%)	111 (34%)
Male	193 (65%)	217 (66%)
Ethnicity		
Hispanic or Latinx	25 (8%)	32 (10%)
Not Hispanic or Latinx	271 (91%)	296 (90%)
Unknown	2 (1%)	0
Race		
American Indian or Alaska Native	0	1 (<1%)
Asian	169 (57%)	173 (53%)
Black or African American	23 (8%)	30 (9%)
Native Hawaiian or other Pacific Islander	1 (<1%)	1 (<1%)
Unknown or not reported	5 (2%)	5 (2%)
White	100 (34%)	118 (36%)
Pre-stroke modified Rankin Scale score		
0	281 (94%)	303 (92%)
1	10 (3%)	17 (5%)
2	6 (2%)	8 (2%)
3	1 (<1%)	0
Time between stroke onset and administration of study drug, min	99·2 (18·7)	101·2 (23·8)
ICH volume, mL	16·5 (13·3)	16·9 (15·6)
IVH volume, mL	1·4 (4·1)	1·7 (5·9)
NIH Stroke Scale score	13 (8–17)	13 (8–17)
Baseline Glasgow Coma Scale score		
8	5 (2%)	8 (2%)
9	8 (3%)	10 (3%)
10	15 (5%)	14 (4%)
11	21 (7%)	19 (6%)
12	11 (4%)	15 (5%)
13	29 (10%)	24 (7%)
14	69 (23%)	50 (15%)
15	140 (47%)	188 (57%)

(Table 1 continues in next column)

	Placebo group (n=298)	Intervention group (n=328)
(Continued from previous column)		
Location of ICH		
Lobar	41 (14%)	35 (11%)
Deep	254 (85%)	287 (88%)
Infratentorial	3 (1%)	6 (2%)
Blood pressure, mm Hg	170/98	173/99
CT angiography performed	254 (85%)	257 (78%)
Spot sign on CT angiography	77 (26%)	71 (22%)
Study medication administered in mobile stroke unit	6 (2%)	11 (3%)
ECG result		
Abnormal, clinically significant	5 (2%)	4 (1%)
Abnormal, not clinically significant	131 (44%)	145 (44%)
ECG not performed	1 (<1%)	3 (1%)
Normal	161 (54%)	176 (54%)
Troponin elevation	50 (17%)	64 (20%)
Ultra-early haematoma growth <10 mL/h	128 (43%)	153 (47%)
Ultra-early haematoma growth, ≥10 mL/h	170 (57%)	175 (53%)

Data are mean (SD), n (%), or median (IQR). ICH=intracerebral haemorrhage. IVH=intraventricular haemorrhage. NIH=National Institutes of Health. ECG=electrocardiogram.

Table 1: **Baseline participant characteristics in the intention-to-treat population**

	Placebo group	Intervention group	OR (95% CI)*	Two-sided p value
Primary outcome				
mRS at 180 days in the intention-to-treat population				
0–2	134/298 (45%)	151/328 (46%)	1·09 (0·79 to 1·51)	0·61
3	76/298 (26%)	80/328 (24%)	..	..
4–6	88/298 (30%)	97/328 (30%)	..	..
mRS at 180 days in the per-protocol population				
0–2	129/286 (45%)	146/308 (47%)	1·12 (0·80 to 1·56)	0·87
3	75/286 (26%)	79/308 (26%)	..	..
4–6	82/286 (29%)	83/308 (27%)	..	..
Secondary outcomes				
Ordinal distribution of the mRS at 90 days				
0–2	113/298 (38%)	132/328 (40%)	1·13 (0·82 to 1·56)	0·87
3	57/298 (19%)	59/328 (18%)	..	..
4–6	128/298 (43%)	137/328 (42%)	..	..
Ordinal distribution of the mRS at 90 days†	3 (2 to 4)	3 (2 to 4)	1·13 (0·86 to 1·51)	0·87
Ordinal distribution of the mRS at 180 days†	3 (2 to 4)	3 (2 to 4)	1·10 (0·83 to 1·47)	0·87
mRS 0–2 at 90 days	113/298 (38%)	132/328 (40%)	1·15 (0·80 to 1·66)	0·87
mRS 0–2 at 180 days	134/298 (45%)	151/328 (46%)	1·12 (0·77 to 1·61)	0·87
Utility-weighted mRs at 90 days	5·5 (2·9)	5·5 (3·0)	..	..
OR (95% CI)	4·78 (4·20 to 5·35)	4·97 (4·40 to 5·53)	..	0·87
Utility-weighted mRs at 180 days	6·1 (2·9)	6·1 (2·9)	..	..
OR (95% CI)	5·27 (4·71 to 5·8)	5·40 (4·86 to 5·94)	..	0·87
Change in ICH volume from baseline to 24 h, mL	5·5 (13·7)	1·9 (7·0)	..	..
OR (95% CI)	4·76 (2·31 to 7·21)	1·0 (–1·39 to 3·38)	..	0·0011
Change in ICH plus IVH volume from baseline to 24 h, mL	7·4 (19·6)	2·2 (8·4)	..	..
OR (95% CI)	7·41 (4·02 to 10·78)	1·99 (–1·31 to 5·28)	..	0·0011
EQ-5D at 90 days	0·5 (0·4)	0·5 (0·4)	..	0·87
OR (95% CI)	0·40 (0·32 to 0·48)	0·40 (0·33 to 0·48)	..	..
EQ-5D at 180 days	0·5 (0·4)	0·5 (0·5)	..	0·87
OR (95% CI)	0·47 (0·39 to 0·54)	0·47 (0·39 to 0·54)	..	..

Data are n (%), median (IQR), or mean (SD), unless otherwise indicated. The imputed dataset included 626 participants. mRS at day 180 was missing for ten participants; data were imputed using multiple imputation. mRS was missing for seven participants at day 30 and for 15 participants at day 90; data were imputed using hot-deck imputation. OR=odds ratio. mRS=modified Rankin Scale. ICH=intracerebral haemorrhage. IVH=intraventricular haemorrhage. EQ-5D=EQ-5D health-related quality of life. *Adjusted common ORs and 95% CIs from a proportional odds regression model are provided for categorical outcomes; least squared means and 95% CIs from a linear regression model are reported for numerical outcomes. Both regression analyses are adjusted for age, baseline ICH volume, baseline IVH volume, and pre-stroke mRS. p values for secondary outcomes were calculated with Hochberg's step-up procedure to adjust for multiple comparisons. †All seven steps of the mRS.

Table 2: **Efficacy outcomes after missing data imputation**

	Placebo group (n=298)	Intervention group (n=328)	Relative risk (95% CI)
Life-threatening thromboembolic complications within 4 days*	4 (1%)	15 (<5%)	3·41 (1·14–10·15)
Life-threatening thromboembolic complications within 90 days*†	11 (4%)	21 (6%)	1·73 (0·85–3·54)
Unstable angina	0	0	..
Deep venous thrombosis (not leading to pulmonary embolism)	4 (1%)	7 (2%)	1·59 (0·47–5·38)
Mortality within 180 days	22 (7%)	20 (6%)	0·83 (0·46–1·48)
mRS 5–6 at 180 days	31 (10%)	37 (11%)	1·08 (0·69–1·70)
Myocardial injury without acute coronary syndrome	30 (10%)	49 (15%)	1·48 (0·97–2·27)
Acute myocardial infarction‡	4 (1%)	3 (1%)	0·68 (0·15–3·02)
Acute cerebral infarction‡	11 (4%)	18 (5%)	1·49 (0·71–3·10)
Acute pulmonary embolism‡	3 (1%)	5 (2%)	1·51 (0·37–6·28)

mRS=modified Rankin Scale. *Defined as a serious adverse event of acute myocardial infarction, acute cerebral infarction, or acute pulmonary embolism. †One life-threatening thromboembolic complication event occurred 97 days after randomisation in the placebo group and was excluded from the secondary safety outcome of life-threatening thromboembolic complications within 90 days. ‡Serious and non-serious adverse events, including small diffusion-positive lesions without any clinical change.

Table 3: **Safety outcomes in the intention-to-treat population**

No difference

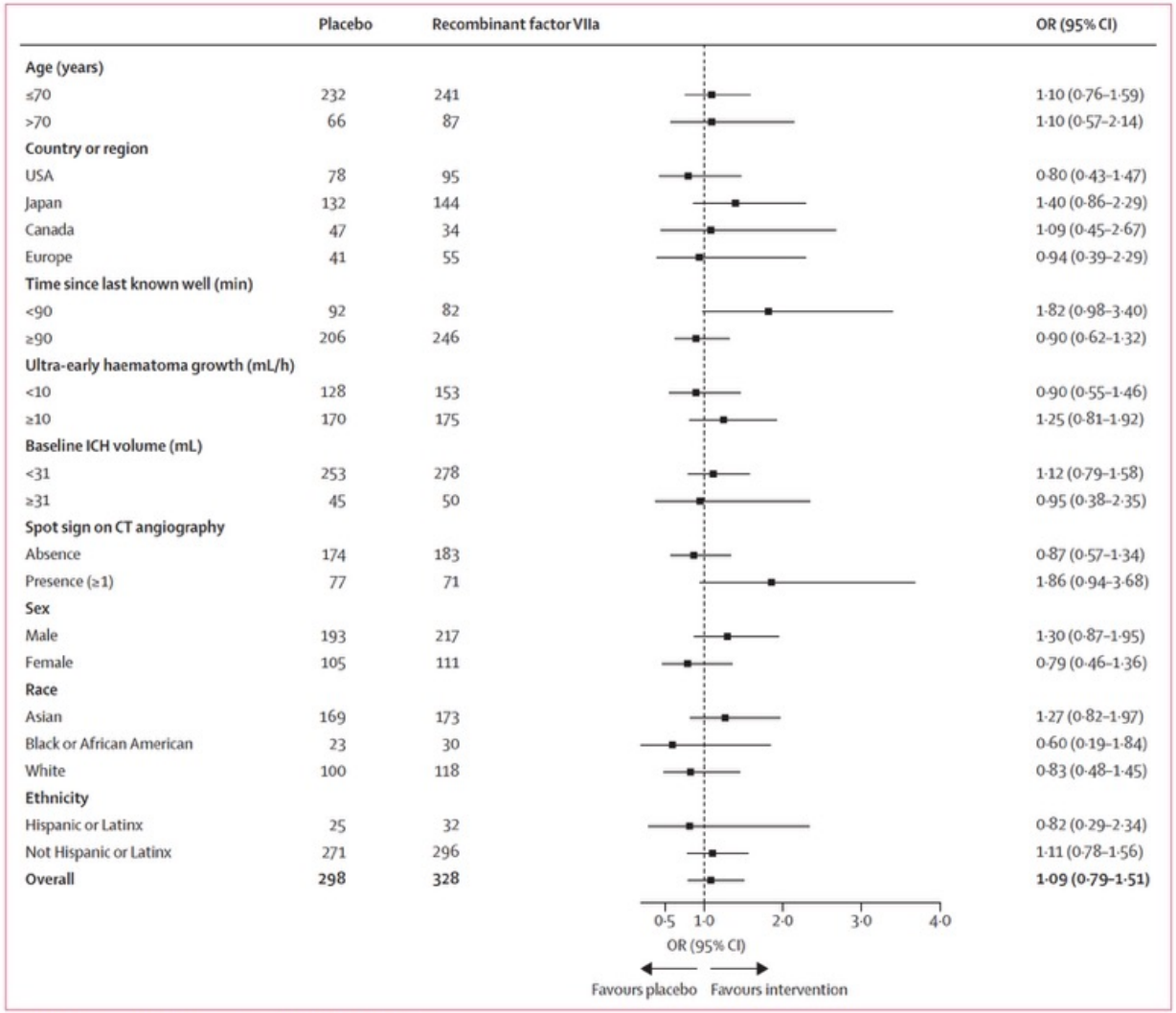

Figure 2: **Prespecified subgroup analyses of mRS at 180 days**
mRS=modified Rankin Scale. OR=odds ratio. ICH=intracerebral haemorrhage.

Research in context

Evidence before this study

Intracerebral haemorrhage (ICH), the second most common type of stroke with the greatest disability and mortality of all stroke subtypes, leads to substantial disability and mortality in direct proportion to the volume of bleeding. We performed a pooled analysis of previous phase 2b and phase 3 trials of recombinant factor VIIa. We also reviewed the treatment trials of ICH summarised in 2025 by the European Stroke Organisation and European Association of Neurosurgical Societies guideline on stroke due to spontaneous ICH in October, 2025. The primary challenge for haemostatic therapy in patients with spontaneous ICH is that almost all bleeding expansion occurs within the first 2–3 h after symptom onset. Recombinant factor VIIa slows bleeding in patients with ICH, but the clinical benefit with this agent observed in a phase 2b trial was not subsequently shown in a larger phase 3 trial. Post-hoc analyses of these two randomised trials indicated that recombinant factor VIIa had its greatest potential for benefit when administered within 2 h in patients aged 70 years and younger who did not have a large ICH or large amount of intraventricular haemorrhage on baseline CT scan of the head. A major unanswered question is the decrease in the volume of bleeding in the brain that is needed to improve functional outcomes in patients with ICH.

Added value of this study

To our knowledge, this multicentre, double-blind, randomised, placebo-controlled, phase 3 trial (FASTEST) is the largest trial to date investigating the hyperacute treatment of patients with ICH. We found that recombinant factor VIIa slowed bleeding but did not improve functional outcomes overall and was associated with a small increase in life-threatening thromboembolic complications. We also show that the agent's haemostatic effects were concentrated in patients with the greatest likelihood of ongoing bleeding: those treated within 90 min or with a spot sign on CT angiography identified within 2 h of onset. This study suggests that the mean volume of decreased haemorrhage growth needed to improve functional outcomes for any haemostatic agent is likely to be at least 6–12 mL. Our findings highlight the importance of CT angiography and rapid treatment in identifying efficacious haemostatic treatments for patients with ICH.

Implications of all the available evidence

Although we report neutral results overall, this trial provides a roadmap for the management of two subgroups of patients with ICH. Additionally, this study provides insight into the amount of haemostasis needed to improve functional outcomes for patients with spontaneous ICH treated with recombinant factor VIIa or other haemostatic agents.

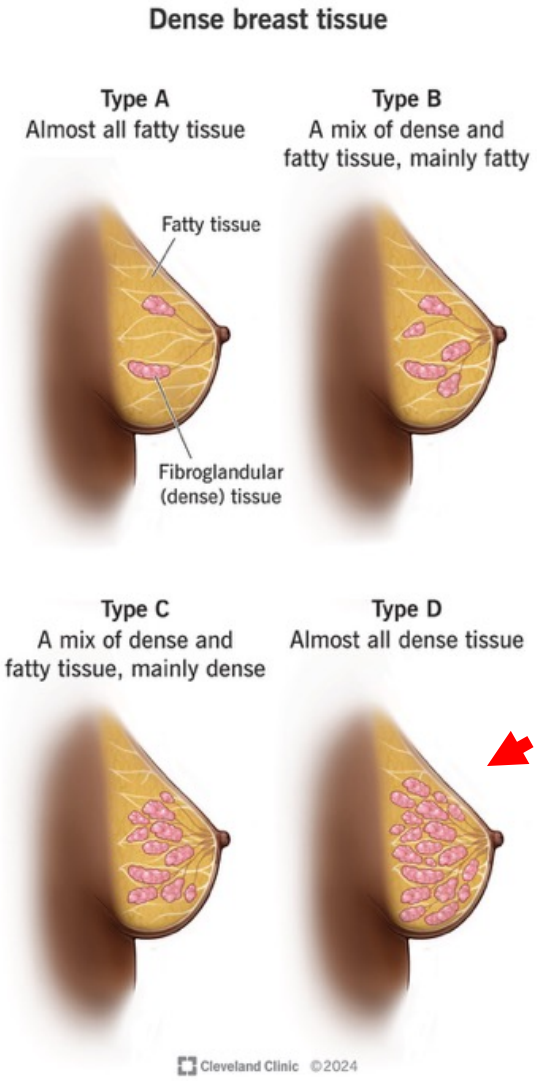

Ultrasound

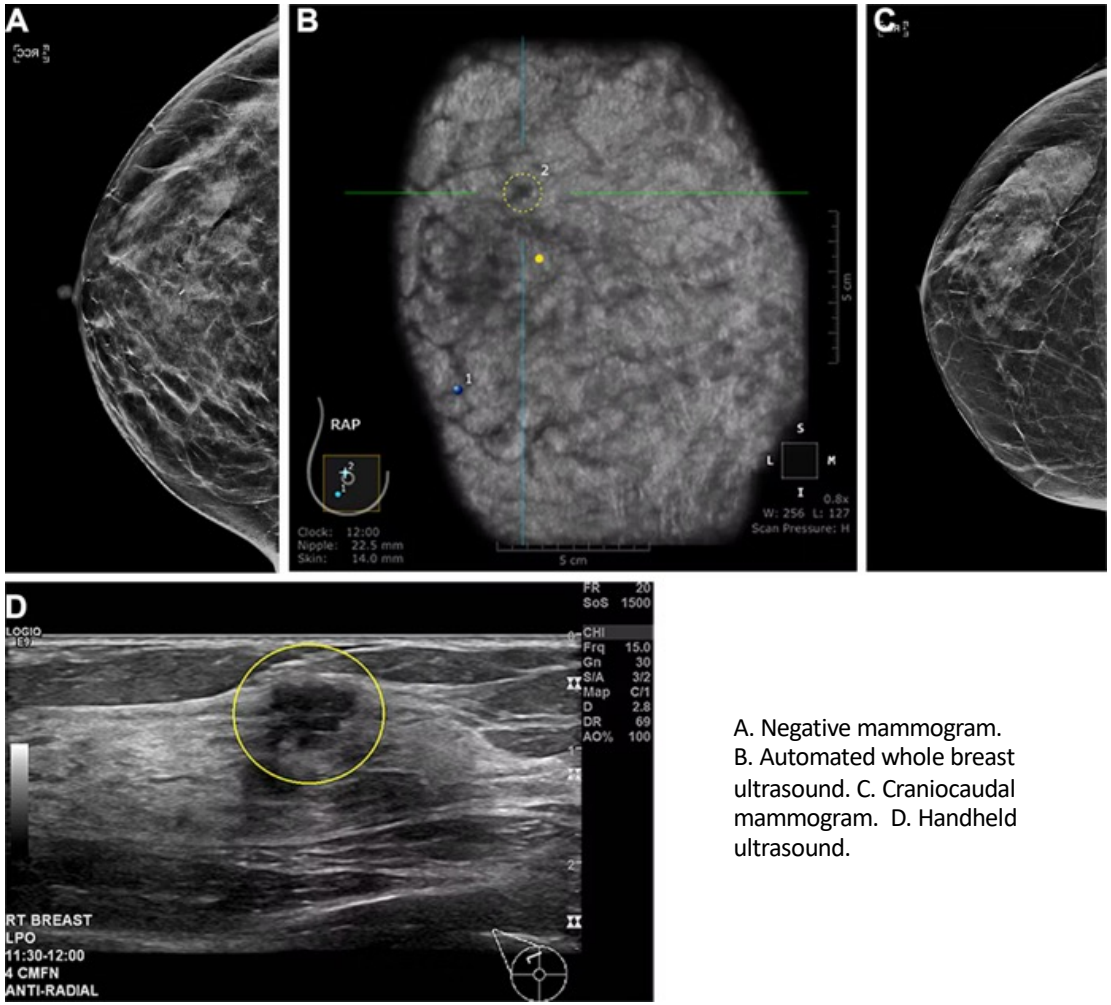

A. Negative mammogram. B. Automated whole breast ultrasound. C. Craniocaudal mammogram. D. Handheld ultrasound.

Cumulative incidence of advanced breast cancer in women aged 40–49 years in the Japan Strategic Anti-cancer Randomised Trial (J-START) of adjunctive ultrasonography: a prespecified secondary analysis

Summary

Background The J-START randomised controlled trial found that adjunctive ultrasonography was associated with significantly higher rates of breast cancer detection than mammography alone. This report aims to evaluate the long-term effect of adjunctive ultrasonography screening on the cumulative incidence of advanced breast cancer as a prespecified secondary outcome of J-START.

Methods We enrolled asymptomatic women in 42 study sites in 23 of 47 prefectures in Japan. Eligible women were aged 40–49 years without a history of breast cancer, including in-situ cancer, or other cancers in the previous 5 years, and who had a life expectancy of more than 5 years. Participants were assigned in a 1:1 ratio to undergo ultrasonography with mammography (intervention group) or mammography alone (control group) twice during a 2-year screening period by individual or cluster randomisation. Participants attended an initial screening appointment and were then asked to return for a second screening after 2 years. This prespecified secondary analysis assessed the cumulative incidence of stage 2 or higher breast cancers based on the TNM classification up to data cutoff on Oct 4, 2024.

Findings Between Aug 2, 2007, and March 31, 2011, 72 661 asymptomatic women aged 40–49 years were randomly assigned (36 723 in the intervention group and 35 938 in the control group). Median follow-up for this secondary analysis was 11·4 years (range 0·0–16·1; IQR 9·3–12·9) in the intervention group and 11·3 years (0·0–16·1; 8·9–12·9) in the control group. Of 894 breast cancers detected in the intervention group, 234 (26%) were advanced cancers, compared with 277 (33%) of 843 detected breast cancers in the control group (hazard ratio 0·83 [95·6% CI 0·70–0·98]; p=0·026). Kaplan–Meier curves suggested a violation of the proportional hazards assumption, with a significant difference in advanced cancer incidence only between 48 months and 96 months. Divergence between groups emerged around year four, widened until year eight, and remained stable thereafter.

Interpretation Adjunctive ultrasonography reduced the cumulative incidence of advanced breast cancer in women aged 40–49 years. These findings highlight the potential value of integrating adjunctive ultrasonography into screening programmes for women with dense breast tissue, particularly in Asian populations, and could inform future breast cancer screening guidelines.

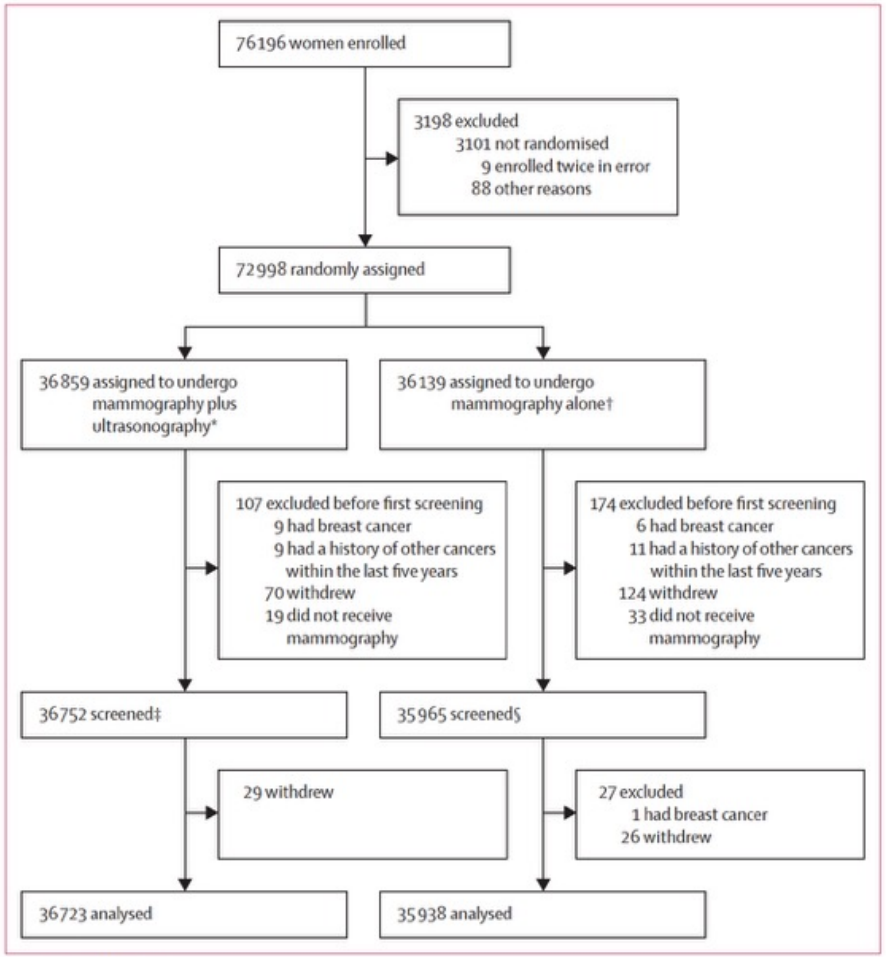

Figure 1: **Trial profile**
Japanese women aged 40–49 years were enrolled and randomly assigned in a 1:1 ratio to undergo mammography with ultrasonography (intervention) or mammography alone (control) every 2 years. *26 434 enrolled by individual randomisation and 10 245 by cluster randomisation. †26 411 enrolled by individual randomisation and 9278 by cluster randomisation. ‡Four women did not undergo ultrasonography. §Five women underwent ultrasonography.

	All participants (n=72 661)	Intervention group (n=36 723)	Control group (n=35 938)
Age at randomisation (years)	44·0 (5·0)	44·0 (5·0)	44·0 (5·0)
Ever undergone breast cancer screening			
Yes	55 798 (76·8%)	28 289 (77·0)	27 509 (76·5%)
No	16 851 (23·2%)	8424 (22·9%)	8427 (23·4%)
Unknown or data missing	12 (<0·1%)	10 (<0·1%)	2 (<0·1%)
Method of most recent breast cancer screening			
Mammography			
Yes	39 498 (54·4%)	20 008 (54·5%)	19 490 (54·2%)
No	16 290 (22·4%)	8279 (22·5%)	8011 (22·3%)
Unknown or data missing	16 873 (23·2%)	8436 (23·0%)	8437 (23·5%)
Ultrasonography			
Yes	10 555 (14·5%)	5452 (14·8%)	5103 (14·2%)
No	45 233 (62·3%)	22 835 (62·2%)	22 398 (62·3%)
Unknown or data missing	16 873 (23·2%)	8436 (23·0%)	8437 (23·5%)
Clinical breast examination			
Yes	50 545 (69·6%)	25 652 (69·9%)	24 893 (69·3%)
No	5243 (7·2%)	2635 (7·2%)	2608 (7·3%)
Unknown or data missing	16 873 (23·2%)	8436 (23·0%)	8437 (23·5%)
Age at menarche (years)			
7–11	15 257 (21·0%)	7656 (20·8%)	7601 (21·1%)
12–13	41 653 (57·3%)	21 077 (57·4%)	20 576 (57·3%)
14–18	15 656 (21·5%)	7939 (21·6%)	7717 (21·5%)
Others or data missing	95 (0·1%)	51 (0·1%)	44 (0·1%)
Menopausal status			
Premenopausal	54 959 (75·6%)	27 715 (75·5%)	27 244 (75·8%)
Perimenopausal	13 389 (18·4%)	6774 (18·4%)	6615 (18·4%)
Postmenopausal	4269 (5·9%)	2207 (6·0%)	2062 (5·7%)
Unknown or data missing	44 (0·1%)	27 (0·1%)	17 (0·1%)
Number of pregnancies			
0	8740 (12·0%)	4423 (12·0%)	4317 (12·0%)
1	8802 (12·1%)	4500 (12·3%)	4302 (12·0%)
2	25 206 (34·7%)	12 650 (34·4%)	12 556 (34·9%)
3–4	24 083 (33·1%)	12 233 (33·3%)	11 850 (33·0%)
5–10	3422 (4·7%)	1752 (4·8%)	1670 (4·6%)
Unknown or data missing	2408 (3·3%)	1165 (3·2%)	1243 (3·5%)

(Table 1 continues in next column)

	All participants (n=72 661)	Intervention group (n=36 723)	Control group (n=35 938)
(Continued from previous column)			
Number of pregnancies delivered			
Nulliparous	9493 (13·1%)	4849 (13·2%)	4644 (12·9%)
1	11 010 (15·2%)	5559 (15·1%)	5451 (15·2%)
2	32 119 (44·2%)	16 164 (44·0%)	15 955 (44·4%)
3	14 969 (20·6%)	7635 (20·8%)	7334 (20·4%)
4–8	2155 (3·0%)	1090 (3·0%)	1065 (3·0%)
Unknown or data missing	2915 (4·0%)	1426 (3·9%)	1489 (4·1%)
Age at first birth (years)			
<20	675 (0·9%)	354 (1·0%)	321 (0·9%)
20–24	14 594 (20·1%)	7465 (20·3%)	7129 (19·8%)
25–29	28 461 (39·2%)	14 387 (39·2%)	14 074 (39·2%)
30–39	15 792 (21·7%)	7883 (21·5%)	7909 (22·0%)
40–49	430 (0·6%)	222 (0·6%)	208 (0·6%)
Unknown or data missing	12 709 (17·5%)	6412 (17·5%)	6297 (17·5%)
Ever breastfed children			
Yes	56 183 (77·3%)	28 415 (77·4%)	27 768 (77·3%)
No	14 953 (20·6%)	7575 (20·6%)	7378 (20·5%)
Unknown or data missing	1525 (2·1%)	733 (2·0%)	792 (2·2%)
Number of first-degree female relatives with breast cancer			
0	69 250 (95·3%)	34 960 (95·2%)	34 290 (95·4%)
1	3342 (4·6%)	1726 (4·7%)	1616 (4·5%)
>1	69 (0·1%)	37 (0·1%)	32 (0·1%)
Ever had breast surgery	1462 (2·0%)	754 (2·1%)	708 (2·0%)
Ever had benign neoplasm	917 (1·3%)	489 (1·3%)	428 (1·2%)
Ever had breast inflammation	538 (0·7%)	264 (0·7%)	274 (0·8%)

Table 1: **Demographic characteristics**

	Intervention group (n=894)					Control group (n=843)				
	1st round (n=198)	1st round interval cancers (n=36)	2nd round (n=105)	Other period (n=555)	Total (n=894)	1st round (n=124)	1st round interval cancers (n=49)	2nd round (n=80)	Other period (n=590)	Total (n=843)
Early cancers	151 (76·3%)	19 (52·7%)	84 (80·0%)	392 (70·6%)	646 (72·3%)	78 (62·9%)	32 (65·4%)	57 (71·3%)	384 (65·1%)	551 (65·4%)
Stage 0	57 (28·8%)	7 (19·4%)	30 (28·6%)	116 (20·9%)	210 (23·5%)	31 (25·0%)	9 (18·4%)	18 (22·5%)	119 (20·2%)	177 (21·0%)
Stage 1	94 (47·5%)	12 (33·3%)	54 (51·4%)	276 (49·7%)	436 (48·8%)	47 (37·9%)	23 (47·0%)	39 (48·8%)	265 (44·9%)	374 (44·4%)
Advanced cancers	44 (22·2%)	17 (47·3%)	21 (20·0%)	152 (27·4%)	234 (26·1%)	45 (36·3%)	16 (32·6%)	23 (28·7%)	193 (32·7%)	277 (32·8%)
Stage 2	33 (16·7%)	14 (38·9%)	18 (17·1%)	121 (21·8%)	186 (20·8%)	37 (29·8%)	13 (26·5%)	20 (25·0%)	163 (27·6%)	233 (27·6%)
Stage 3	10 (5·0%)	2 (5·6%)	2 (1·9%)	25 (4·5%)	39 (4·3%)	6 (4·9%)	3 (6·1%)	3 (3·7%)	26 (4·4%)	38 (4·5%)
Stage 4	1 (0·5%)	1 (2·8%)	1 (1·0%)	6 (1·1%)	9 (1·0%)	2 (1·6%)	0	0	4 (0·7%)	6 (0·7%)
Unknown	3 (1·5%)	0	0	11 (2·0%)	14 (1·6%)	1 (0·8%)	1 (2·0%)	0	13 (2·2%)	15 (1·8%)
Number of deaths*	..	..	..	..	297 (100%)	..	..	..	..	280 (100%)
Breast cancer	..	..	..	..	21 (7·1%)	..	..	..	..	21 (7·5%)
Any cause	..	..	..	..	223 (75·1%)	..	..	..	..	207 (73·9%)
Unknown	..	..	..	..	53 (17·8%)	..	..	..	..	52 (18·6%)

*Percentages in the stage-distribution section are calculated using the total number of breast cancer cases in each period as the denominator. Percentages in the deaths section are calculated using total deaths in each group (297 in the intervention group and 280 in the control group) as the denominator.

Table 2: **Stage distribution of breast cancer and number of deaths stratified by cause**

Advanced breast cancer (can the numbers be reduced?)

Overall breast cancer

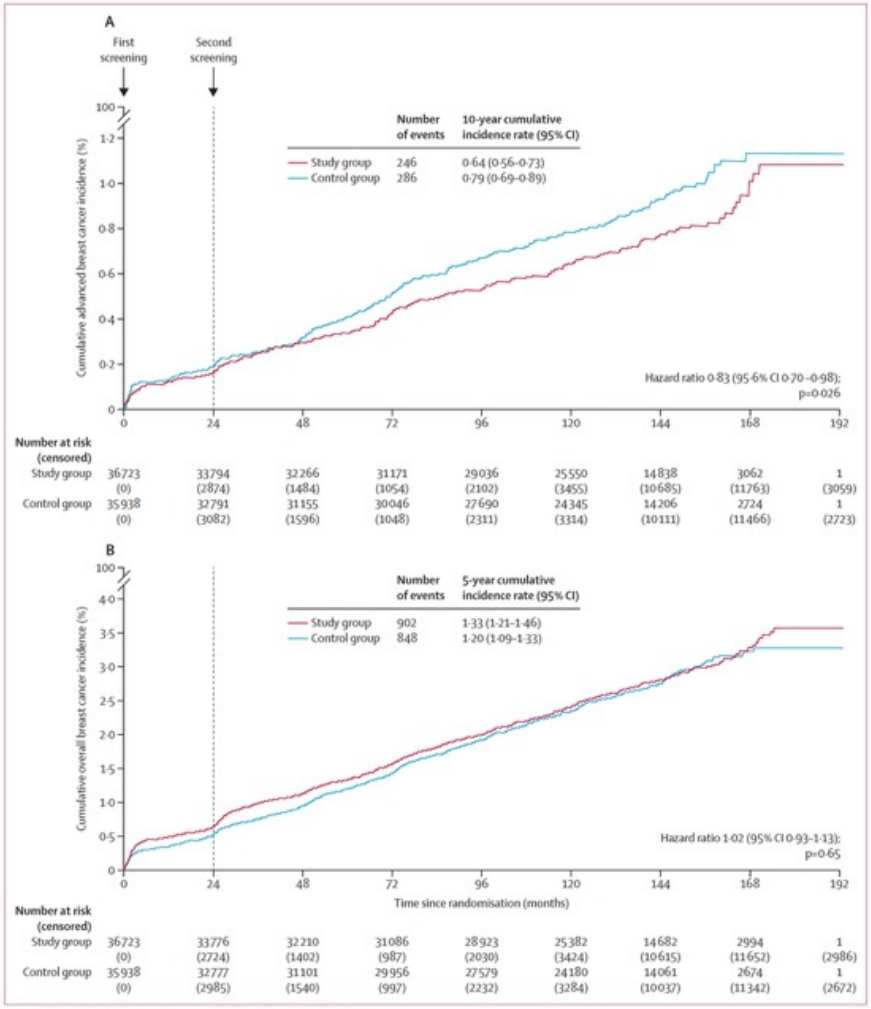

Figure 2: **Kaplan-Meier curve for cumulative incidence of breast cancer**
(A) Cumulative incidence of advanced breast cancer in the intervention group (red) and control group (blue). The graph shows the percentage of patients who were diagnosed with advanced breast cancer or who died due to breast cancer of unknown stage (y-axis) over a follow-up period of 192 months (x-axis). (B) Cumulative incidence of overall breast cancer in the intervention group (red) and control group (blue). The graph shows the percentage of patients who were diagnosed with breast cancer (y-axis) or who died over a follow-up period of 192 months (x-axis). Arrows indicate the timing of the first and second screenings. Numbers below the graph indicate the number of participants at risk and number of events at different timepoints for both groups.

Research in context

Evidence before this study

We searched the Cochrane Database of Systematic Reviews, which published a comprehensive analysis in 2023 evaluating the added value of ultrasonography to mammography in breast cancer screening. The review included eight studies: two prospective cohort studies, five retrospective cohort studies, and one randomised controlled trial (J-START), which was assessed to have low risk of bias. To identify any additional randomised controlled trials published since then, we conducted an updated search of the Cochrane Database of Systematic Reviews, as well as MEDLINE and PubMed on Aug 5, 2025 for studies published between Nov 22, 2014, and Aug 5, 2025, using keywords related to "breast cancer", "screening", "mammography", "ultrasound", and "randomised controlled trial". This search identified the BRAID trial, in which abbreviated MRI and contrast mammography detected three times more invasive cancers than automated whole breast ultrasound. BRAID differs from J-START in age, modality, and follow-up.

Added value of this study

This report presents the extended follow-up results of J-START, a large-scale randomised controlled trial investigating the effect of adjunctive ultrasonography in breast cancer screening among women aged 40–49 years. Unlike previous reports, this analysis focused specifically on the cumulative incidence of advanced breast cancer. Our findings show that the addition of ultrasonography significantly reduced the incidence of advanced breast cancer for up to 8 years following the second screening. The study included 72 661 women followed up over more than 15 years (Aug 2, 2007, to Oct 4, 2024), with a minimal loss to follow-up. These results suggest that adjunctive ultrasonography with mammography is a highly effective strategy for the early detection of breast cancer in Asian women aged between 40 and 49 years with dense breast tissue, who are the target population of J-START.

Implications of all the available evidence

This study is the first randomised controlled trial to show a reduction in the cumulative incidence of advanced breast cancer, which could translate into decreased breast cancer mortality in the future. In cancer screening trials, mortality is often the most important endpoint; however, the favourable prognosis of breast cancer limits the number of mortality events that can be observed within a short follow-up period. Despite the fact that an observed reduction in advanced cancer might suggest a potential decline in mortality, the validity of using advanced cancer incidence as a surrogate endpoint remains under debate. Although current evidence is still limited, our findings might contribute to the use of advanced breast cancer incidence as a potential surrogate indicator. Continued follow-up is warranted to confirm whether adjunctive ultrasonography reduces breast cancer mortality.

Fibroblast Growth Factor 21 (FGF21) ist ein metabolisches Hormon, das hauptsächlich in der Leber produziert wird und den Zucker- sowie Fettstoffwechsel reguliert. Es fördert die Insulinsensitivität, wirkt gewichtsreduzierend, entzündungshemmend und gilt als potenzielles „Verjüngungshormon“. FGF21 wird durch Fasten, Sport (Krafttraining) und spezielle Ernährungsweisen (weniger tierisches Eiweiß) angeregt.

Wichtige Eigenschaften von FGF21:

- **Stoffwechselregulation:** FGF21 verbessert die Glukoseaufnahme, senkt Triglyceride und steigert den Energieverbrauch.
- **Gesundheitseffekte:** Es fördert die Herz-Kreislauf-Gesundheit, wirkt der Fettleibigkeit entgegen und schützt vor Diabetes.
- **Appetitkontrolle:** FGF21 kann das Verlangen nach Süßem und Alkohol reduzieren.
- **FGF21-Resistenz:** Bei adipösen Patienten können trotz erhöhter Spiegel im Blut Anzeichen einer Resistenz auftreten, was auf eine verringerte Wirkung hindeutet.
- **Therapeutisches Potenzial:** Aufgrund seiner Fähigkeit, Stoffwechselstörungen zu korrigieren, wird FGF21 als Wirkstoff zur Behandlung von Adipositas und Typ-2-Diabetes erforscht.

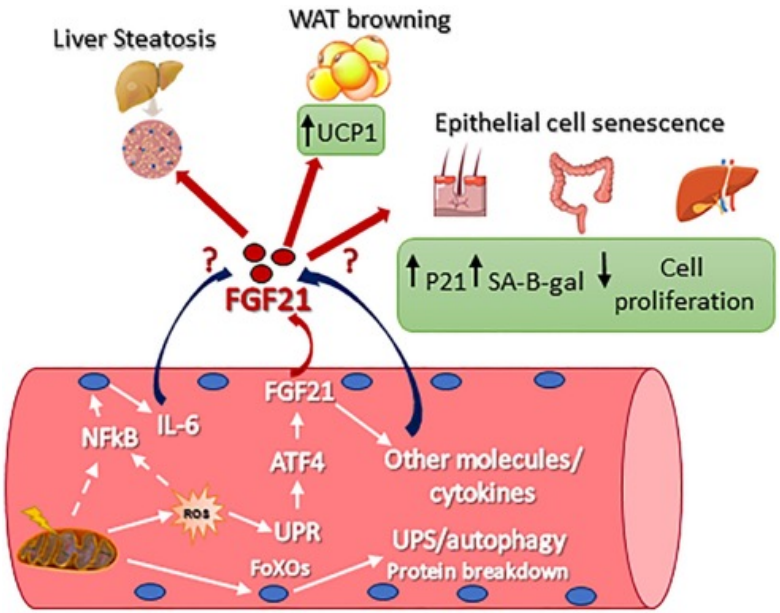

Efimosfermin alfa (BOS-580) once per month in people with metabolic dysfunction-associated steatohepatitis with F2 or F3 fibrosis: results from a 24-week, randomised, double-blind, placebo-controlled, phase 2 trial

Summary

Background The growing prevalence of metabolic dysfunction-associated steatohepatitis (MASH) underscores the unmet need for effective and safe liver-targeted therapies to prevent fibrosis and disease progression. The aim of this study was to evaluate the efficacy and safety of efimosfermin alfa (henceforth referred to as efimosfermin, formerly BOS-580), an FGF21 analogue taken once per month, in patients with MASH and moderate or advanced fibrosis.

Methods This 24-week, randomised, double-blind, placebo-controlled, phase 2 trial evaluated the safety and efficacy of efimosfermin in participants aged 18–75 years with a BMI of at least 27 kg/m² and MASH and F2 or F3 fibrosis present on a diagnostic liver biopsy done either during screening or within 6 months before the first day of dosing, and total activity Nonalcoholic Fatty Liver Disease Activity Score (NAS) of at least 4 with a minimum score of 1 point for all three NAS components (steatosis, hepatocyte ballooning, and lobular inflammation). The trial was conducted at 34 clinical research study sites in the USA. Participants were randomly assigned 1:1 to efimosfermin 300 mg or placebo administered by subcutaneous injection every 4 weeks (Q4W) over 24 weeks, stratified by MASH fibrosis stage (F2 *vs* F3 stage). Participants, investigators, and those assessing outcomes were masked to group assignment. The primary endpoint was safety and tolerability (ie, treatment-emergent adverse events, changes from baseline to week 24 in blood pressure and heart rate, and the incidence of grade 3 and grade 4 laboratory abnormalities at week 24), analysed in all participants who received at least one dose. This trial is registered with ClinicalTrials.gov (NCT04880031) and was completed on Sept 18, 2024.

Findings Between May 4, 2023, and March 22, 2024, of 1171 participants screened, 84 participants were randomly assigned to efimosfermin 300 mg Q4W (n=43) or placebo (n=41); 44 (52%) were female and 40 (48%) were male. 48 (57%) had F2 fibrosis and 36 (43%) had F3 fibrosis; 65 had evaluable week-24 biopsy results. All 43 in the efimosfermin group and 40 of 41 participants in the placebo group received at least one dose. Adverse events were reported in 29 (67%) of 43 participants receiving efimosfermin and 22 (55%) of 40 receiving placebo. The majority of treatment-emergent adverse events were mild (24 [56%] of 43 in the efimosfermin group *vs* 15 [38%] of 40 in the placebo group) or moderate (18 [42%] *vs* 14 [35%]) in severity. Most frequent adverse events were gastrointestinal events, which were transient and occurred within the first few weeks of treatment. There were no clinically meaningful changes in vital signs between treatment and placebo groups, and no clinically significant grade 3 or higher laboratory abnormalities observed for either group. No deaths or adverse events greater than grade 3 were observed during the study.

Interpretation In this phase 2 trial, treatment with efimosfermin once per month was generally well tolerated in participants with biopsy-confirmed MASH and F2 or F3 fibrosis. These results support the further development of efimosfermin for treatment of MASH-related fibrosis.

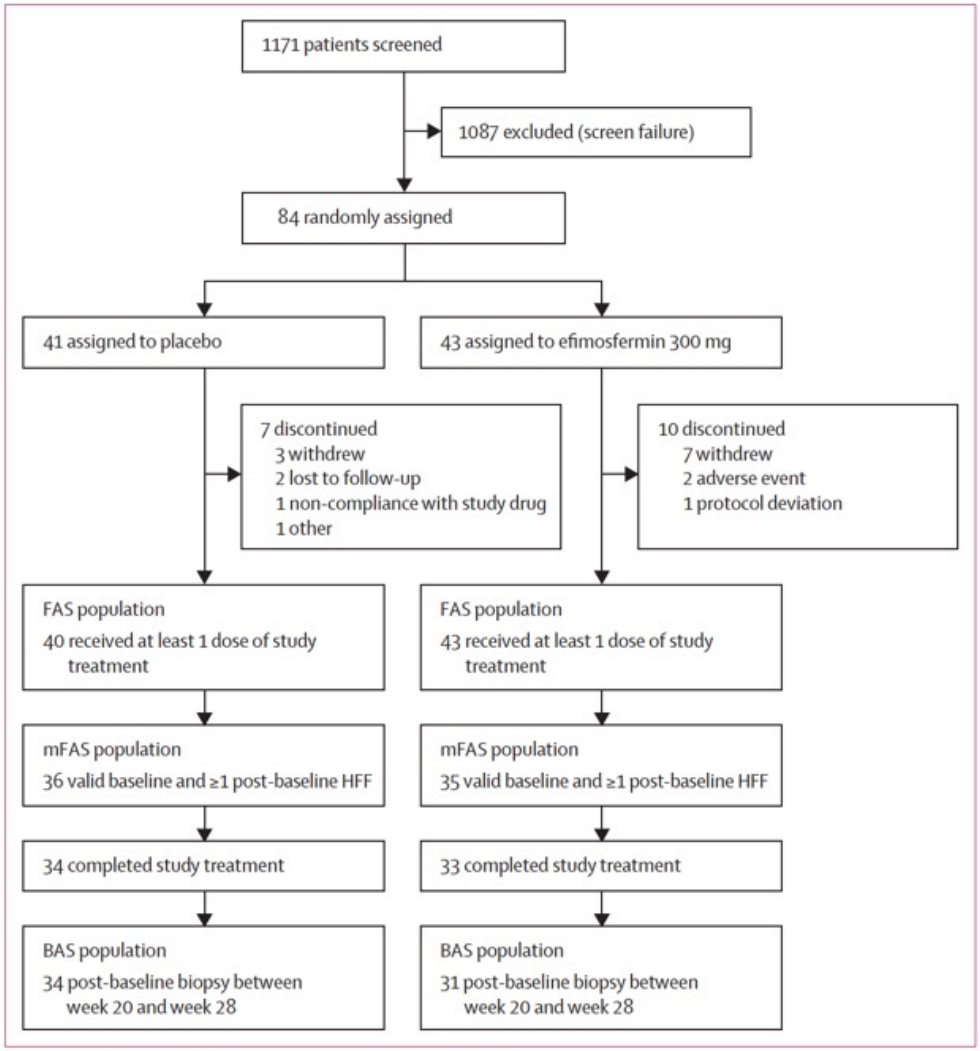

Figure 1: **Participant disposition (CONSORT flow diagram)**
BAS=biopsy analysis set. FAS=full analysis set. mFAS=modified full analysis set.

	Placebo (n=41)	Efimosfermin 300 mg Q4W (n=43)	Total (N=84)
Age, years	54·6 (10·2)	52·9 (11·7)	53·7 (10·9)
Sex, female*	21 (51%)	23 (53%)	44 (52%)
Sex, male*	20 (49%)	20 (47%)	40 (48%)
Ethnicity			
Hispanic or Latino	34 (83%)	28 (65%)	62 (74%)
Not Hispanic or Latino	7 (17%)	15 (35%)	22 (26%)
Race†			
American Indian or Alaska Native	0	1 (2%)	1 (1%)
Black or African American	1 (2%)	0	1 (1%)
White	36 (88%)	40 (93%)	76 (90%)
Other	4 (10%)	2 (5%)	6 (7%)
Weight, kg	103·2 (17·6)	106·5 (20·2)	104·9 (18·9)
BMI, kg/m²	37·2 (6·0)	37·5 (5·7)	37·3 (5·8)
Type 2 diabetes	20 (49%)	28 (65%)	48 (57%)
HbA_{1c}, mean percentage (SD)	6·4% (1·1)	6·7% (1·1)	6·6% (1·1)
Liver histology			
Fibrosis stage, F2‡	23 (56%)	25 (58%)	48 (57%)
Fibrosis stage, F3‡	18 (44%)	18 (42%)	36 (43%)
NAS	5·1 (0·9)	5·1 (0·9)	5·1 (0·9)
HFF, mean percentage (SD)	21·2% (6·5)	19·6% (8·3)	20·4% (7·5)
Pro-C3, ng/mL	56·3 (20·7)	49·6 (16·8)	52·9 (19·0)
VCTE LSM, kPa	12·1 (3·9)	11·4 (3·0)	11·7 (3·5)
ALT, IU/L	57·0 (25·3)	63·5 (44·1)	60·3 (36·1)
AST, IU/L	43·1 (18·0)	51·4 (37·7)	47·3 (29·9)
Adiponectin, µg/L	4078·3 (2147·6)	4227·9 (2479·4)	4154·0 (2308·5)
Triglycerides, mmol/L	2·3 (1·4)	1·8 (0·7)	2·0 (1·1)
HDL-C, mmol/L	1·2 (0·3)	1·2 (0·3)	1·2 (0·3)
LDL-C, mmol/L	2·9 (0·9)	2·7 (1·0)	2·8 (1·0)
Total cholesterol, mmol/L	5·1 (1·2)	4·7 (1·1)	4·9 (1·1)
Concomitant medications			
Antihypertensive	27 (66%)	17 (40%)	44 (53%)
Antidiabetic	18 (44%)	24 (56%)	42 (50%)
Lipid lowering	13 (32%)	14 (33%)	27 (32%)

Data are mean (SD) or n (%) unless otherwise stated. ALT=alanine aminotransferase. AST=aspartate aminotransferase. EAS=enrolled analysis set. HbA_{1c}=glycated haemoglobin. HFF=hepatic fat fraction. Pro-C3=N-terminal propeptide of type 3 collagen. NAS=Nonalcoholic Fatty Liver Disease Activity Score. Q4W=every 4 weeks. VCTE LSM=vibration-controlled transient elastography liver stiffness measurement. *Sex was defined on the basis of a binary categorisation (male or female) that is usually designated at birth and generally refers to a set of biological attributes that are associated with physical and physiological features. †Race was defined on the basis of standard racial categories and was captured via self-report. ‡All participants were either fibrosis stage 2 (F2) or stage 3 (F3).

Table 1: **Participant demographics and baseline clinical characteristics (EAS population)**

	Placebo (n=40)	Efimosfermin 300 mg Q4W (n=43)	Total (N=83)
Any adverse event	22 (55%)	29 (68%)	51 (61%)
Any serious adverse event	0	2 (5%)*	2 (2%)
Any adverse event leading to discontinuation of efimosfermin 300 mg or placebo	0	2 (5%)†	2 (2%)
Any adverse event by severity			
Grade 1 mild	15 (38%)	24 (56%)	39 (47%)
Grade 2 moderate	14 (35%)	18 (42%)	32 (39%)
Grade 3 severe	0	2 (5%)	2 (2%)
Grade 4 life-threatening consequences	0	0	0
Grade 5 death related to adverse event	0	0	0
Any adverse event leading to death	0	0	0
Most frequent (≥10%) treatment-emergent adverse events			
Nausea	5 (13%)	14 (33%)	19 (23%)
Diarrhoea	3 (8%)	10 (23%)	13 (16%)
Vomiting	1 (3%)	7 (16%)	8 (10%)

Data are n (%). Participants were only counted once per system organ class and preferred term. FAS=full analysis set. Q4W=every 4 weeks. *One participant with biliary colic (grade 3) and one participant with gastritis (grade 3, considered to be non-drug related by the investigator). †One participant with abdominal pain, nausea, and vomiting and one participant with dehydration.

Table 2: **Adverse events (FAS population)**

Fibrosis improvement

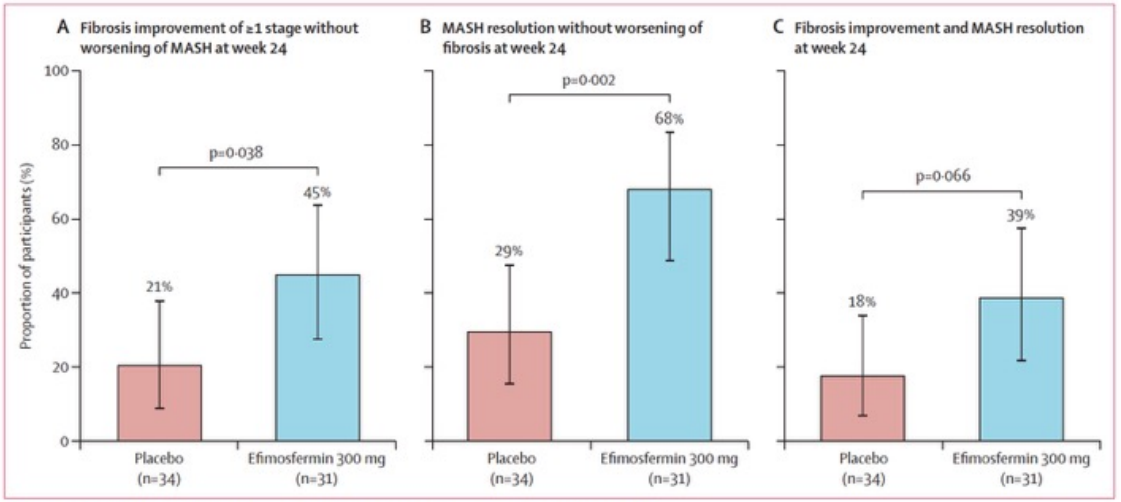

Figure 2: **Proportion of participants reaching histology endpoints at week 24 (BAS population)**
(A) Proportion of participants with improvement in liver fibrosis by at least one stage and no worsening of steatohepatitis (defined as no increase in NAS for ballooning, inflammation, or steatosis) at week 24. (B) Proportion of participants with MASH resolution (defined as NAS of 0 for ballooning and 0–1 for inflammation) without worsening of fibrosis at week 24. (C) Proportion of participants who achieved fibrosis improvement and MASH resolution at week 24. p values comparing efimosfermin 300 mg response rates to placebo response rates were estimated by Cochran–Mantel–Haenszel tests stratified by baseline fibrosis stage. Error bars indicate 95% CIs. BAS=biopsy analysis set. MASH=metabolic dysfunction-associated steatohepatitis. NAS=Nonalcoholic Fatty Liver Disease Activity Score.

	Placebo	Efimosfermin 300 mg Q4W
Liver fat and fibrosis biomarkers		
HFF percentage*†		
Number of patients	31	34
Absolute least-squares mean change from baseline (SE) at week 28, percentage points	−2·8 (1·1)	−10·8 (1·0)
95% CI	−4·9 to −0·6	−12·9 to −8·8
Least-squares mean treatment difference (95% CI), percentage points	−8·1 (−11·0 to −5·1)	..
p value	<0·001	..
Relative least-squares mean change from baseline (SE) at week 28, percentage points	−15·6 (4·9)	−49·4 (4·7)
95% CI	−25·3 to −5·8	−58·7 to −40·1
Least-squares mean treatment difference (95% CI), percentage points	−33·8 (−47·4 to −20·2)	..
p value	<0·001	..
Pro-C3 percentage†‡§		
Number of patients	33	31
Absolute least-squares mean change from baseline (SE) at week 24, percentage points	−10·6 (2·2)	−24·4 (2·3)
95% CI	−15·0 to −6·2	−28·9 to −19·8
Least-squares mean treatment difference (95% CI), percentage points	−13·8 (−20·2 to −7·3)	..
p value	<0·001	..
Relative least-squares mean change from baseline (SE) at week 24, percentage points	−16·6 (4·2)	−44·6 (4·4)
95% CI	−25·1 to −8·1	−53·4 to −35·9
Least-squares mean treatment difference (95% CI), percentage points	−28·0 (−40·3 to −15·7)	..
p value	<0·001	..
VCTE LSM†‡, kPA		
Number of patients	33	37
Absolute least-squares mean change from baseline (SE) at week 28, kPA	−1·5 (0·6)	−1·9 (0·6)
95% CI	−2·7 to −0·3	−3·0 to −0·7
Least-squares mean treatment difference (95% CI), kPA	−0·4 (−2·1 to 1·3)	..
p value	0·64	..

(Table 3 continues in next column)

(Continued from previous column)

	Placebo	Efimosfermin 300 mg Q4W
Relative least-squares mean change from baseline (SE) at week 28, kPA	−9·3 (4·8)	−16·4 (4·5)
95% CI	−18·9 to 0·3	−25·5 to −7·3
Least-squares mean treatment difference (95% CI), kPA	−7·1 (−20·4 to 6·2)	..
p value	0·29	..
ELF score†‡		
Number of patients	31	32
Absolute least-squares mean change from baseline (SE) at week 24	−0·2 (0·1)	−0·7 (0·1)
95% CI	−0·5 to 0·0	−0·9 to −0·5
Least-squares mean treatment difference (95% CI)	−0·5 (−0·8 to −0·2)	..
p value	0·005	..
Cardiometabolic biomarkers		
Adiponectin†‡, µg/L		
Number of patients	33	31
Absolute least-squares mean change from baseline (SE) at week 24, µg/L	13·7 (409·6)	2988·6 (422·6)
95% CI	−805·3 to 832·7	2143·6 to 3833·6
Least-squares mean treatment difference (95% CI), µg/L	2975·0 (1798·1 to 4151·8)	..
p value	<0·001	..
Relative least-squares mean change from baseline (SE) at week 24, µg/L	−0·9 (6·1)	68·3 (6·3)
95% CI	−13·1 to 11·2	55·8 to 80·9
Least-squares mean treatment difference (95% CI), µg/L	69·3 (51·8 to 86·7)	..
p value	<0·001	..
HbA_{1c} percentage†‡		
Number of patients	33	31
Absolute least-squares mean change from baseline (SE) at week 24, percentage points	0·0 (0·1)	−0·4 (0·1)
95% CI	−0·2 to 0·3	−0·6 to −0·1
Least-squares mean treatment difference (95% CI), percentage points	−0·4 (−0·8 to 0·0)	..
p value	0·041	..

(Table 3 continues in next column)

(Continued from previous column)

	Placebo	Efimosfermin 300 mg Q4W
Triglycerides†‡, mmol/L		
Number of patients	33	31
Absolute least-squares mean change from baseline (SE) at week 24, mmol/L	0·0 (0·1)	−0·5 (0·1)
95% CI	−0·3 to 0·2	−0·7 to −0·2
Least-squares mean treatment difference (95% CI), mmol/L	−0·4 (−0·8 to 0·0)	..
p value	0·030	..
Relative least-squares mean change from baseline (SE) at week 24, mmol/L	5·2 (6·8)	−20·6 (7·0)
95% CI	−8·4 to 18·8	−34·6 to −6·6
Least-squares mean treatment difference (95% CI), mmol/L	−25·8 (−45·6 to −6·1)	..
p value	0·011	..
HDL cholesterol†‡, mmol/L		
Number of patients	32	31
Absolute least-squares mean change from baseline (SE) at week 24, mmol/L	0·0 (0·0)	0·2 (0·0)
95% CI	−0·1 to 0·0	0·1 to 0·2
Least-squares mean treatment difference (95% CI), mmol/L	0·2 (0·1 to 0·3)	..
p value	<0·001	..
Relative least-squares mean change from baseline (SE) at week 24, mmol/L	−2·6 (2·5)	16·4 (2·5)
95% CI	−7·6 to 2·3	11·4 to 21·4
Least-squares mean treatment difference (95% CI), mmol/L	19·1 (12·1 to 26·1)	..
p value	<0·001	..
LDL cholesterol†‡, mmol/L		
Number of patients	30	31
Absolute least-squares mean change from baseline (SE) at week 24, mmol/L	−0·1 (0·1)	−0·1 (0·1)
95% CI	−0·3 to 0·2	−0·3 to 0·1
Least-squares mean treatment difference (95% CI), mmol/L	−0·1 (−0·4 to 0·3)	..
p value	0·76	..
Relative least-squares mean change from baseline (SE) at week 24, mmol/L	3·5 (4·6)	−0·5 (4·5)
95% CI	−5·7 to 12·6	−9·5 to 8·4
Least-squares mean treatment difference (95% CI), mmol/L	−4·0 (−16·9 to 8·9)	..
p value	0·54	..

(Table 3 continues in next column)

(Continued from previous column)

	Placebo	Efimosfermin 300 mg Q4W
Total cholesterol†‡, mmol/L		
Number of patients	32	31
Absolute least-squares mean change from baseline (SE) at week 24, mmol/L	−0·1 (0·1)	−0·2 (0·1)
95% CI	−0·4 to 0·2	−0·4 to 0·1
Least-squares mean treatment difference (95% CI), mmol/L	0·0 (−0·4 to 0·3)	..
p value	0·85	..
Relative least-squares mean change from baseline (SE) at week 24, mmol/L	−0·7 (2·7)	−1·6 (2·7)
95% CI	−6·0 to 4·7	−7·0 to 3·8
Least-squares mean treatment difference (95% CI), mmol/L	−1·0 (−8·7 to 6·7)	..
p value	0·80	..
Bodyweight, kg		
Number of patients	40	43
Absolute least-squares mean change from baseline (SE) at week 24, kg	−1·0 (0·1)	−1·5 (0·9)
95% CI	−2·7 to 0·7	−3·2 to 0·2
Least-squares mean treatment difference (95% CI), kg	−0·5 (−2·9 to 2·0)	..
p value	0·70	..
Relative least-squares mean change from baseline (SE) at week 24, kg	−1·1 (0·8)	−1·5 (0·8)
95% CI	−2·8 to 0·5	−3·1 to 0·1
Least-squares mean treatment difference (95% CI), kg	−0·4 (−2·7 to 1·9)	..
p value	0·75	..

The p values reflect the comparison of the least-squares mean change (or percent change) between placebo and efimosfermin groups. ALT=alanine aminotransferase. AST=aspartate aminotransferase. ELF=Enhanced Liver Fibrosis. FAS=full analysis set. HbA_{1c}=glycated haemoglobin. HFF=hepatic fat fraction. mFAS=modified full analysis set. Pro-C3=N-terminal propeptide of type 3 collagen. Q4W=every 4 weeks. VCTE LSM=vibration-controlled transient elastography liver stiffness measurement. *Data reported from participants in the mFAS population (ie, participants in FAS with valid baseline and week 28 HFF results). †Least-squares mean, SE, 95% CI, and p values were based on ANCOVA models with change or percentage change from baseline as the dependent variable, and baseline and treatment as covariates. ‡Data reported from participants in the FAS population. §Pro-C3 values are based on the Roche Cobas e801 (Nordic BioScience) assay.

Table 3: Change from baseline at week 24 or week 28 in key liver and cardiometabolic biomarkers (mFAS and FAS populations)

Hepatic fat fraction

Reduction rate

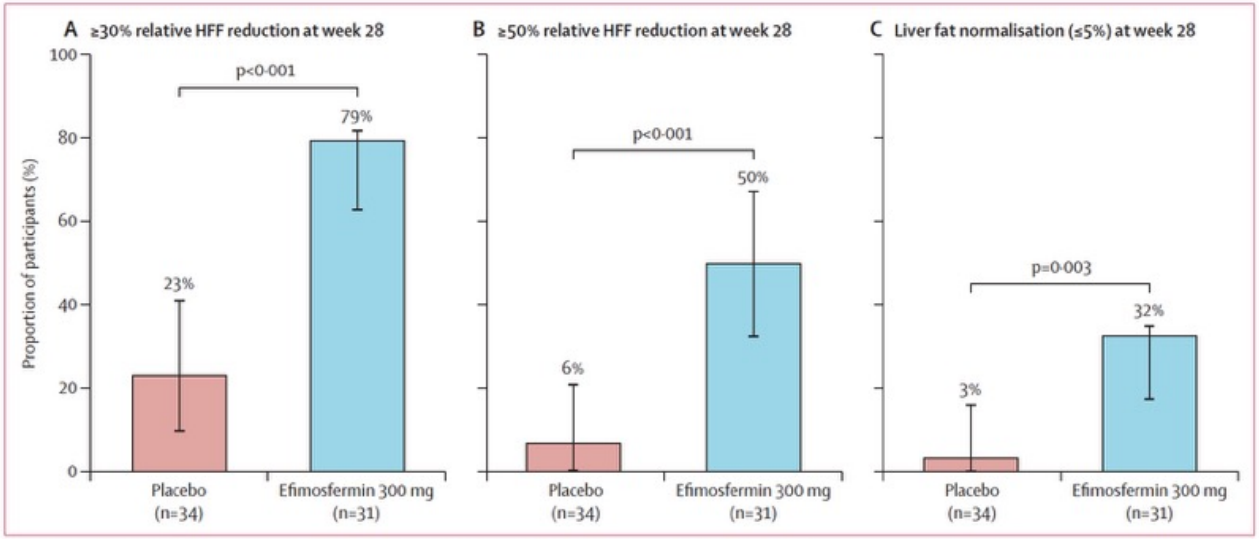

Figure 3: **Proportion of participants achieving HFF reduction thresholds and liver fat normalisation at week 28 (mFAS population)**
(A) Proportion of participants who reached at least a 30% relative HFF reduction at week 28. (B) Proportion of participants who reached at least a 50% relative HFF reduction at week 28. (C) Proportion of participants who reached liver fat normalisation (≤5%) at week 28. p values comparing efimosfermin 300 mg response rates with placebo response rates were estimated by Cochran-Mantel-Haenszel tests stratified by baseline fibrosis stage. Errors bars indicate 95% CIs, which were estimated using the binomial exact method. HFF=hepatic fat fraction. mFAS=modified full analysis set.

Research in context

Evidence before this study

We did a literature review using PubMed between Feb 17, and Feb 28, 2025, focusing on English-language clinical studies. Our search included the terms "NASH" or "NAFLD", given that Medical Subject Headings terms have not yet adopted the updated metabolic-related terminology, alongside keywords such as "fibroblast growth factor 21", "FGF21 analogue", and "FGF21 agonist" and identified 143 articles. FGF21 agonists have been shown to reduce hepatic steatosis, improve insulin sensitivity, and improve metabolic markers of disease. In clinical trials, FGF21 analogues with balanced agonism across FGFR1c, FGFR2c, and FGFR3c have further shown histological improvement in fibrosis and metabolic dysfunction-associated steatohepatitis (MASH) resolution with beneficial changes in non-invasive markers of liver and cardiometabolic health in patients with MASH. Efruxifermin, an Fc-fusion FGF21 analogue, and pegozafermin, a glycopegylated analogue, are among those evaluated in phase 2b trials with either weekly or biweekly dosing, showing antifibrotic activity within 24 weeks of treatment in patients with moderate or advanced fibrosis, or up to 96 weeks in those with compensated cirrhosis due to MASH. Published results from the phase 2a 12-week trial of once-per-month efimosfermin in phenotypic MASH reported a favourable safety profile, improvements in indicators of hepatic and metabolic health, and a significant proportion of patients who met liver fat reduction thresholds associated with histological response.

Added value of this study

This phase 2 study is the first, to our knowledge, to evaluate a once-per-month FGF21 analogue in participants with moderate-to-advanced fibrosis due to MASH. Long-acting formulations, such as efimosfermin, offer the potential to enhance patient compliance and reduce treatment burden. In the present study, participants treated with efimosfermin 300 mg Q4W reached fibrosis improvement of at least one stage without worsening of MASH, and MASH resolution without worsening of fibrosis after 24 weeks, with both histological endpoints showing statistically significant differences versus placebo. Improvements in lipids and glycaemic control, including clinically meaningful reductions in HbA_{1c} among those with type 2 diabetes, indicate a broader cardiometabolic benefit of efimosfermin beyond its hepatic effects. Efimosfermin was generally well tolerated over the 24-week treatment period.

Implications of all the available evidence

As the number of individuals affected by MASH continues to rise and treatment options remain scarce, there is a clear unmet need for therapies that are well tolerated, reduce treatment burden, and improve rates of fibrosis regression as a major determinant of liver-related outcomes. Notably, the histological and cardiometabolic improvements observed with efimosfermin once-per-month dosing were achieved over a relatively short 24-week treatment period, suggesting that longer-acting formulations are feasible and might improve long-term adherence and reduce patient burden—important considerations in the management of a serious and chronic condition such as MASH. Overall, findings from this phase 2 study support the continued development of efimosfermin as a promising therapy for MASH and warrant further investigation in phase 3 trials of longer duration.

Leprosy

Leprosy, also known as Hansen's disease, is a curable granulomatous condition caused by *Mycobacterium leprae* or *Mycobacterium lepromatosis*, disproportionately affecting impoverished communities across the globe. The bacteria's tropism for dermal histiocytes, endothelial cells, and Schwann cells causes neuronal and dermal damage that often results in disability, permanent disfigurement, stigma, and social exclusion. Despite important achievements in the understanding of the disease, its elimination has been hampered by the scarcity of sensitive diagnostic tools, sub-optimal integration and implementation of coordinated and financially stable preventive interventions, persistent stigmatisation, and failure to efficiently and sustainably address the socioeconomic and demographic factors associated with an increased risk of leprosy. In this Seminar, we provide an update on key public health and clinical aspects of the disease.

Skin, vessels, and nerves

You do not have to go to Africa to get leprosy

Panel 1: **Patient's perspective**

"My experience with getting diagnosed with leprosy has been a rough journey. I saw many doctors before a diagnosis was made; I was initially told I had lupus. At the beginning, there were a lot of medications, and I was in and out of the hospital because of chronic pain. I still have flare-ups, and it was very hard. I am a lot better now; I just have to take my medications to avoid more flare-ups. I have a lot of scars and my skin has changed colour. I stayed home for 2 years because of the way I looked; only my family knew what was going on. People would often stare at me and that's why I stayed inside for so long—because yes, I was treated differently by people who didn't know me. I have nerve damage in my right leg that I will probably always have, but I'm thankful that I'm better now, even though I still have some difficulties. It hasn't been easy; I was in deep depression for 2 years, but I am mostly recovered now that I have accepted the change of my body. I am feeling much better for the most part. There are days I can't do much because of the pain, but I just get through it." This patient is female, age 43 years, and resides in Oklahoma, USA, without history of residence or travel abroad or to any other state within the USA.

The primary facility for treating leprosy (Hansen's disease) in the USA is the National Hansen's Disease Program (NHDP) Clinical Center in Baton Rouge, Louisiana, which serves as the central hub for diagnosis, treatment, and research. While the historic Carville Leprosarium (later the Gillis W. Long Hansen's Disease Center) in Louisiana operated for over a century, the NHDP now manages a network of outpatient clinics nationwide.

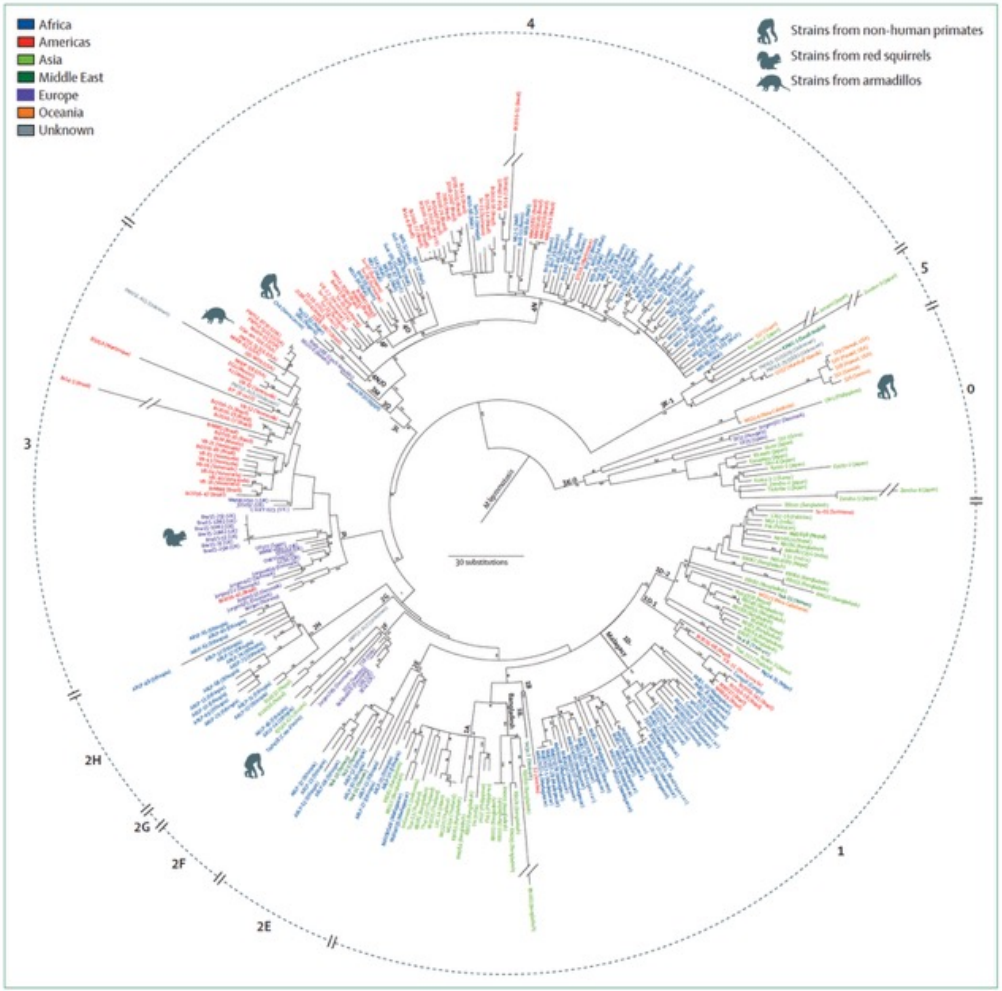

Figure 1: **Phylogenetic tree of 324 *Mycobacterium leprae* strains**
The tree was built using the Maximum Parsimony method in MEGA-X using an alignment of 4812 genome-wide homozygous single-nucleotide polymorphisms, allowing for 20% missing data. *Mycobacterium lepromatosis* was used as an outgroup. Bootstrap support was estimated from 500 replicates; branches with greater than 80% bootstrap support are denoted. Branch lengths of certain hypermutator strains (depicted by ||) are shortened for aesthetic purposes. Strains are colour-coded according to continent of origin using UN macro-geographical regions. The nine major *Mycobacterium leprae* branches are denoted in grey and the genotypes in black.

	Clinical characteristics	Pathology	Bacillary index[64]	Differential diagnosis[65]
Tuberculoid leprosy	One to three hypoesthetic or anaesthetic lesions (lesions in face can have normal sensation); hairless, and sometimes scaly erythematous plaque with raised well defined outer borders; thickened and irregular peripheral nerves can be palpable close to the lesion; cold abscesses can develop along the path of a peripheral nerve	Mature granuloma with well developed epithelioid cells with variable presence of Langhans cells surrounded by a dense lymphocyte infiltrate extending to the epidermis without an over-riding clear zone; when discernible, nerves are densely infiltrated within the granuloma	Usually 0, rarely 1+	Sarcoidosis; lupus vulgaris; granuloma annulare; pityriasis rosea; vitiligo; chromoblastomycosis; mycosis fungoides
Tuberculoid borderline leprosy	Usually, five to 25 asymmetrically distributed macules or plaques that are larger in size than tuberculoid leprosy lesions; satellite or finger-like lesions; loss of sensation is less conspicuous than tuberculoid leprosy; nerves are asymmetrically and irregularly thickened	Similar to tuberculoid leprosy except for the presence of a subepidermal clear zone; when noticeable, the nerves are densely infiltrated leading to reduced innervation	1–2+	Discoid lupus; tinea corporis; pityriasis versicolor; psoriasis; eczematous reaction; secondary syphilis; drug eruptions; anergic cutaneous leishmaniasis; post-kala-azar dermal leishmaniasis; lobomycosis; systemic lupus erythematosus; neurofibromatosis; Kaposi's sarcoma; differential diagnosis of nerve involvement: Déjérine–Sottas's disease, diabetic neuropathy, compression neuropathy, medication-induced neuropathy, and syringomyelia
Borderline-borderline leprosy	Typically, more than 25 asymmetrically distributed annular appearing macules or plaques with normal appearing skin in the centre surrounded by a well defined inner border and poorly defined outer border giving the appearance of punched out lesions; asymmetrical enlarged peripheral nerves	Epithelioid cells are scattered in the granuloma and are not contained by a lymphocyte zone; Langhans giant cells are absent; nerve bundles are easily identified with a variable degree of lymphocyte infiltration	2–3+	As for tuberculoid borderline leprosy
Borderline lepromatous leprosy	Innumerable symmetrically distributed macules and plaques with associated infiltrative nodular lesions; lack of infiltration of ear lobes, madarosis, keratitis, iritis, and normal-appearing skin between nodules which tend to dimple; enlarged peripheral nerves have a more symmetrical distribution than borderline-borderline leprosy	Histiocytes have the propensity to evolve into epithelioid cells; no foamy changes, or histiocytes with foamy changes but without clumps of acid-fact bacilli (*globi*); lymphocytes are present in the perineural cuffs or in an entire section of the granuloma; the structure of the nerve is severely affected but without increased cellularity	3–4+	As for tuberculoid borderline leprosy
Lepromatous leprosy	Widespread symmetrically distributed macules, plaques, and nodular lesions; thickened facial skin with loss of eyebrows; nasal mucosa, eyes, and larynx can be affected; symmetrical involvement or nerves can lead to so-called glove-and-stocking anaesthesia	Histiocytes are inactive and filled with host lipids (Virchow cells), associated with absence of lymphocytes; nerves show structural damage but without infiltration	4–6+	As for tuberculoid borderline leprosy

The bacterial index is the number of bacilli per oil immersion field(s). 1+: 1–10 bacilli per 100 fields; 2+: 1–10 bacilli per 10 fields; 3+: 1–10 bacilli per field; 4+: 10–100 bacilli per field; 5+: 100–1000 bacilli per field; and 6+: More than 1000 bacilli per field."

Table: **Clinicopathological correlation of disease staging according to the Ridley–Jopling classification[62,63]**

Figure 2: **Clinical spectrum of leprosy**

Diverse cutaneous and neurological manifestations of leprosy. (A) A patient with polar tuberculoid leprosy with a large solitary hypopigmented macule with ill-defined borders. (B) A patient with borderline tuberculoid leprosy with finger-like satellite lesions extending beyond the edges. (C) A patient with borderline lepromatous leprosy with large asymmetrically distributed plaques with raised erythematous borders suggestive of type 1 reversal reaction. (D) Involvement of the ulnar and median nerve with the clinical aspect of claw hand with bone involvement and loss of fingers. (E) Damage of the common peroneal nerve with ulceration on the lateral aspect of the feet with loss of digits. (F) Corresponds to a patient with polar lepromatous leprosy experiencing a type 2 reaction with painful hand oedema, dactylitis, and skin ulceration.

Clinical suspicion

Any of the following:
- Skin lesions: hypopigmented or erythematous macules or papules
- Sensory loss: diminished or absent sensation within the skin lesions; loss of thermal sensitivity usually precedes loss of tactile sensitivity
- Nerve involvement: thickened peripheral nerves, especially the ulnar, radial, median, posterior tibial, and common peroneal nerves

Multibacillary disease: more than five skin lesions, nerve involvement, or positive skin smear

Ancillary diagnostics

Slit-skin smear
- Sample typical lesions and at least six sites (both earlobes, elbows, and knees)

Skin biopsy
- Histopathological analysis aids with disease classification especially for the borderline forms

Nerve biopsy
- Better sensitivity than skin biopsy
- Invasive and can lead to irreversible nerve damage

PCR
- Most sensitive and specific assay
- Lack of availability and standardisation precludes widespread use

Serological tests
- A negative test does not exclude leprosy (especially paucibacillary disease)

High resolution ultrasound of nerves
- Can detect nerve enlargement before clinically evident
- Operator dependent

Emerging mobile technologies
- Useful in resource-constrained endemic regions

Treatment

Screening
- When feasible, consider screening for G6PD deficiency and *HLA-B**13:01 before prescribing dapsone
- Screen for HIV, latent tuberculosis, strongyloidiasis, and hepatitis B and C
- Screen for *Trypanosoma cruzi* in endemic areas of Latin America (continental America, excluding the Caribbean)

Antimicrobial treatment
- Monthly rifampicin 600 mg and clofazimine 300 mg plus daily dapsone 100 mg and clofazimine 50 mg, respectively
  - 12 months for multibacillary disease
  - 6 months for paucibacillary disease
    - Two drugs can be used: rifampicin 600 mg monthly plus dapsone 100 mg daily
  - Alternative treatment regimen should be ideally provided under research protocols

Monitor for development of reactions
- Educate patients that their development does not imply treatment failure and to seek immediate care to prevent disability

Assess nerve function and physical and psychological disability
- Provide self-care information
- Referral to rehabilitation services and surgical specialties if clinically indicated
- Promote interventions aimed at reducing stigmatisation

Contact tracing and prophylaxis
- Provide single-dose rifampicin to close contacts after exclusion of tuberculosis and active leprosy

Figure 3: **Diagnostic and therapeutic algorithm of leprosy**

Panel 2: **Important advances and future directions in leprosy**

Pathophysiology

- The identification of phenolic glycolipid 3 is being explored as a novel therapeutic target. The molecule is a potent immunostimulatory glycolipid that provides immunity against infection and might also play a role in leprosy reactions.[145]
- The role of regulatory T cells and T-helper-17 cells in the pathogenesis of leprosy and its reactions could help to elucidate potential therapeutic applications.[58]
- Advances in genetic sequencing technologies, together with the development of functional models through genome editing and cell reprogramming, have expanded the understanding of the role that genetic polymorphisms play in the susceptibility to disease and clinical phenotype.[146]

Diagnostics

- A wide array of complementary serological, molecular, and host-derived diagnostic methods including point-of-care tests could help reduce misclassification of multibacillary as paucibacillary disease, improve the recognition of latent infections in communities with high disease burden, and provide a rapid evaluation of the effect of preventive and therapeutic measures.[91]
- Emerging mobile technologies such as the Leprosy Alert and Response Network System and SkinApp are promising tools to aid frontline health-care workers in expediting diagnosis and treatment.[91,147]
- Development of a molecular viability assay based on the measurement of hsp18 and esxA transcripts could help fast-track development of shorter treatment courses and early identification of treatment failure or relapse.[105–107]

Treatment

- Preliminary data support the effectiveness of better tolerated regimens such as the monthly administration of moxifloxacin, rifampicin, and minocycline, the shortening of multidrug therapy to a uniform 6-month regimen irrespective of the bacillary index, and the repurposing of new drugs such as bedaquiline.[99–104] The implementation of a molecular viability assay in larger confirmatory studies could help advance the potential application of new treatment regimens.
- Telacebec (Q203), an inhibitor of the cytochrome bcc:aa3 terminal oxidase, the only terminal electron acceptor in *Mycobacterium leprae*, is a promising treatment candidate and has shown potent antibacterial activity in the mouse footpad model.[148]
- Immunosuppressive therapy remains the cornerstone of leprosy reactions treatment. The effect of potential new leprosy treatment regimens on the incidence and severity of these reactions should be considered during the design of clinical studies. The concomitant administration of vaccines developed against leprosy could reduce the incidence of reactions.[149]
- Immunomodulatory therapies for erythema nodosum leprosum such as the combination of methotrexate, prednisolone, and metformin are being evaluated in clinical trials.[150,151] The Medicines Development for Global Health has received US Food and Drug Administration clearance to conduct a global phase 2 clinical trial with dovralimast, a phosphodiesterase-4 inhibitor, for treatment of erythema nodosum leprosum.[152]

Prevention

- Rifapentine has been shown to be more effective than rifampicin for postexposure prophylaxis in low levels of endemicity.[140] Enhanced postexposure regimens are being explored, such as rifampicin (150–600 mg) and clarithromycin (150–500 mg), administered every 4 weeks for a total of three doses, and bedaquiline with rifampicin, with dose depending on age and proximity to an index case.[141,142]
- Beyond their potential role in preventing infection, several leprosy vaccine candidates are being evaluated as adjunct immunotherapy given alongside multidrug therapy with the aim of enhancing bacterial clearance and possibly shortening treatment duration. The efficacy of post-exposure prophylaxis could improve with concomitant administration of leprosy vaccines.[143,149]

Stigma and discrimination

- People living with leprosy continue to be segregated from society and their families. A list of current laws and regulations that discriminate against people living with leprosy and their families can be found in the International Federation of Anti-Leprosy Associations website.
- In response, the UN Human Rights Council (UNHRC) adopted a resolution on elimination of discrimination against persons affected with leprosy and their family members in 2008. A Special Rapporteur was appointed in 2017 by UNHRC on the elimination of discrimination.[80]

Conclusion

In an era of shifting global dynamics, effectively reducing the burden of leprosy requires adapting to an evolving landscape. This adaptation hinges on the integration of robust public health policies with community-based initiatives. Concurrent investment in biomedical research and operational innovation must be underpinned by sustained political will and reliable funding. Such coordinated action, supported by an unwavering commitment to equity, is essential to eliminate leprosy as a public health issue.

Global health leap: an urgent call to action

The ongoing global health crisis presents a pivotal opportunity to transform and reform the fragmented global health architecture. This Viewpoint issues an urgent call for coordinated action—a Global Health Leap—and urges all stakeholders to unite around a shared scope, clear objectives, and principles and a process for transformative change. Throughout the past 50 years, major health emergencies such as HIV/AIDS, severe acute respiratory syndrome, Ebola virus, and COVID-19, coupled with a general optimism around the Millennium Development Goals and multilateralism, have driven expansion of the global health architecture. Today's funding challenges, by contrast, are leading to initiatives calling for reform, streamlining, and downsizing (table).[10–12] These calls build on a long-standing recognition that the global health institutional architecture has become top-heavy and duplicative after years of mission creep, during which organisations have expanded outside their core mandates in the absence of overall coordination.[13]

So far, the response to funding cuts from multiple agencies has been piecemeal cost-cutting as a route to short-term survival. Unless the current funding crisis is addressed urgently, constructively, and in a coordinated manner, a disorderly collapse of crucial health programmes could place the world's most vulnerable populations at greater risk.

Global health institutions have played a major role in keeping our world safe, driving equitable health outcomes, and helping countries develop their health systems.[4,14] All stakeholders in this architecture—governments, donors, civil society, academia, think tanks, the private sector, and global and regional health initiatives—should therefore align on a much bolder approach, a Global Health Leap, to urgently reform the global health architecture. This approach should be underpinned by consensus on these core questions: what is in scope? What is the overarching objective? What principles and process will drive reform, and which stakeholders can lead us to a Global Health Leap?

	Stakeholders	Lead	Timeline	Outputs
Future of Global Health Initiative*	Multistakeholder, including national governments, donors, civil society, international organisations, and academic representation	Norway and Kenya	2021–23	Lusaka Agenda (December, 2023)[1]
Friends of the Lusaka Agenda[2]	Multistakeholder, including national governments, donors, civil society, international organisations, and academic representation	UK Government and Malawi Government	2023 to present	Not applicable—informal group
Sevilla Platform of Action Initiative: Towards a renewed global health ecosystem: Navigating Challenges and Opportunities for financing inclusive, resilient and sustainable health systems[3]	Multistakeholder, including national governments, donors, civil society, international organisations, and academic representation	Spain	June, 2025 to present	TBC
Bold ideas for a reformed global health system*	Five regional public health experts	Wellcome Trust	June to August, 2025	Experts' proposal (August, 2025)[4]
The Accra Reset Initiative[5]	Governments and development experts	President John Dramani of Ghana	August, 2025 to present	Presidential High Level Task Force on Global Health Governance; Health Fund; SUSTAIN tool
Report on the implementation of the EU Global Health Strategy	European Commission	European Commission	July, 2025	Report[6]
Health Architecture Reimagined Civil Society Organizations	Multiple global, regional, and national civil society and community networks and organisations, including WACI Health, UHC2030 Civil Society Engagement Mechanism, STOPAIDS, Noncommunicable Diseases Alliance, Global Fund Advocates Network, Global Network of People Living with HIV, and the International Treatment Preparedness Coalition	Steering group composed of a consortium of civil society and community networks and organisations	July, 2025 to present	TBC
The Gavi Leap[7]	Gavi-supported countries	Gavi Secretariat	January, 2025 to present	Transformed Gavi Secretariat and country operating model aligned with Gavi Leap principles
Africa CDC's vision for a new public health order[8]	Africa CDC	Africa CDC	September, 2022	*Lancet* Comment[9]

CDC=Centres for Disease Control and Prevention. TBC=to be confirmed. *Status completed; others are active and ongoing.

Table: **Selected initiatives feeding into global health architecture reform**

Panel 1: Key messages

- There is an urgent need to use the present global health crisis as a catalyst for strategic reform of the global health ecosystem, with all stakeholders aligned on an agreed scope, objectives, and process for reform.
- The objective of reform should be to reimagine the role of every institution and focus on four priorities: generating global public goods, enabling positive impact at a large scale, merging operations at the last mile, and strengthening support for fragile contexts.
- The transformation of Gavi, the Vaccine Alliance (the Gavi Leap) has been developed in the context of broad change in the global health architecture. The four principles of the Gavi Leap can inform a broader global health leap.
- A panel, coordinated by WHO, which is supported by all countries, led by heads of state from donor and implementing countries, and supported by a technical committee, could drive restructuring and simplify the global and regional health architecture. Country support units and a standing committee of health agency leads should be subsequently institutionalised.
- The global goods function of the future global health ecosystem should be sustainably and predictably financed in the future, whereas tiered transition plans should be put in place for countries as long as a shortfall exists between donor official development assistance and domestic resourcing. A separate mechanism should be put in place for fragile and humanitarian settings.

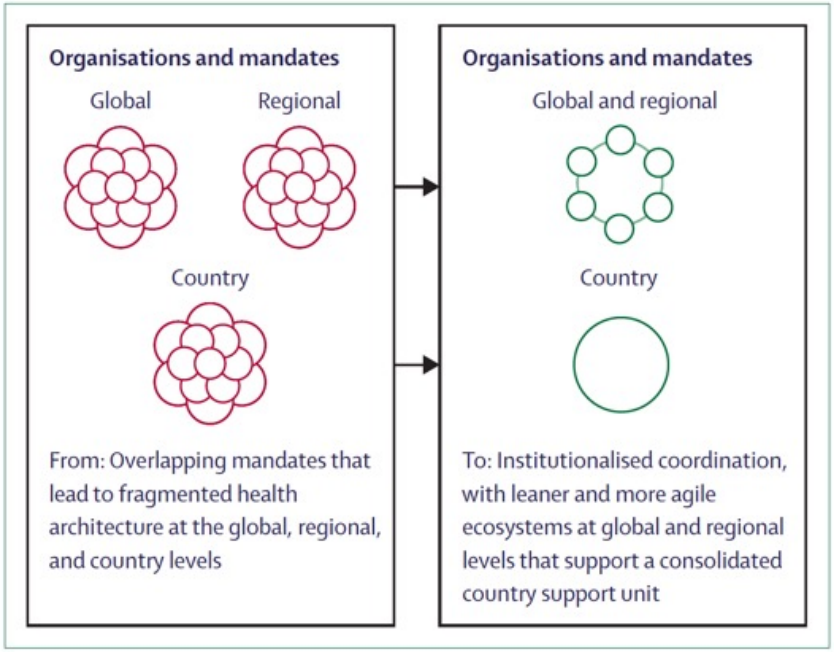

Figure 1: **From fragmentation and overlaps to a reimagined global health architecture**

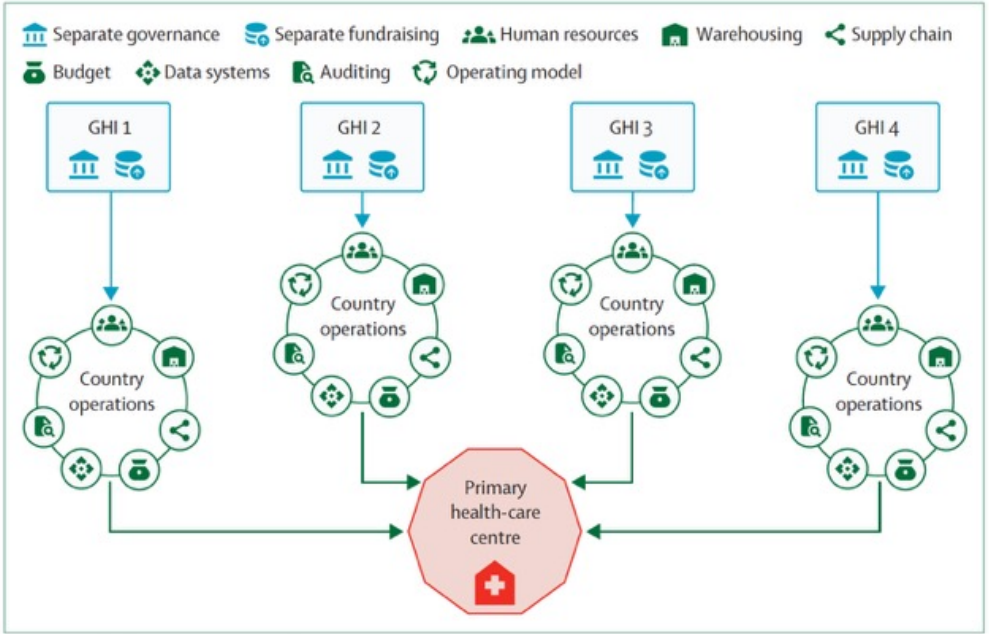

Figure 2: **Collaboration potential across various organisations**

Panel 2: The road to the Gavi Leap

When I joined Gavi, the Vaccine Alliance in early 2024, a pivotal shift in global health was evident. A new approach was needed to build on Gavi's enormous success in a rapidly changing world where funding constraints coexisted with material risks from conflict, climate change, and disease outbreaks. Opportunities were emerging as low-income countries showed increasing leadership in terms of health. Our response was the Gavi Leap: a transformation in the broader context of needed changes in the global health architecture, the reforming principles of which are already bringing tangible change to how we work, how we support countries, and how we sustain impact.

The Gavi Leap places countries and national self-reliance at the heart of everything we do; giving countries more agency over how Gavi support is deployed, radical simplification of our country-operating and grant-making models to reduce the administrative burden on countries, the use of country systems coupled with investments in public finance management, a drive towards merging at the last mile for reasons explained in the appendix, investments in Africa's future through vaccine manufacturing,[21] agile and differentiated approaches for fragile and humanitarian contexts, the imposition of checks and balances through investments in processes that strengthen transparency and accountability, and support for unlocking sustainable financing for long-term resilience. These radical shifts in ways of working will enable Gavi to reduce Secretariat size by 33% by the end of January, 2026.[22] Ultimately, our aim is to bring forward the day when Gavi has fully served its purpose. The Gavi Leap shows the feasibility of radical reform of the global health architecture.[23] We are committed to sharing our experiences and pain points along the way, in the hope that our transformation creates insights that can help inform others.

The need for reform is now broadly agreed upon, but action is still urgently required to establish a process for this reform. One option to establish a political process is to convene a panel coordinated by WHO that all countries endorse, led by heads of state from both implementing and donor countries, with full participation of regional bodies, national ministries of finance and planning, and other stakeholders, including civil society. Such a panel must be sufficiently robust to prevent narrow interests from dominating, and should be grounded in scientific and technical expertise, potentially informed by a *Lancet* Commission or similar entity. The panel must focus on the matter of predictably financing the global goods function of the future global health ecosystem and establish a consensus on tiered transition plans for countries to sustain health systems in light of the sudden reduction in official development assistance. Merging operations at the last mile can be driven by agencies supported by countries. Donors can play an important role in forging consensus. Improving delivery in humanitarian and fragile contexts requires new collaborative approaches with humanitarian actors and a focus on avoiding duplication.

Organoide sind im Labor gezüchtete, winzige, dreidimensionale Gewebestrukturen, die echten Organen (wie Gehirn, Darm oder Lunge) in Aufbau und Funktion ähneln. Sie entstehen aus Stammzellen, organisieren sich selbstständig und ermöglichen es Forschern, menschliche Krankheitsentwicklungen, Medikamentenwirkungen und Organentwicklung außerhalb des Körpers in Echtzeit zu untersuchen.

•**Herstellung:** Organoide werden aus adulten Stammzellen, embryonalen Stammzellen oder induzierten pluripotenten Stammzellen (iPS-Zellen) kultiviert.

•**Größe:** Die Strukturen sind meist nur wenige Millimeter groß, da ihnen die Gefäßversorgung fehlt.

•**Vorteile:**

Sie schließen die Lücke zwischen Tierversuchen und menschlicher Physiologie, da sie menschliches Gewebe statt tierisches nutzen

.

•**Anwendungen:**

- •**Krankheitsforschung:** Untersuchung von entzündlichen Prozessen oder Krebs (Tumoroide).
- •**Medikamententests:** Testen von Wirkstoffen auf spezifische Organstrukturen.
- •**Regenerative Medizin:** Potenzial zur Reparatur von geschädigtem Gewebe.

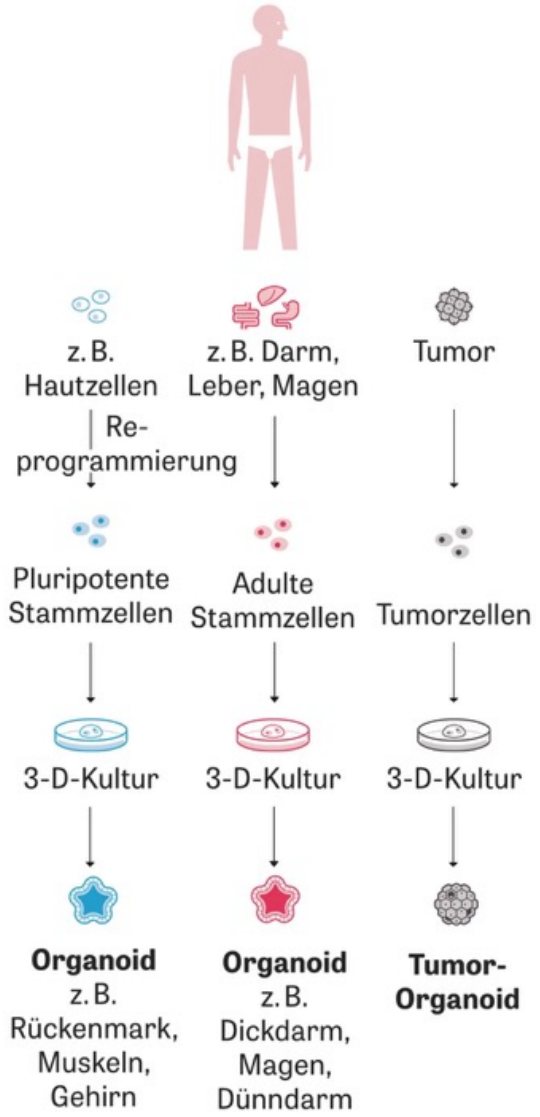

Cyborg pancreatic islet organoids

Bio-nanoelectronic islets are new tools for diabetes research and therapy

Stem cells can be manipulated to form organoids— three-dimensional structures that mimic the vital functions of organs. Organoids are useful for research into developmental, physiological, and pathophysiological mechanisms, and for improving therapies. The ability to monitor and steer organoid maturation in situ, noninvasively, in real time, and over months has the potential to transform biomedical research and regenerative medicine but poses considerable biotechnological challenges. Li et al. report the differentiation of human pluripotent stem cells into pancreatic islet micro-organs containing microelectrodes. These cyborg pancreatic organoids enable cell-specific long-term monitoring of islet cell activities, opening new avenues in diabetes research and cell therapy.

Pancreatic islets are complex networks of endocrine cells, including glucagon-secreting a cells and insulin-secreting β cells, that raise and lower blood glucose concentrations, respectively. The destruction or dysfunction of β cells, as well as α-cell dysregulation, are present in both type 1 and type 2 diabetes, which are chronic diseases that affect 10% of people worldwide.

Islet cells use bioelectric signals to transduce nutrient and neuro-hormonal inputs into secretion of hormones. These electric signals, which are difficult to detect with extracellular probes, have different durations and amplitudes compared with those of neurons and cardiomyocytes. Ever since extracellular electrodes were used to record electrical activity in islets isolated from rodents and humans (primary islets), substantial progress has been made using planar microelectrode arrays and organic electrochemical transistor arrays. These tools have also been used to study islets derived from the differentiation of human stem cells in culture.
Li *et al*. combined measurements of gene expression (transcriptomics) at cellular resolution and electrical field potentials, in an approach they called electro-sequencing. The authors' flexible bio-nanoelectronic platform enabled gene expression profiling and electrical recording at multiple sites at the same time in islet organoids. This approach made it possible to track islet functional maturation over weeks, whereas previous studies were limited to electrical recordings at the end of the differentiation protocol. This technology goes further than a previous application of the patch-sequencing technique that correlated single-cell transcriptomics with the electrical properties of islet cells to characterize dysfunction in islets obtained from patients with diabetes.

Der Glukose-Sensor

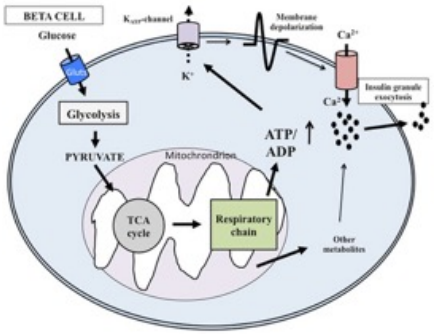

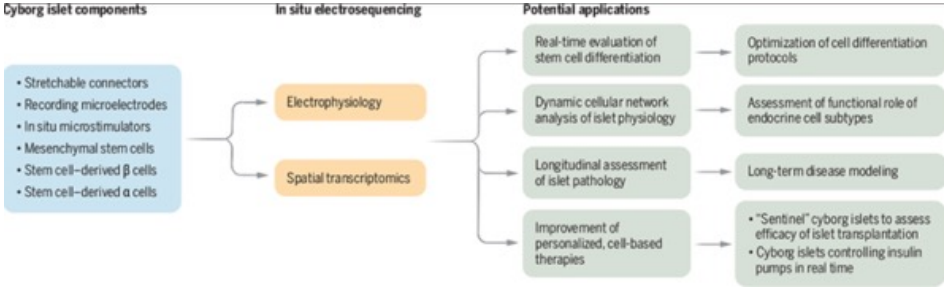

Bio-nanoelectronic islet organoids and their applications
Human stem cell–derived islet organoids that contain both recording microelectrodes and microstimulators enable monitoring of the functional maturation of islets in response to metabolic cues or electrical stimulation. These cyborg islets allow single-cell, noninvasive, high-speed, and long-term electrophysiological monitoring coupled with analysis of gene expression (transcriptomics). Cyborg islets have multiple applications in diabetes research and therapy.

INTRODUCTION: Human pluripotent stem cell–derived islets (SC-islets) hold promise for diabetes research and therapy but show functionally immature glucose responsiveness. Although several strategies promote maturation, SC-islets still fall short of the precision and dynamics of hormone secretion in primary islets. Whether this reflects poor coordination among α and β cells or intrinsic heterogeneity is unknown. Progress requires tools to decipher how individual cell functions specialize and synchronize within intact three-dimensional (3D) tissue over time.

RATIONALE: Recent advances in flexible, tissue-like nanoelectronics enable integration of stretchable electrodes into organoids during development, allowing long-term, noninvasive, single-cell electrophysiology, an opportunity not yet applied to SC-islet cells. We therefore integrated tissue-like, stretchable electronics into human pluripotent stem cell–derived pancreatic organoids to create "cyborg" pancreatic organoids, enabling months-long, single cell–resolved electrophysiology during pancreatic organoid maturation.

RESULTS: Cyborg pancreatic organoids enabled continuous recording of single-unit extracellular spiking activity within intact pancreatic organoids. Spike sorting isolated and clustered spikes to individual cells, allowing simultaneous capturing of single SC-α and -β cell electrical activities, distinguished by their characteristic responses to glucose. SC-α cells fired more rapid action potentials under low versus high glucose, which is consistent with glucagon secretion, whereas SC-β cells showed the opposite pattern, which is consistent with insulin release. Pharmacological perturbations further validated cell type–specific electrical behaviors. In situ electro-sequencing bridged these electrical signatures to transcriptionally defined SC-α and -β cells. Longitudinal tracking showed that SC-α and -β cells occupy either low or high basal firing electrical states and that increased organoid-level hormone responsiveness stems from increased electrical activity of SC-α and -β cells adopting both low and high basal firing states. Entrainment to daily metabolic cycles further demonstrated that circadian hormone secretion rhythms reflect synchronized oscillations in both SC-α and -β action potential firing rates and waveform profiles. Lastly, implanted electrical stimulators enabled electrical stimulation that selectively enhanced glucose-stimulated activity in SC-α and -β cells.

CONCLUSION: Cyborg pancreatic organoids provide a platform for continuous, single cell–resolved tracking of α and β cell electrical maturation within intact 3D tissue during maturation, uncovering mechanisms that enhance glucose responsiveness and cellular synchronization. This platform potentiates discovery of regulators of SC-islet maturation and provides a route toward engineering fully functional, tunable human islets, supporting future applications in disease modeling, drug discovery, and regenerative therapies for diabetes.

Ein **Cyborg** (ein Kofferwort aus dem Englischen für *cybernetic organism*) ist ein Wesen, das sowohl aus biologischen als auch aus künstlichen (elektronischen, mechanischen oder robotischen) Bestandteilen besteht.

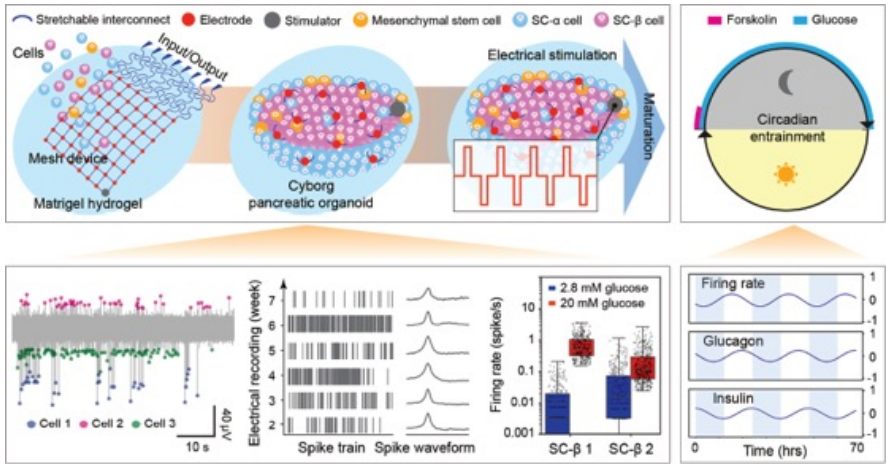

Cyborg pancreatic organoids. (Left, top and bottom) Stretchable mesh nanoelectronics integrated with stem cell–derived pancreatic cells generated "cyborg" pancreatic organoids. Single-unit electrical activities from SC-α and -β cells were captured through spike sorting and linked to transcriptional identity through in situ electro-sequencing. Long-term recordings tracked cell-specific dynamics. Electrical stimulation enhanced glucose-dependent electrical responses. (Right, top and bottom) Entrainment to daily metabolic cycles coordinated circadian electrical-secretory rhythms that enhanced organoid activity in vitro.

Entrainment bezeichnet allgemein das Mitreißen, Einfangen oder Synchronisieren von Systemen. Es beschreibt, wie ein externer Rhythmus einen internen (biorhythmischen) Prozess anpasst, oder wie turbulente Strömungen Umgebungsluft einbeziehen. Der Begriff ist zentral in der Biologie (Synchronisation), Meteorologie (Luftmischung) und Verfahrenstechnik (Mitreißen).

‘Highly likely’ that rare poison killed Putin nemesis Navalny, Europeans say

LONDON — It is “highly likely” that Russian opposition leader Alexei Navalny was killed by a rare toxin found in poison dart frogs, five European nations said in a statement Saturday, adding that Russia had the “means, motive and opportunity” to administer the deadly dose when Navalny died in an Arctic prison two years ago.

The statement, by the United Kingdom, Sweden, France, the Netherlands and Germany, provided official Western government validation of the belief — widely held by Navalny’s family and thousands of his supporters — that he was murdered by Russian authorities, perhaps on a direct order from the Kremlin.

"Given the toxicity of epibatidine and reported symptoms, poisoning was highly likely the cause of his death," the allies said. "Navalny died while held in prison, meaning Russia had the means, motive and opportunity to administer this poison to him."

Russian Foreign Ministry spokeswoman Maria Zakharova dismissed the joint statement, saying it was intended to "distract attention from the pressing problems of the West." Russian officials said they will comment further if testing involved in the investigation is released, Zakharova told the Russian outlet RBC.

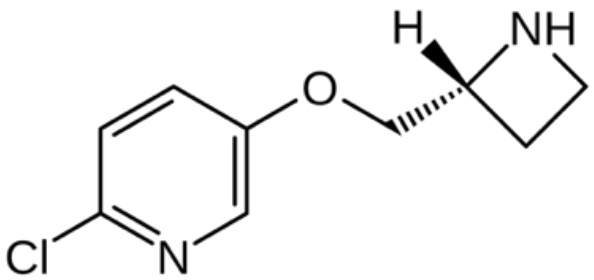

Succinylcholine and epibatidine are **structurally different but share similar pharmacological actions** as potent agonists of nicotinic acetylcholine receptors. Epibatidine is effectively orally absorbed. Determined by LC-MS.

Epibatidin ist ein hochgiftiges chlorhaltiges Alkaloid, das 1974 im Hautdrüsensekret von Baumsteigerfröschen der Gattung *Epipedobates* in Ecuador gefunden und dessen bicyclische Struktur 1992 aufgeklärt wurde.
Es ähnelt in seiner Wirkung anderen nikotinergen Acetylcholinrezeptor-Agonisten wie beispielsweise Nicotin des Tabaks, Anatoxin A, einiger Cyanobakterien, Cytisin des Goldregens und Arecolin der Betelnüsse.